UNIVERSITY OF HULL

Development of personalised optimisation of advanced-stage non-small cell lung cancer patients treated with volumetric modulated arc radiotherapy

being a Thesis submitted for the Degree of Doctor of Philosophy in the University of Hull

by

Nilesh Suresh Tambe

2022

Abstract

Background and Aim of the study: Lung cancer is the third most common cancer in the UK. A significant number of these patients are diagnosed with inoperable advanced-stage non-small cell lung cancer. Until recently, the standard of care for these patients was radiotherapy with or without chemotherapy but the overall survival remained poor, with a 5-year survival of only 13%. Recent studies showed significant improvement in overall survival in patients who are suitable for, and have received, immunotherapy, in addition to chemotherapy and radiotherapy. Radiotherapy aims to deliver tumoricidal doses to the target volume whilst minimising doses to the surrounding organs at risk (OAR). However, achieving this goal could be challenging especially when treating advanced-stage tumours, as it could increase OAR doses and increase toxicities to an unacceptable level. Furthermore, several factors affect the achieved dose distribution including, patient's geometry, treatment technique, planner's experience, beam geometry, optimisation parameters, and interventions used during treatments. It is therefore important to develop methods to personalise treatment plan optimisation for advanced-stage non-small cell lung cancer (NSCLC) patients to achieve minimum OAR doses without compromising target doses using patient-specific parameters. This study aims to develop knowledge-based planning models (KBP) using patient-specific factors to determine personalised treatment planning optimisation for advanced-stage NSCLC patients treated with volumetric modulated arc therapy (VMAT) to reduce OAR doses whilst delivering intended doses to the target volume.

Methods: Four KBP models were developed using patient-specific dose and volume parameters to predict minimum achievable OAR doses, identify optimal arc parameters, trigger adaptive radiotherapy and estimate doses to adapted gross tumour volume using

patients' geometry. The KBP models were verified using independent patient data sets. Change in treatment plan optimisation could increase modulation and affect plan deliverability therefore, several modulation indexes were calculated and plans were measured on the clinical linear accelerator to assess the effect of change in optimisation on treatment plan delivery.

Results: The KBP models developed showed that relatively simple models can predict OAR doses and arc parameters and help identify patients for adaptive radiotherapy. The models can accurately estimate personalised and progressive dose escalation. The KBP resulted in a significant reduction in plan variability in all three studied dosimetric parameters, volume of lungs receiving 5Gy (V_5), 20Gy (V_{20}) and mean lung dose (MLD) by 4.9% (p=0.007, 10.8% to 5.9%), 1.3% (p=0.038, 4.0% to 2.7%) and 0.9Gy (p=0.012, 2.5Gy to 1.6Gy), respectively. The individualised arc geometry resulted in a significant reduction in lungs (V_5 = - 15.1%, MLD = - 1.0Gy) and heart (MHD = - 1.4Gy) doses without compromising target coverage. The models, which were developed to predict changes in PTV coverage ($\Delta V95^{PTV}$) using a specific biomarker (Programmed death-ligand 1 (PD-L1 expression)) and the difference in 'planning' and 'fraction' planning target volume (PTV) centre of the mass (characterised by mean square difference, MSD), could predict change in PTV coverage within ± 1.0% for 77% of the total fractions. Furthermore, the models developed for predicting personalised and progressive dose escalation predicted doses within 0.4% and 0.7% respectively. Additionally, the plan complexity and deliverability measurements show that plan complexity could increase but may not affect treatment delivery significantly.

Conclusion: The studies performed show that altering the 'standard' treatment planning optimisation approach could significantly reduce OAR doses and improve target

coverage. This will help reduce toxicities and improve local control and overall survival and outcome for inoperable advanced-stage NSCLC patients.

Acknowledgements

First and foremost I am extremely grateful to my supervisors, Prof. Andrew W Beavis, Dr. Isabel M Pires and Dr. Craig Moore for their invaluable advice, continuous support, and patience during my PhD study. Their immense knowledge and plentiful experience have encouraged me throughout my research. I would also like to thank Dr. Andrew Wieczorek and Dr. Sunil Kumar Upadhyay for their clinical expertise in my studies. I would like to thank all the members of the radiation physics department. It is their kind support that has made my study enjoyable. I also like to thank Varian Medical Systems for lending us the Velocity adaptive radiotherapy software for this research.

Finally, I would like to express my gratitude to my parents, my wife, Yogita and my children, Sharvil and Shanay. Without their tremendous understanding and encouragement over the past few years, it would be impossible for me to complete my study.

Table of Contents

Publications to date

1. Andrzej Wieczorek*, Tambe, N. S.*; 'The Role of Radiotherapy in the Management of Lung Carcinoma, Frontiers in Lung Cancer Perspectives in LungCancer 2020,1:214.https://doi.org/10.2174/9789811459566120010013.
2. Tambe, N. S.; Pires, I. M.; Moore, C.; Cawthorne, C.; Beavis, A. W., Validation of in-house knowledge-based planning model for advance-stage lung cancer patients treated using VMAT radiotherapy. Br J Radiol 2020, 93 (1106), 20190535.
3. Tambe, N. S.; Pires, I. M.; Moore, C.; Wieczorek, A.; Upadhyay S.; Beavis, A. W., Predicting personalized optimal arc parameters using knowledge-based planning model for in-operable locally advanced-stage NSCLC lung cancer patients to reduce organs at risk doses. Biomed. Phys. Eng. Express, 2021. 7.065016.
4. Tambe, N. S.; Pires, I. M.; Moore, C.; Wieczorek, A.; Upadhyay S.; Beavis, A. W., Validation of in-house knowledge-based planning model for predicting change in target coverage during VMAT radiotherapy to in-operable advanced-stage NSCLC lung cancer patients. Biomed. Phys. Eng. Express, 2021. 7.065002.
5. Tambe, N. S.; Pires, I. M.; Moore, C.; Wieczorek, A.; Upadhyay S.; Beavis, A. W., Predicting personalised and progressive adaptive dose escalation to gross tumour volume using knowledge-based planning models for inoperable advanced-stage non-small cell lung cancer patients treated with volumetric modulated arc therapy. Biomed. Phys. Eng. Express, 2022. 8.035001.

CONFERENCE PRESENTATIONS

Poster presentation

1. Validation of a novel knowledge-based planning (KBP) model for lung cancer treatments with VMAT: Tambe, N. S, Moore, C., Pries, I. M., Cawthorne, C. and Beavis, A. (2019) 'EP-1836 Validation of a novel knowledge-based planning (KBP) model for lung cancer treatments with VMAT', Radiotherapy and Oncology, 133, pp. S996. ESTRO 2019.

2. RapidArc with avoidance sectors for the treatment of lung and oesophagus cancers: Tambe, N. S., Moore, C., Pries, I. M., Cawthorne, C. and Beavis, A. (2019) 'E-038 RapidArc with avoidance sectors for the treatment of lung and oesophagus cancers'. UKIO, 2019.

3. Nilesh S Tambe, Isabel M Pires, Craig Moore, Andrew Wieczorek, Sunil Upadhyay, Andrew W Beavis, ‘Adaptive dose escalation for non-small cell lung cancer patients treated with VMAT’, ESTRO 2021.

List of Tables

Chapter 1

Chapter 2

Chapter 3

Chapter 4

List of Figures

Chapter 1

Chapter 2

Chapter 3

Chapter 4

Chapter 5

Chapter 6

Chart

List of acronyms

3D-CT	Three-dimensional computerised tomography
4D-CT	Four-dimensional computerised tomography
ADC	Adenocarcinoma
ART	Adaptive radiotherapy
BED	Biological effective dose
BEV	Beam's eye view
CBCT	Cone beam computerised tomography
CI	Conformity index
CRT	Conformal radiotherapy
CT	Computerised tomography
CTV	Clinical target volume
DMLC	Dynamic multi-leaf collimator
DRR	Digitally reconstructed radiograph
DVH	Dose-volume histogram
EPID	Electronic portal imaging device
ESAPI	Eclipse scripting application plug-in
FB	Free-breathing
GI	Gastrointestinal
GTV	Gross tumour volume
Gy	Gray
HI	Homogeneity index
HRA	Health Research Authority
HU	Hounsfield units

ICD	Immune checkpoint inhibitors
ICRU	International Commission on Radiation Units and measurement
IGRT	Image-guided radiotherapy
IMRT	Intensity-modulated radiotherapy
ITV	Internal target volume
KBP	Knowledge-based planning
MDT	Multidisciplinary team meetings
MHD	Mean heart dose
MLC	Multi-leaf collimator
MLD	Mean lung dose
MPE	Medical physics expert
MRI	Magnetic resonance imaging
MSD	Mean square difference
MU	Monitor Units
MV	Megavoltage
NHS	National Health Service
NSCLC	Non-small cell lung cancer
NTO	Normal tissue objective
OAR	Organs at risk
OBI	Onboard imaging
OVH	Overlap volume histogram
PD-1	Programmed cell death protein
PDIP	Portal dose image prediction
PD-L1	Programmed cell death-ligand 1

PET	Positron emission tomography
PRV	Planning organ at risk volume
PTV	Planning target volume
QA	Quality assurance
RP	Radiation-induced pneumonitis
RPM	Real-time positioning management
SABR	Stereotactic ablative body radiotherapy
SAS	Small aperture score
SCC	squamous cell carcinoma
SCLC	Small cell lung cancer
SUV	Standardized uptake volume
TCP	Tumour control probability
TPS	Treatment planning system
VMAT	Volumetric modulated radiotherapy
WHO	World Health Organisation

1.0 Introduction

This chapter is published in a book, and therefore the text presented here is adapted from the article. My contribution consisted in performing a literature search and writing the manuscript with input from the co-author. Reference: Andrzej Wieczorek*, Tambe, N. S.*; 'The Role of Radiotherapy in the Management of Lung Carcinoma, Frontiers in Lung Cancer Perspectives in LungCancer 2020,1:214. https://doi.org/10.2174/97898114595 6612001 0013.

1.1 Lung cancer

Lung cancer is triggered due to exposure to inhaled carcinogens (e.g. tobacco smoke, arsenic, asbestos, beryllium, cadmium, coal and coke fumes, silica, nickel, and radon) to the bronchial epithelium cells. The biological changes eventually lead to carcinoma by the activation of carcinogens or inactivation of tumour suppression genes (p-4, Jeremic, 2011) (Jeremic, 2011; Massion P P, 2016). In addition to the environmental factors, lung cancer can have a familial origin due to common genetic or environmental factors among family members (Kanwal, Ding and Cao, 2017). Almost 8% of total lung cancers occur due to familial factors (Kanwal, Ding and Cao, 2017).

1.1.1 Incidence of lung cancer

Lung cancer is the third most common cancer in the UK, accounting for 13% of the total cancer patients and resulting in 35,137 deaths per year (Cancer Research UK, 2019). In years 2015 to 2017, approximately 47,800 new lung cancer cases were reported in the UK per year (Cancer Research UK, 2019). A recent study reported 1.32 fold increase in lung cancer cases over twenty years (Chen, Mo and Yi, 2022). Lung cancer incidence is

highly related to age, with the highest incidence rate in the older population. On average, 44% of total new lung cancer cases are in people aged 75 years and over (see Figure 1.1) and the median age at presentation of lung cancer is 70 years (see Figure 1.2) (Cancer Research UK, 2019). The majority of these patients have smoking-related co-morbidities such as emphysema and cardiovascular disease (Kanwal, Ding and Cao, 2017; Cancer Research UK, 2019). As a result, many of these patients are not suitable for surgery (Leary, 2012; Maconachie *et al.*, 2019). Radiotherapy with or without chemotherapy is considered the standard of care for those patients who are not suitable for surgery (Leary, 2012; Maconachie *et al.*, 2019).

For those diagnosed with lung cancer, the median life expectancy in the 19th century was about 13.2 months (Fowler J K, 1898). This has improved over the years but not significantly, with the average five-year or more survival in the UK only 8% to 11% (Neal and Hoskin, 2012; Cancer Research UK, 2016). In the last 40 years, five years of overall survival had only improved by 3% to 5% in the UK despite the advancement in the treatment modalities (Cancer Research UK, 2016).

1.1.2 Lung Cancer Classification

There are two main types of lung cancer: small-cell lung cancer (SCLC) and non-small cell lung cancer (NSCLC) (Kernstine and Reckamp, 2010). SCLC accounts for about 10 - 15% of lung cancer patients whereas the majority are diagnosed with NSCLC (Kernstine and Reckamp, 2010). NSCLC is further divided into lung adenocarcinoma (ADC, the most common type of NSCLC), lung squamous cell carcinoma (SCC), and lung large cell carcinoma. Accurate histological diagnosis to assess cancer subtypes is very important as SCLC and NSCLC cancers grow and spread very differently (Sher, Dy and Adjei, 2008; Zappa and Mousa, 2016). SCLC generally spreads quite rapidly, whereas NSCLC spreads

relatively slowly (Sher, Dy and Adjei, 2008; Zappa and Mousa, 2016). The standard of care for SCLC patients is chemotherapy with or without radiotherapy; surgery is performed in approximately 2% of patients (Cancer Research UK, 2016). However, for a majority of NSCLC patients standard of care is radiotherapy with or without chemotherapy; in these patients, surgery is performed in approximately 15% of patients (Cancer Research UK, 2016). The majority of all lung cancer patients are diagnosed with advanced disease, stage III or IV (see Figure 1.3) (Cancer Research UK, 2016).

1.2 Treatment of NSCLC

This thesis is focused on the personalised optimisation of radiotherapy treatment planning for NSCLC patients, as the majority of lung cancer patients are diagnosed with NSCLC and the standard of care for inoperable patients is radiotherapy with or without chemotherapy (Cancer Research UK, 2016; Maconachie *et al.*, 2019; Cancer Research UK, 2019). In recent years, the gold standard in oncology is the use of a combination of treatment modalities (Maconachie *et al.*, 2019). The selection of treatment modality(s) for NSCLC patients is dependent on tumour staging, age, lung function, and performance status (see Tables 1.1 and 1.2) (Maconachie *et al.*, 2019). Early-stage lung cancer patients with performance status 2 (see Table 1.2 for description) (Maconachie *et al.*, 2019) and who are suitable for lobectomy are treated with limited surgical resection. If not, these patients are treated with stereotactic radiotherapy or radical radiotherapy depending on tumour size and location (i.e., centrally located tumours are treated with radical radiotherapy). In addition, a standard of care for patients with stage III disease is chemotherapy plus radiotherapy, but patients with impaired performance status may undergo palliative radiotherapy to control symptoms (Maconachie *et al.*, 2019). Treatment options based on staging are displayed in Table 1.1.

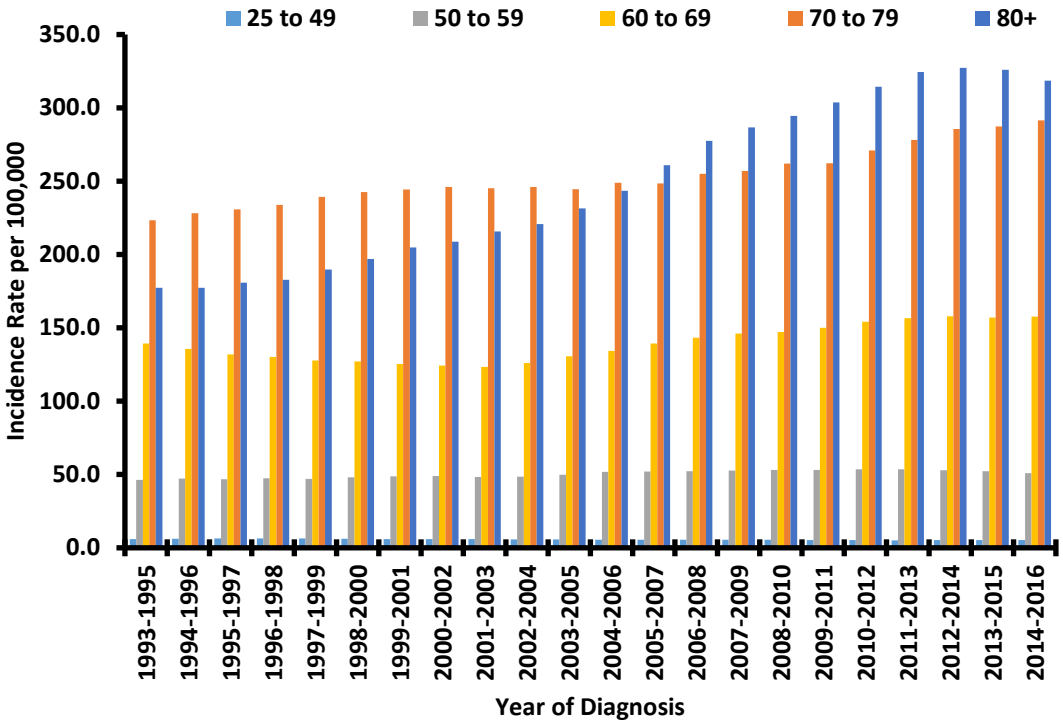

Figure 1.1: Incidence of lung cancer by age in the UK between 1993 and 2016

Lung cancer incidence is higher in elderly patients compared to younger patients. The data show an increase in the incidence of lung cancer in patients aged 80 years and above in recent years (Cancer Research UK, 2016; Cancer Research UK, 2019).

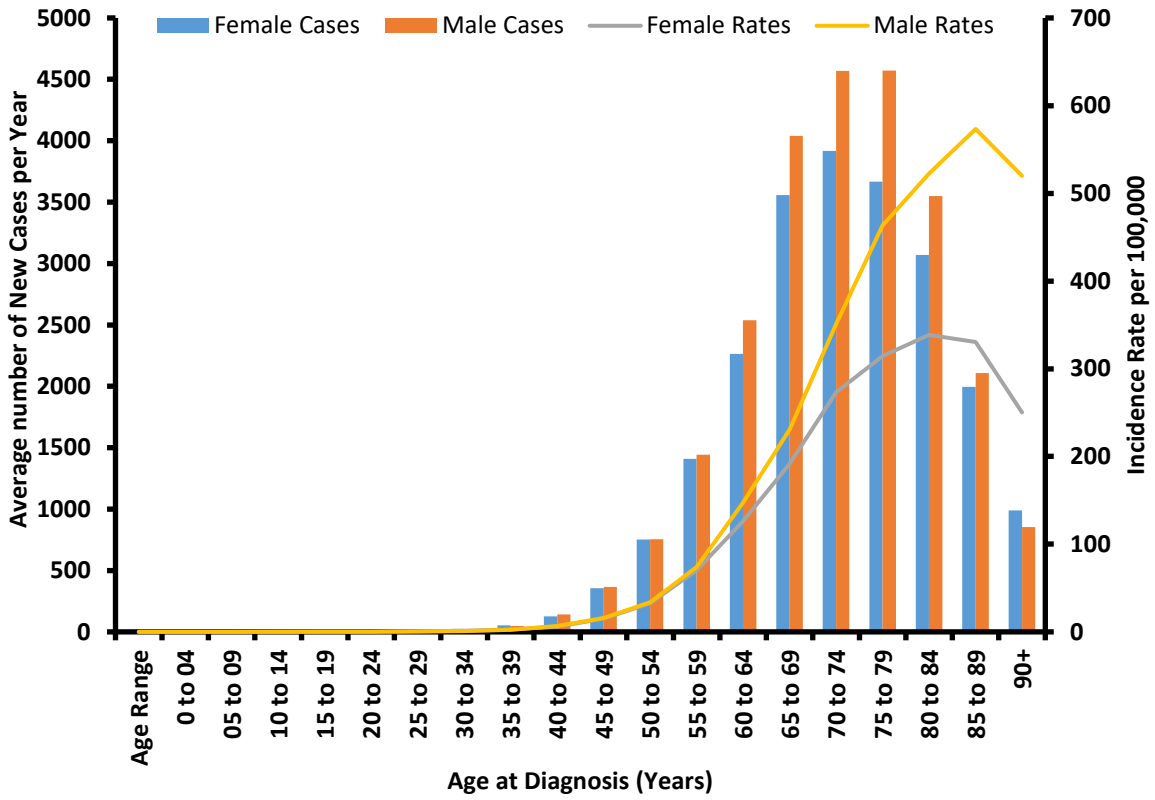

Figure 1.2: Age-specific incidence of lung cancer

The figure shows the average number of new lung cancer cases diagnosed per year and age-specific incidence rates per 100,000 population, in the UK (Cancer Research UK, 2019).

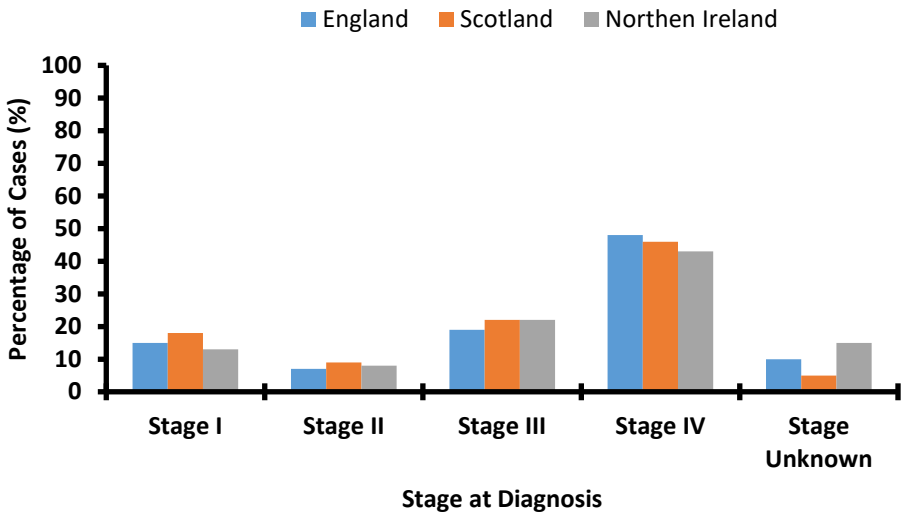

Figure 1.3: Lung cancer staging at diagnosis in England, Scotland and Northern Ireland

The proportion of lung cancer cases at each stage, all ages, in England, Scotland and Northern Ireland. It can be seen that a significant number of patients are diagnosed at an advanced stage (Cancer Research UK, 2016).

Table 1.1 Lung cancer staging and management (p-3 to 15) (Cox, Chang and Komaki, 2007)

Staging	Treatment
Stage I and II	Surgery ± adjuvant chemotherapy Patients unfit for surgery or patients who prefer SABR or radiotherapy to surgery – SABR or radiotherapy
Stage IIIA and IIIB	Chemotherapy + Radiotherapy +/- adjuvant immunotherapy or radiotherapy alone (if patient unfit or patient preference)
Stage IV	Chemotherapy, targeted therapy, immunotherapy, palliative RT

Table 1.2 Performance status defined by World Health Organisation (Maconachie *et al.*, 2019)

Grade/Status	Explanation of activity
0	Fully active, able to carry on all pre-disease performance without restriction
1	Restricted in physically strenuous activity but ambulatory and able to carry out work of a light or sedentary nature, e.g., light housework, office work
2	Ambulatory and capable of all self-care but unable to carry out any work activities. Up and about more than 50% of waking hours
3	Capable of only limited self-care, confined to bed or chair for more than 50% of waking hours
4	Completely disabled. Cannot carry on any self-care. Confined to a bed or chair
5	Dead

1.2.1 Surgery

Surgery is a standard of care for NSCLC patients with limited/early-stage disease and who are suitable for operation (Maconachie *et al.*, 2019). Lung surgical resections are generally pneumonectomy, lobectomy, or wedge recession (Maconachie *et al.*, 2019). However, surgical resections have 2% to 4% associated fatal side effects (Cancer Research UK, 2016; Maconachie *et al.*, 2019). Survival of patients undergoing surgery is higher for limited/early-stage cancer patients compared to advanced-stage disease, mainly due to remaining microscopic diseases (p-5, Cox, Chang and Komaki) (Cancer Research UK, 2019; Cox, Chang and Komaki, 2007). A number of studies have reported that the overall survival of advanced-stage non-small cell lung cancer (NSCLC) patients undergoing surgery is similar to the patients who have had chemo-radiotherapy (p-5, Cox, Chang and Komaki) (Pöttgen *et al.*, 2017; Cox, Chang and Komaki, 2007). However, Pöttgen *et. al.* 2017 also reported that early mortalities (within 6 months of the treatment) were higher in patients treated with surgery (Pöttgen *et al.*, 2017).

1.2.2 Chemotherapy

Chemotherapy is considered for patients with stage II and III NSCLC who are not suitable or have declined surgery (Maconachie *et al.*, 2019). Cisplatin-based combination chemotherapy can be offered to patients with tumour stage T1A–4, N1–2, M0 and WHO performance status of 0 or 1 in the postoperative setting or a preoperative setting for patients with tumour staging TIIIA–N2 (Maconachie *et al.*, 2019). Radiotherapy with or without chemotherapy is the standard of care for patients who are not suitable for surgery (Maconachie *et al.*, 2019). Chemotherapy is given either sequentially (i.e. course of chemotherapy is completed before starting radiotherapy) or concomitantly (i.e. chemotherapy is given during radiotherapy) depending on the patient's age and lung

function (Maconachie *et al.*, 2019). Concomitant chemo-radiotherapy improves patient survival but it also results in higher toxicity compared to sequential chemo-radiotherapy (Maconachie *et al.*, 2019). The survival of patients that receive sequential chemo-radiotherapy is approximately 4% less than those that receive concomitant chemo-radiotherapy (Curran *et al.*, 2011). In addition, most chemotherapy agents used have associated normal tissue toxicities (Rancati *et al.*, 2003).

1.2.3 Radiotherapy

The aim of radiotherapy is to deliver the intended dose to a target volume whilst minimising the dose to healthy tissues (organs-at-risk, OARs), but achieving the desired target coverage whilst minimising the OAR dose can be challenging, especially, when the target volume is in close proximity with the dose-limiting structures (e.g. spinal cord) (Newhauser, 2009). Unlike systemic treatments (e.g. chemotherapy), radiotherapy is a localised treatment modality. Most commonly, radiotherapy treatment is delivered using a linear accelerator (see Figure 1.4) producing high-energy (megavoltage (MV)) x-rays (p-40, Khan, 2012) (Khan, 2012; Symonds *et al.*, 2012). The treatment beams are shaped to the tumour volume using multi-leaf collimators (MLC) to minimise radiation dose spillage into healthy tissues surrounding the tumour volume (p-230, Khan, 2012, p-160, Symonds, 2012) (Khan, 2012; Symonds *et al.*, 2012). This reduction of dose to healthy tissues is highly important to reduce post-treatment toxicities (p-28, Symonds, 2012) (Symonds *et al.*, 2012). The radiation dose deposited is characterised by the energy imparted per unit mass of a given material, and the unit of dose is the Gray (Gy); 1 Gy = 1 J/kg (Leary, 2012).

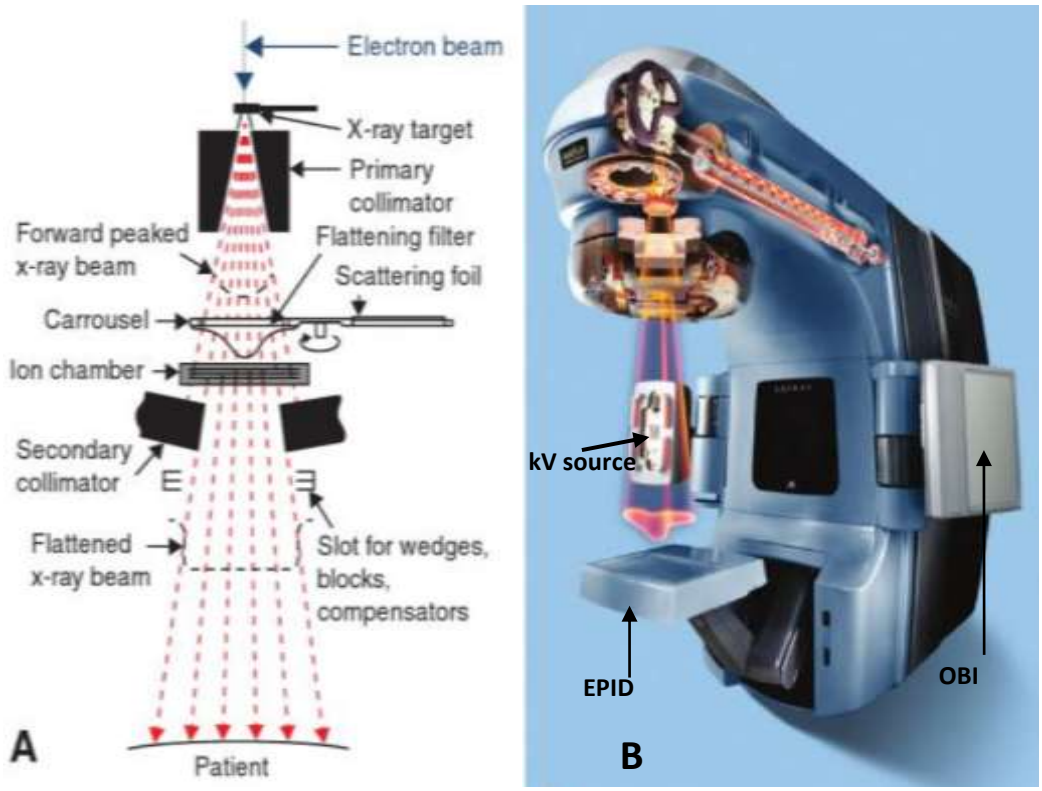

Figure 1.4. Schematic of a linear accelerator, p43 (Khan, 2012)

Image A shows a schematic of the X-ray mode of a Varian linear accelerator and image B shows a Varian linear accelerator with On-Board Imaging (OBI). OBI is used for acquiring 3D cone beam computerised tomography (CBCT) and/ or 2D planar kilo-voltage images (2D-kV) images). An electronic portal imaging device (EPID) panel is also shown this is used to acquire megavoltage (MV) 2D images and/ or portal dose image prediction (PDIP) measurement to assess the deliverability of treatment plans.

1.2.3.2 Radiotherapy treatment pathway

Treatment management of cancer patients is decided in multidisciplinary team meetings (MDT: a team that includes experts from different disciplines/specialties of medicine, e.g. medical speciality, clinical oncology, medical oncology, surgery, radiology, pathology), taking multiple factors into account including disease stage, prognosis, lung function, cardiovascular function, and age. Once the decision has been made and if the patient is to have radiotherapy, they are referred to a consultant clinical oncologist. The clinical oncologist discusses treatment (dose and fractionation) and related toxicities with the patients and gains informed consent from the patient. Patients then undergo the following processes at Hull University Teaching Hospitals (HUTH), see chart 1.1.

CT simulation

At HUTH, a treatment-planning CT scan is acquired on a Siemens Pro™ CT scanner. The CT scan is performed, to obtain a volumetric data set to be used for delineating targets and organs at risk volumes. CT images are reconstructed from measured exit radiation fluence, having irradiated the patient with an x-ray beam over a 360-degree arc. An attenuation coefficient (Hounsfield Units (HU)) can be determined from these scans, to characterise tissue density and is used for treatment plan optimisation and dose calculations. The acquired CT images allow the generation of a digitally reconstructed radiograph (DRR) and/ or the CT volumetric data set can be used for treatment verification prior to delivering treatment (p-29, Beets-Tan, Oyes and Valentini 2020) (Beets-Tan, Oyen and Valentini, 2020).

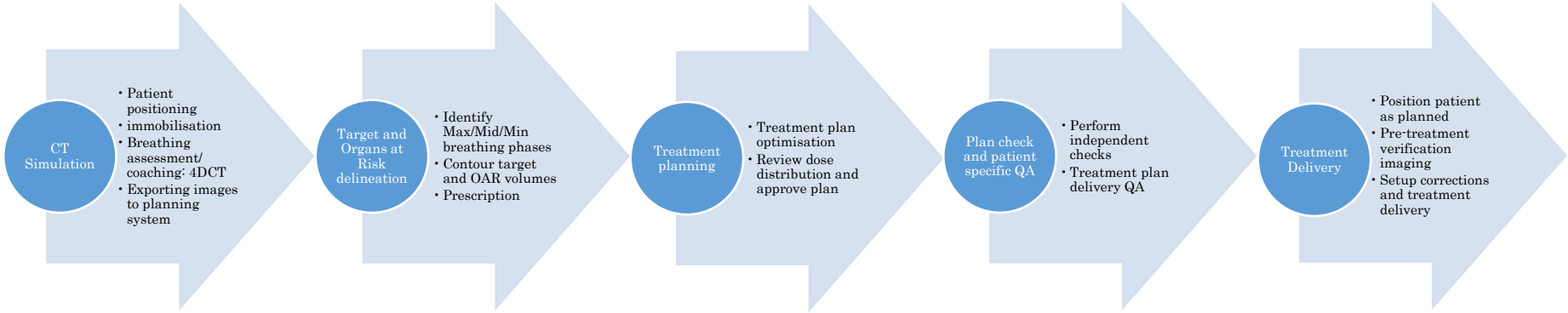

Chart 1.1: Showing radiotherapy patient pathway at HUTH.

Patient positioning and immobilisation: Lung cancer patients are positioned supine with their arms above their head (to avoid treating through arms) using a wing board with hand poles and knee rest. If both arms cannot be raised above the head, then every attempt is made to raise one arm only. Both the wing board and knee rest are fixed to the couch using locking bars. The position of the locking bars, arm poles and head position is recorded on the patient setup sheet to ensure consistent patient positioning during radiotherapy treatment as the CT simulation scan is carried out only once prior to starting treatment. Any deviation from the planned/simulated treatment position could introduce errors in treatment delivery (especially if pre-treatment imaging is not performed), (p-150, Marcu, Bezak and Allen, 2012) (Marcu, Bezak and Allen, 2012). Immobilisation devices limit patient motion during treatment so that treatment can be delivered as planned (p-132, Marcu, Bezak and Allen, 2012) (The Royal College of Radiologists, 2008; Marcu, Bezak and Allen, 2012).

Target and organs at risk (OAR) volume delineation: At HUTH, target volumes used are consistent with international standards: gross tumour volume (GTV: includes the tumour volume (primary and nodes) that can be seen by the eye (or palpation) either on the patient or with the help of imaging), no additional margins are added to this structure); clinical target volume (CTV: is a volume that contains the GTV and/or subclinical microscopic malignant disease); and planning target volume (PTV: includes gross tumour and clinical target volumes with a margin added for set-up errors) (International Commission on Radiological Units, 1993; International Commission on Radiological Units, 1999; Newhauser, 2009). Target volumes, GTV, nodes and CTV are contoured by clinical oncologists and the clinician also construct PTV by adding a marging to CTV.

In addition, organs at risk (OAR) volumes including lungs (i.e. lungs excluding GTV), heart, spinal cord, and spinal cord PRV are contoured on the averaged 4D-CT scan (a scan reconstructed using average pixel density from the binned data). The PRV is the planning organ at risk volume: the PRV includes a margin to compensate for setup variations similar to the PTV, ensuring the critical tissues/ structures do not exceed the dose limit) (International Commission on Radiological Units, 1993; International Commission on Radiological Units, 1999). At HUTH, the spinal cord PRV is generated by adding a 0.5 cm isotropic margin for setup errors to ensure the dose to the spinal cord does not exceed the acceptable limit.

Treatment planning: Individualised treatment plans are then produced for each patient. The goal of treatment planning is to deliver the intended dose to the target volume whilst keeping OAR doses within the clinical constraints and/or reducing as low are reasonably practicable beyond the dose constraint (Emami *et al.*, 1991; Newhauser, 2009; Bentzen *et al.*, 2010; Marks *et al.*, 2010b; Appelt *et al.*, 2014). Different techniques are used to produce conformal treatment plans and treat lung cancer patients.

Radiotherapy dose and fractionation: Radiotherapy is conventionally delivered in several smaller doses, called fractions, over a period of weeks to a total prescribed dose value (Newhauser, 2009; Maconachie *et al.*, 2019). The conventional fractionation regime delivers a radiation dose of 1.8 Gy – 2 Gy per fraction (per day) for five days a week (Newhauser, 2009). Generally, the total radiotherapy dose varies between 60 Gy – 70 Gy, delivered in 30 – 35 fractions over six to seven weeks (Nyman *et al.*, 2016; Maconachie *et al.*, 2019). The fractionation schedule allows normal tissues to recover from the sub-lethal damage caused by radiation (p-127, Whitson, 1972) (Whitson, 1972). The time between fractionations also allows the redistribution of tumour cells from a radio-

resistant phase of the cell division cycle (i.e., S phase) to more radio-sensitive phases (i.e., late G2 and M) (p-185, 191, Whitson, 1972) (Whitson, 1972). Furthermore, it allows re-oxygenation of hypoxic tumour cells, improving tumour cell killing (p-194, Whitson, 1972) (Whitson, 1972). Repair and repopulation of the normal cells during a break between fractionations also improve the tolerance of normal tissue (p-104, Whitson, 1972) (Whitson, 1972). One of the disadvantages of long-scheduled fractionation is the unwanted repopulation of tumour cells that starts after 4 weeks of treatment (Withers, Taylor and Maciejewski, 1988; Maciejewski and Majewski, 1991; Petereit *et al.*, 1995; Kim and Tannock, 2005; Chen *et al.*, 2011). This can be avoided by accelerated treatment schedules or by hypo-fractionated dose regimes (e.g. 55 Gy delivered in 20 fractions). These fractionated regimes are recommended for unresectable stage III (T1-T3/N0-N2) lung cancer patients (Maconachie *et al.*, 2019). Hyper-fractionated dose regimes, where smaller doses per fraction are delivered more than once a day, can be considered for advanced-stage NSCLC patients (Maconachie *et al.*, 2019).

In recent years, early-stage inoperable cancers are treated using stereotactic ablative body radiotherapy (SABR) (see Table 1.1). The SABR fractionation regime differs significantly from the conventional fractionation regime, delivering a high radiation dose over a short period of time (54 Gy/ 3#s: SABR lung) to potentially ablate early-stage NSCLC (UK SABR Consortium, 2016; Nyman *et al.*, 2016; Bergsma *et al.*, 2017; Dan and Williams, 2017; Kennedy, Corkum and Louie, 2017; Shah and Loo, 2017; Sun *et al.*, 2017; Boon *et al.*, 2017; Yu, Dai and Xu, 2017; UK SABR Consortium, 2019). Finally, an emerging technique and one of the major and promising breakthroughs in radiation oncology is FLASH-radiotherapy (FLASH-RT) (Bourhis *et al.*, 2019; Vozenin, Bourhis and Durante, 2022). It delivers ultra-fast radiation doses with an intra-pulse dose rate higher than

$1.8x10^5$ Gy/s helping to limit normal tissue toxicities and hence could allow dose escalation (Bourhis *et al.*, 2019; Vozenin, Bourhis and Durante, 2022). FLASH therapy has the additional benefits of reducing treatment time and issues related to organ motion. The pre-clinical animal studies show promising results, but due to technological challenges it might take a few years for being used routinely for treating cancer patients (Bourhis *et al.*, 2019; Vozenin, Bourhis and Durante, 2022).

The biologically effective dose (BED) is a way of comparing the biological effects of the dose delivered by a particular combination of dose per fraction and total dose to a given tissue characterised by a specific α/β ratio. BED delivered with different fractionation regimes can be calculated using equation 1.1.

$$BED = d \times f \left(1 + \frac{d}{\alpha/\beta}\right) \qquad \textbf{Equation 1.1}$$

Here, d is the dose per fraction, f is the total number of fractions (d x f = total prescription dose), and α/β is used to quantify the fractionation sensitivity of the tissues (Steel, 2002). The α/β ratio describes the dose where the linear, as well as the quadratic component, cause the same amount of cell killing. A low α/β (0.5 – 6 Gy) value is characteristic of late-responding normal tissues, and higher values (7 – 20 Gy) are characteristic of early-responding normal tissues and tumours (Steel, 2002).

Tumour control and normal tissues complication probability (TCP/ NTCP): TCP is a parameter used to quantify the percentage of tumour killing for a given radiation dose whereas, its effect on normal tissue damage is defined as NTCP. Both TCP and NTCP depend on fractionation dose and cell biology such as repopulation, repair, redistribution and re-oxygenation (Nuraini and Widita, 2019).

In this thesis, TCP was calculated using Biosuite software (Uzan and Nahum, 2012) and the estimated TCP values were used for comparing the clinical and test plans. The Biosuite software uses a dose-volume histogram and a number of set parameters (describing how different tissues will respond to the given ionising radiation) to predict TCP and NTCP. For more information about the parameters and the values used in the thesis please see section 6.2.3.

Organs at risk (OAR) dose constraints: OAR dose constraints (i.e., tolerance dose), that is, doses related to acceptable or tolerable side-effects, are obtained based on previous experiences, as reported by Emami et al (Emami et al., 1991) and QUANTEC (Marks et al., 2010b). Dose constraints include maximum dose, mean dose and/or dose to a percentage of volume. For example, to limit the risk of symptomatic radiation pneumonitis below 20%, the dose to 30 to 35% of healthy lung tissue should be less than 20 Gy (i.e., V20Gy < 30-35%) and/ or a mean lung dose should be lower than 20 to 23 Gy (Bradley et al., 2005; Marks et al., 2010a).

Lower OAR doses are associated with lower toxicities, which can be achieved with IMRT and/or VMAT treatments (Yom *et al.*, 2007; Jiang *et al.*, 2012). Numerous studies have compared treatment outcomes for patients treated with 3D-CRT and IMRT/VMAT and reported that the rate of grade 3 and/or higher toxicities are significantly lower for patients treated with IMRT/VMAT compared to 3DCRT patients (Yom *et al.*, 2007; Jiang *et al.*, 2012). This was despite treating larger target volumes with IMRT (Yom *et al.*, 2007; Jiang *et al.*, 2012). In addition, Wijsman et al compared toxicities and outcomes for advanced-stage NSCLC patients treated with IMRT and VMAT; the study found no significant differences in the acute and late pulmonary toxicities, however, the VMAT patients showed higher acute oesophageal toxicities compared to the IMRT patients

(Wijsman *et al.*, 2017). This study did not find any differences in the overall survival between patients treated with IMRT or VMAT (Wijsman *et al.*, 2017).

Radiotherapy planning techniques: The radiotherapy treatment planning pathway for the management of cancer patients includes clinical and technical treatment planning (see Chart 1.1). Clinical planning dictates treatment intent, treatment modality, radiation dose prescription to the target volumes and clinical structures. Conversely, the technical plan derives the patient's position, immobilisation, treatment beam geometry, aperture and X-ray beam energy to produce individualised optimal treatment plans (p-5, Xia, 2018) (Xia *et al.*, 2018).

Different radiotherapy treatment planning and delivery techniques have been developed over the years. Even after megavoltage, radiotherapy became the norm following the introduction of Co-60 and linear accelerator units in the 1950s and 1960, treatment was planned using 2D images acquired on a conventional simulator (p-17, Barrett, Dobbs and Roques, 2009) (Barrett, Dobbs and Roques, 2009). Treatment fields were defined based on poorly differentiated anatomical and tumour boundaries and dose distribution and treatment times were calculated manually using 2D dosimetric data until the early development and introduction of computer treatment planning in the 1960s and 1970s (p-210, Levitt et al, 2008; p-49, Xia, 2018) (Levitt *et al.*, 2008; Xia *et al.*, 2018). Following the development of the CT scanner in the 1970s, there has been a significant improvement in radiotherapy planning (Bortfeld, 2006). 3D CT images are used for delineating target volumes and establishing a true 3D target volume. After 1999, the further development and wider availability of 3D treatment planning systems (TPS) and multi-leaf collimators (MLC) allowed the shaping of treatment beam apertures to the target volume using the beam's eye view (BEV) resulting in the superior conformation of

isodoses to the target volume whilst minimising dose to OARs (Barrett, Dobbs and Roques, 2009). In 3D-CRT, multiple static fields are placed around the target volume using the beam's eye view (BEV). BEV helps to avoid and/or minimise beam incidence through critical structures (p-21, Barrett, Dobbs and Roques, 2009) (Barrett, Dobbs and Roques, 2009). 3D-CRT treatment plans are optimised by changing treatment beam weighting, using wedges to compensate for body obliquity or increasing the number of beams and changing collimator angles. Target conformity increases in 3D-CRT plans compared to 2D plans (p-21, Barrett, Dobbs and Roques, 2009) (Barrett, Dobbs and Roques, 2009). However, delivering intended doses to target volumes can be limited due to the proximity of OAR volumes (p-21, Barrett, Dobbs and Roques, 2009) (Barrett, Dobbs and Roques, 2009). Furthermore, one of the limitations of this technique is that the dose to the OAR volume located in the groove region of a concave target volume sometimes cannot be reduced below the prescription dose unless target coverage is compromised (Cho, 2018; Maconachie *et al.*, 2019).

In 1982, the intensity-modulated radiotherapy (IMRT) planning technique was first proposed by Brahme et al (Cho, 2018). Since then, the use of IMRT in clinical practice has increased significantly and it has become a standard of care for treating a range of cancer sites. IMRT is a more complex form of conformal radiation therapy where dose conformity to the target, or more specifically dose to exclusion to the OARs, is achieved by using the beams with modulated intensity (Barrett, Dobbs and Roques, 2009) which adds to create exquisite dose distribution. Each IMRT field consists of multiple segments/beamlets shaped using MLC, whose individual intensities (defined by the associated monitor (MUs)) superpose within the overall irradiated field to produce the beam modulation.

IMRT can produce significantly more conformal dose distribution compared to 3DCRT (p-21, Barrett, Dobbs and Roques, 2009) (Barrett, Dobbs and Roques, 2009). In addition, IMRT can produce homogeneous dose distribution across PTV and achieve sharper dose fall-off at the PTV edge (Barrett, Dobbs and Roques, 2009). Sharper dose fall-off from the PTV boundary allows for a significant reduction of the volume of OAR receiving higher doses (p-23, Barrett, Dobbs and Roques, 2009) (Barrett, Dobbs and Roques, 2009). These features may allow dose escalation to target volume whilst keeping OAR doses in tolerance to improve treatment outcomes. Reduction in OAR doses reduces the complication rate and improves the quality of life (p-23, Barrett, Dobbs and Roques, 2009) (Barrett, Dobbs and Roques, 2009).

IMRT plans are delivered either in 'step and shoot' or dynamic techniques (p-145, Webb, 2015) (Webb, 2015). In 'step and shoot' treatments, the radiation beam is turned off whilst MLCs are moving to the next segment and between gantry rotations, whereas in dynamic delivery, the radiation beam is only off during gantry rotation (moving to the next planned position) (p-143, Webb, 2015) (Webb, 2015).

The Volumetric Modulated Arc Therapy (VMAT) was first introduced in 2007 (Teoh *et al.*, 2011), it is an even more complex strategy for dynamic delivery because the beam remains on during gantry rotation; gantry speed, dose rate and MLC speed change continuously during treatment delivery (Teoh *et al.*, 2011; Hoskin, 2012). VMAT plans can be more conformal compared to IMRT plans as there are more degrees of freedom (Teoh *et al.*, 2011; Hoskin, 2012). The total number of monitor units in VMAT plans are significantly lower compared to IMRT plans (Rana, 2013) which allow faster treatment delivery. However, a larger volume of normal tissues can be exposed to low radiation dose (i.e., increased low dose bath) in VMAT plans compared to IMRT and 3DCRT plans

due to the nature of delivery (i.e., arc delivery) (p-314, Gunderson and Tepper, 2015; p-60, Xia, 2018) (Gunderson and Tepper, 2015; Xia *et al.*, 2018).

Treatment plan optimisation: Treatment plans are optimised using forward planning or inverse planning depending on the treatment technique (p-8-9, Xia, 2018) (Xia *et al.*, 2018). In the forward planning technique, beam angle, aperture shape, beam weighting, wedge (if needed), and wedge angle are iteratively adjusted, by an experienced human, until the desired uniform dose to the target volume is achieved. 2D and 3D conformal plans are created using forward planning (p-8-9, Xia, 2018) (Xia *et al.*, 2018).

With the inverse planning technique, optimisation objectives are entered into a computer optimizer (i.e. the Treatment Planning System) with appropriate priorities (the optimiser assigns a cost function to each of the clinical goals to be achieved, based on constraints, priorities and weights. The cost function is a measure of how close the achieved dose distribution is to the desired dose distribution) to achieve optimal dose distribution for both IMRT and VMAT treatments (p-311, Gunderson and Tepper 2015; p-464 Winchester, 2006; p-12, 14, Xia, 2018) (Winchester *et al.*, 2006; Gunderson and Tepper, 2015; Xia *et al.*, 2018). Inverse plan optimisation is performed either directly or in two steps. In two-step optimisation, the optimizer generates an ideal fluence without taking the physical and mechanical limitations of the treatment machine (e.g. dynamic MLC (DMLC) and dose rate) into account and then the generated fluence is converted into an actual deliverable fluence using the leaf motion calculator within the treatment planning system (TPS) (p-8-9, Xia, 2018) (Xia *et al.*, 2018). The second step ensures that the fluence can be delivered but it could reduce the quality of the original fluence. In direct aperture optimisation, the aperture shapes and weights of beams or arcs are optimised simultaneously and MLC constraints (i.e., physics and mechanical parameters of the

treatment machine) are considered during the optimisation process. This method produces deliverable plans without losing the quality of plans (p-8-9, Xia, 2018) (Xia *et al.*, 2018).

In inverse planning, clearly defined planning objectives are extremely important, as any conflicting/competing objectives may result in an undesired effect on dose distribution (p-9-11, Xia, 2018) (Xia *et al.*, 2018). The optimiser then finds an optimal solution by minimising the cost function (p-9-11, Xia, 2018) (Tol *et al.*, 2015a; Xia *et al.*, 2018). The optimisation processes are done by the optimiser, whereas plan objectives are set by the human planner during optimisation. Higher objectives are set for PTV to achieve the desired coverage (e.g. at least 99% of PTV receives 95% of the prescription dose). Whereas, low dose objectives are set to limit the volume of PTV receiving higher (≥ 107% of the prescription dose) doses (e.g. at most 0% of PTV receives 107% of prescription dose). Similarly, OAR doses are limited by setting lower objectives. The quality of treatment plans depends on the plan objectives set during optimisation (p-11, Xia, 2018) (Xia *et al.*, 2018). Therefore, any variation in the plan objective setting by planners can increase variability in the plan dosimetry achieved. This highlights the importance of patient-specific optimisation objective setting during optimisation, as every patient's anatomy and target volume is different. Variations in plan quality between planners can be reduced significantly using knowledge-based planning techniques.

Knowledge-based planning: KBP methods have been developed to tackle challenges in radiotherapy and to improve quality and efficiency (Ge and Wu, 2019). Knowledge (i.e., dose distributions) gained from previously treated patients (i.e., past clinical plans) is utilised to predict achievable dose distributions for prospective patients (Schreibmann and Fox, 2014; Fogliata *et al.*, 2015b; Nwankwo *et al.*, 2015; Tol *et al.*, 2015b; Chang *et al.*,

2016; Delaney *et al.*, 2017; Powis *et al.*, 2017; Wang *et al.*, 2017; Wall, Carver and Fontenot, 2018). Mainly there are two approaches for KBP, the rule-based approach (also known as automated planning systems). This utilizes planning knowledge to automatically generate beam angle, optimisation structures and optimisation objectives to produce clinically acceptable plans (Zhang *et al.*, 2011b; Ge and Wu, 2019). The second is a data-driven method, where the knowledge is gained from retrospective clinical plans/data-sets to develop models predicting achievable treatment plans for prospective patients (Ge and Wu, 2019). The data (including anatomical information, dose distribution and arc parameter, biomarker, variation in day-to-day treatment setup, and anatomical changes during treatment) can be used effectively to develop KBP models. This thesis presents four knowledge-based planning models developed using linear regression and multivariate analysis. Patient-specific dose and volume information was collected and analysed to develop the models. The method used for each model is described in the following chapters. Several KBP models have been developed and evaluated for prostate and head and neck planning but it had not been fully explored for lung cancer patients (Schreibmann and Fox, 2014; Fogliata *et al.*, 2015b; Nwankwo *et al.*, 2015; Tol *et al.*, 2015b; Chang *et al.*, 2016; Delaney *et al.*, 2017; Powis *et al.*, 2017; Wang *et al.*, 2017; Wall, Carver and Fontenot, 2018). In addition, a commercial knowledge based KBP engine, the RapidPlan™, is available and being used clinically (Fogliata *et al.*, 2014b; Fogliata *et al.*, 2014a; Fogliata *et al.*, 2015b; Fogliata *et al.*, 2015a; Hussein *et al.*, 2016; Chin Snyder *et al.*, 2016; Fogliata *et al.*, 2017; Foy *et al.*, 2017). The RapidPlan™ is a statistical model that is produced from a library of high-quality clinical plans using principal component analysis (PCA) to identify the strongest co-relation between geometric and dosimetric features. The geometric features include the percentage overlap between the target volume and OAR and the dosimetric features include the

fraction of OAR receiving a given radiation dose. The model estimates DVH for the new patient, which could be achieved if the patient is planned using the same technique as the library plans. The model can also generate optimisation objectives to achieve the predicted DVH (Hussein *et al.*, 2016). However, RapidPlan software was not available in our clinic at the time of the study, and it has cost implications. In addition, the RapidPlan software cannot predict arc parameters or trigger adaptive radiotherapy or estimate dose escalation. Therefore, in-house knowledge-based planning models were developed in this thesis.

Dose calculations: Radiation doses are calculated using two different types of calculation algorithms, type A and type B (p-160, Jeremic, 2011) (Jeremic, 2011). The type A algorithm (e.g. pencil beam algorithm) is a simple calculation algorithm, relatively faster and does not require high computational power. However, these algorithms do not take into account varying lateral scatter produced from different-density tissues (p-160, Jeremic, 2011) (Jeremic, 2011). The type B algorithm (e.g. Monte Carlo, AcurosXB) requires higher computational power, relatively slow but accounts for lateral scatter generated from different-density tissues (p-160, Jeremic, 2011) (Jeremic, 2011). Type B algorithms are highly recommended for dose calculation where tissue heterogeneity is higher (e.g. lung), whereas, type A algorithms are only recommended for dose calculation in water-equivalent tissues (e.g. prostate) (p-143, Battista, 2019) (Battista, 2019).

Treatment plan assessment: The treatment plan or planned dose distribution is assessed qualitatively by reviewing doses on CT images and quantitatively on the dose-volume histogram (DVH). Although the DVH is a quick and effective tool to assess doses, it does not provide any spatial information (p-323, Hoskin, 2012) (Hoskin, 2012). Therefore, it is also important to review doses on planning scans (Figure 1.5). DVH is a

two-dimensional plot that summarises planned/simulated dose distribution to the volume of interest of a patient. (Figure 1.5). DVHs allow quantitative assessment of treatment plans, e.g., to assess if OARs exceed the tolerance doses or target achieves expected coverage (p-323, 326, Hoskin, 2012) (Neal and Hoskin, 2012; Hoskin, 2012). DVHs are generated only for volumes that are contoured in the planning system. In addition, DVHs can be used for comparing two plans by putting them on the same plot and this helps determine the optimal plan for an individual patient (p-323, Hoskin, 2012) (Hoskin, 2012).

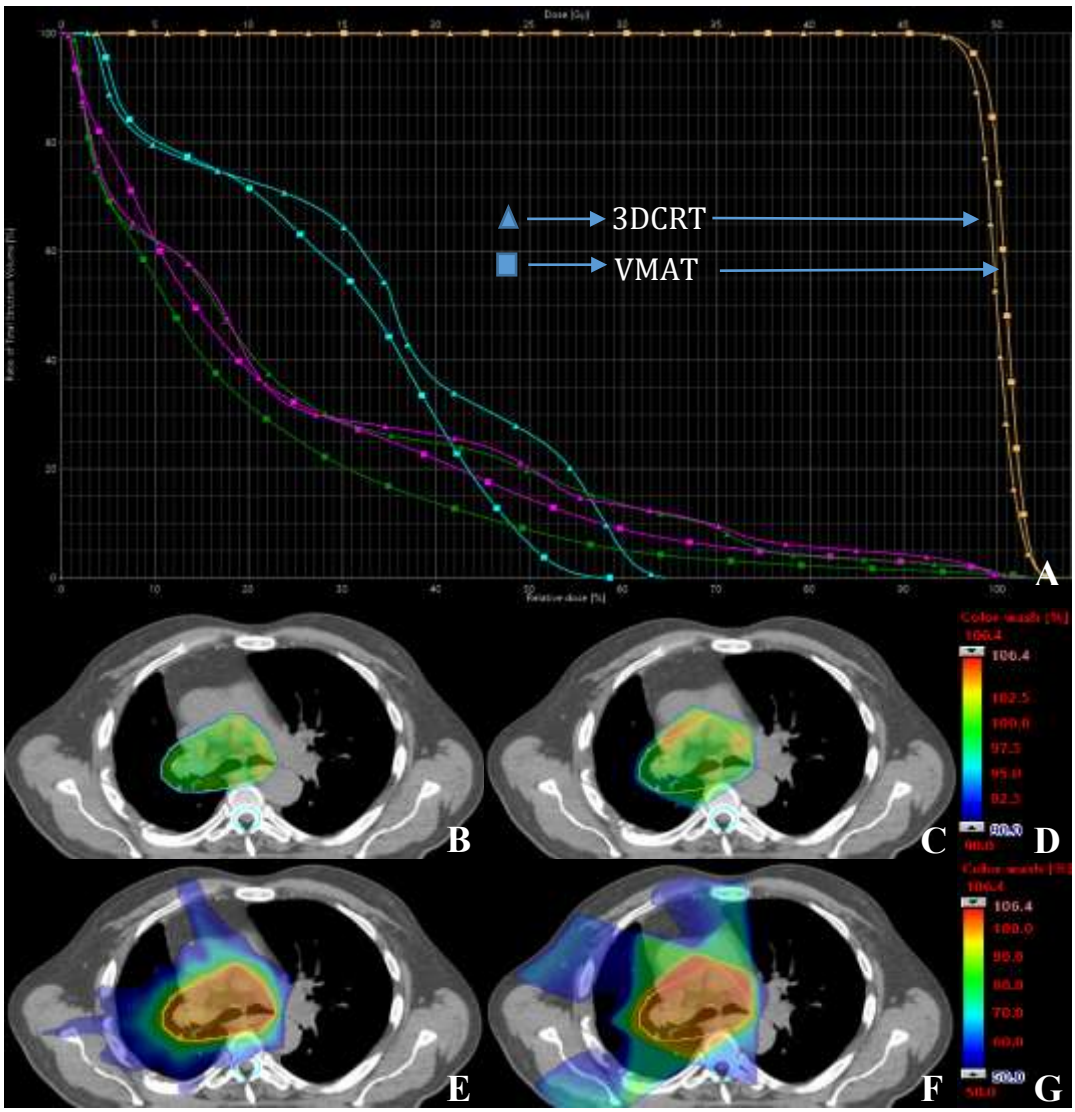

Figure 1.5: Comparing dose distributions produced by 3D CRT and VMAT plans.

Image A: dose-volume histogram (DVH) displaying lung (pink), spinal cord PRV (cyan), heart (green) and PTV (orange) curves for both 3DCRT (in a triangle) and VMAT (in square) plans. It can be seen from the DVH plot that VMAT (B and E) increases the volume receiving lower doses and reduces the volume receiving higher doses compared to the 3DCRT (C and F) plans. The axial slices show dose distribution in a colour wash display, B and C: colour wash with 90% dose threshold and E and F: with 50% dose threshold. It can be seen from these images that dose conformity is significantly higher in the VMAT plan (B and E) compared to the 3DCRT plan (C and F). D and G: dose legend scale.

***Plan check and patient-specific QA*:** At HUTH, following the plan approval, all plans are independently checked. In addition, due to the nature of the treatment technique (i.e., associated complexity of arc modulation), patient-specific quality assurance is performed for all patients to ensure that the treatment can be delivered as planned. In addition, the source of errors between planned and delivered doses can be identified by calculating complexity metrics. The higher the modulation/complexity, the greater the potential for error in the delivery. The level of modulation depends on dosimetric constraints used for optimising plans, patient-specific volumes, and optimisation algorithms. The plan complexity can be quantified using machine parameters and different plan properties, such as fluence, and MLC parameters: aperture, speed, position, dose rate, gantry speed, and MU (Olofsson, 2012; Crowe *et al.*, 2014; Younge *et al.*, 2016; Miften *et al.*, 2018; Chiavassa *et al.*, 2019). In this thesis, several plan complexity metrics are calculated and delivery measurements were performed for both the clinical and test plans to assess the deliverability.

Treatment delivery and image guidance: Image-guided radiotherapy (IGRT) has become a standard of radical treatment (The Royal College of Radiologists, 2008). Treatment is delivered in a fractionated regime. For each treatment fraction, patients are positioned on a linear accelerator couch in the same position as the treatment planning CT simulation (The Royal College of Radiologists, 2008). 2D (planar kV or MV) or 3D cone beam computerised tomography (CBCT) images are acquired prior to treatment delivery to confirm the treatment position (The Royal College of Radiologists, 2008). Pre-treatment CBCT images are compared/ matched with planning 3DCT images and the 2D planar images are compared with a digitally reconstructed radiograph (DRR) generated within the planning system (The Royal College of Radiologists, 2008).

Any errors in the position of a patient are corrected prior to treatment delivery. Locally, volumetric (CBCT) imaging is performed prior to each fraction for lung cancer patients. CBCT images display both soft tissues and bony anatomy whereas 2D planar images mostly display bony anatomy (Figure 1.6). Anatomical changes (internal or external anatomy) can be visualised in CBCT images, which help to assess if a patient required adaptive radiotherapy planning (ART). In ART, the treatment plan is adjusted to fit the anatomical changes seen in images (Bertelsen *et al.*, 2011). Recent development in onboard imaging technology allows performing 4D-CBCT, which enables assessing tumour motion prior to treatment delivery. In addition, CBCT images can be used to assess treatment response during treatment (Jabbour *et al.*, 2015).

Post-radiotherapy toxicities: OARs are categorised into serial and parallel organs (p-212, Hoskin, 2012) (Hoskin, 2012). Serial organs are organs where damage to a small part of the organ could result in loss of function (e.g. spinal cord), whereas for parallel organs damage to a small part of the organ only reduces the function of the organ as undamaged parts of the organ function normally (e.g. lungs) (p-212, Hoskin, 2012) (Hoskin, 2012). For serial organs, the dose limit is the maximum dose received by the organ, whereas for parallel organs dose limit is applied to the volume (e.g. mean dose). Therefore, target coverage (i.e. dose received by the target volume) is compromised near the serial organ to keep the dose within the tolerance limit (Tepper, 2020).

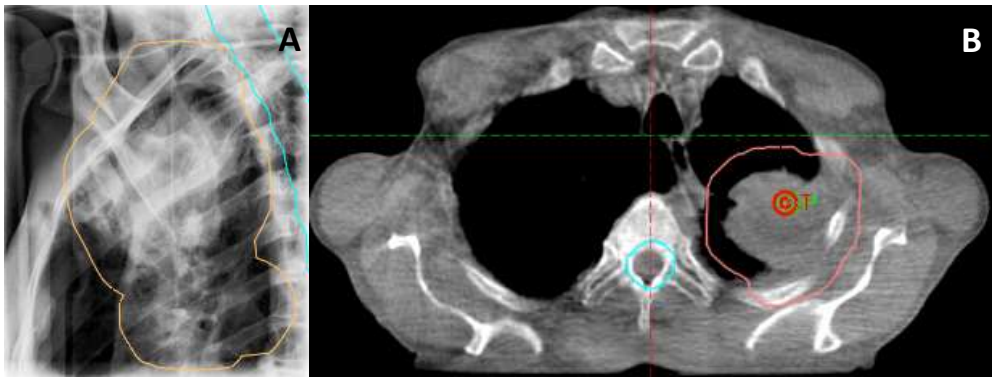

Figure 1.6: Images acquired on the treatment machine prior to the treatment delivery

Image A: is a planar image acquired with the gantry at 90^{o} and B: is a CBCT image with planning target volume (PTV) and spinal cord PRV (planning at risk volume) volume.

1.2.4 Radiotherapy for NSCLC

Radiotherapy is an important modality for the management of lung cancer as more than 40 – 50% of lung cancer patients require radiotherapy during their lifetime (p-27, Cox, Chang and Komaki) (Cox, Chang and Komaki, 2007; Chan *et al.*, 2014). Radiotherapy is used to cure primary lung cancer patients (also known as radical radiotherapy, p-377 Balci et. al., 2013), as well as to palliate symptoms (known as palliative radiotherapy, p-411 Balci et. al., 2013) (Balcı, 2013; Maconachie *et al.*, 2019). Radiotherapy is used primarily in combination with systemic treatment, and/or less frequently with surgery in various therapeutic sequences (Balcı, 2013; Maconachie *et al.*, 2019). However, in early-stage NSCLC, radiotherapy can be used as the mono-therapy with curative intent (p-378 Balci et. al., 2013) (Balcı, 2013; UK SABR Consortium, 2016; Boon *et al.*, 2017; Maconachie *et al.*, 2019; UK SABR Consortium, 2019).

***Selection of NSCLC patients for radiotherapy*:** Radical radiotherapy is indicated for patients with stage I to III NSCLC who have a WHO performance status of 0 or 1: (see Tables 1.1 and 1.2) (Maconachie *et al.*, 2019). Patients with better performance status may also be considered for radical (curative) radiotherapy (See Tables 1.1 and 1.2) after a careful assessment of lung function (Maconachie *et al.*, 2019).

***Treatment simulation for lung cancer patients*:** One of the challenges when treating lung cancer patients with radiotherapy is tumour motion due to breathing (p-134, Jeremic, 2011) (Jeremic, 2011). Significant tumour motion could lead to geometric miss (i.e., not treating the entire tumour volume due to motion), therefore, it is important to account for the tumour motion during radiotherapy treatment planning and delivery (p-134, Jeremic, 2011) (Jeremic, 2011). To account for tumour motion, lung cancer patients with regular breathing undergo four-dimensional (4D) CT scans (p-64, Cox, Chang and

Komaki) (Cox, Chang and Komaki, 2007). The 4D-CT scanning enables capturing tumour motion due to the respiratory breathing cycle (p-134, Jeremic, 2011; p-64, Cox, Chang and Komaki, 2007; p-256, Dieterich, 2015) (Cox, Chang and Komaki, 2007; Jeremic, 2011; Dieterich *et al.*, 2015). Patients with irregular breathing may not be suitable for 4D-CT as it could cause significant motion artefacts in the resultant scans and could affect target delineation (p-39, Ehrhardt and Lorenz, 2013) (Ehrhardt and Lorenz, 2013). Patients with irregular breathing undergo a traditional 3D-CT scan. During 4D-CT acquisitions, the patient's breathing cycle is monitored and recorded with Varian's respiratory gating for scanners (RGSC) system at HUTH. The RGSC system captures the breathing trace/ signal using external surrogates (e.g. infrared-reflective marker block position on the patient's chest/ abdomen) (see Figure 1.7) and the signal is stored in the database.

Following the completion of the scan, each breathing cycle is split into different phase bins (6 to 12 bins; 10 bins are used in our clinic) with respect to time, and the CT slices are sorted by bin (p-64, Cox, Chang and Komaki; p-256, Dieterich, 2015) (Cox, Chang and Komaki, 2007; Dieterich *et al.*, 2015). Each bin is reconstructed into a 3DCT data set (representing an equal percentage of the breathing cycle), resulting in ten 3DCT data sets for ten bins. In amplitude binning, the data are binned based on the amplitude within each breathing cycle. An average scan is produced using the binned images; the target structures contoured on phased images are transferred on to the average scan. This scan is used for treatment plan optimisation and dose calculation (p-34, Beets-Tan, Oyes and Valentini 2020) (Beets-Tan, Oyen and Valentini, 2020).

NSCLC target and OAR delineation at HUTH: For patients with a 4D-CT scan, GTV is contoured on selected phases (e.g. maximum inhale, maximum exhale or mid-phase) (see Figure 1.8A, 1.8D and 1.8K) ensuring full tumour travel is captured (p-35, Ehrhardt and

Lorenz, 2013) (Ehrhardt and Lorenz, 2013). CTV (0.6 cm for SCC and 0.8 cm for ADC), is also contoured on the corresponding phase images by applying a symmetric margin to account for microscopic spread (Giraud *et al.*, 2000; Ozyigit, Selek and Topkan, 2016; Maconachie *et al.*, 2019). For 4D-CT patient scans, the term CTV is not used and instead the term internal target volume (ITV: is the volume encompassing CTV, which takes into account the variation in position, shape and size of the CTV) is used, as this volume incorporates target motion (International Commission on Radiological Units, 1999; Ozyigit, Selek and Topkan, 2016) (Figure 1.9). The ITV may be modified such that healthy structures (e.g. vertebral body) are edited out if they are included inappropriately. The planning target volume (PTV) is produced by adding an isotropic margin to the ITV accounting for setup errors (e.g. ITV + 0.5 cm). For 3D-CT patients, the PTV is produced by applying large asymmetric margins to account for setup error and tumour motion, and in our clinic, we use 1.2 cm superior-inferior and 0.9 cm circumferentially.

In addition, organs at risk (OAR) volumes including lungs (i.e., lungs excluding GTV), heart, spinal cord, and spinal cord PRV are contoured on the averaged 4D-CT scan (a scan reconstructed using average pixel density from the binned data) by the planning staff. The PRV - planning organ at risk volume: includes a margin to compensate for setup variations similar to the PTV ensuring the critical tissues/ structures do not exceed the dose limit) (International Commission on Radiological Units, 1993; International Commission on Radiological Units, 1999). At HUTH, for lung cancer patients, the spinal cord PRV is generated by adding a 0.5 cm isotropic margin for setup errors to ensure the dose to the spinal cord does not exceed the acceptable limit.

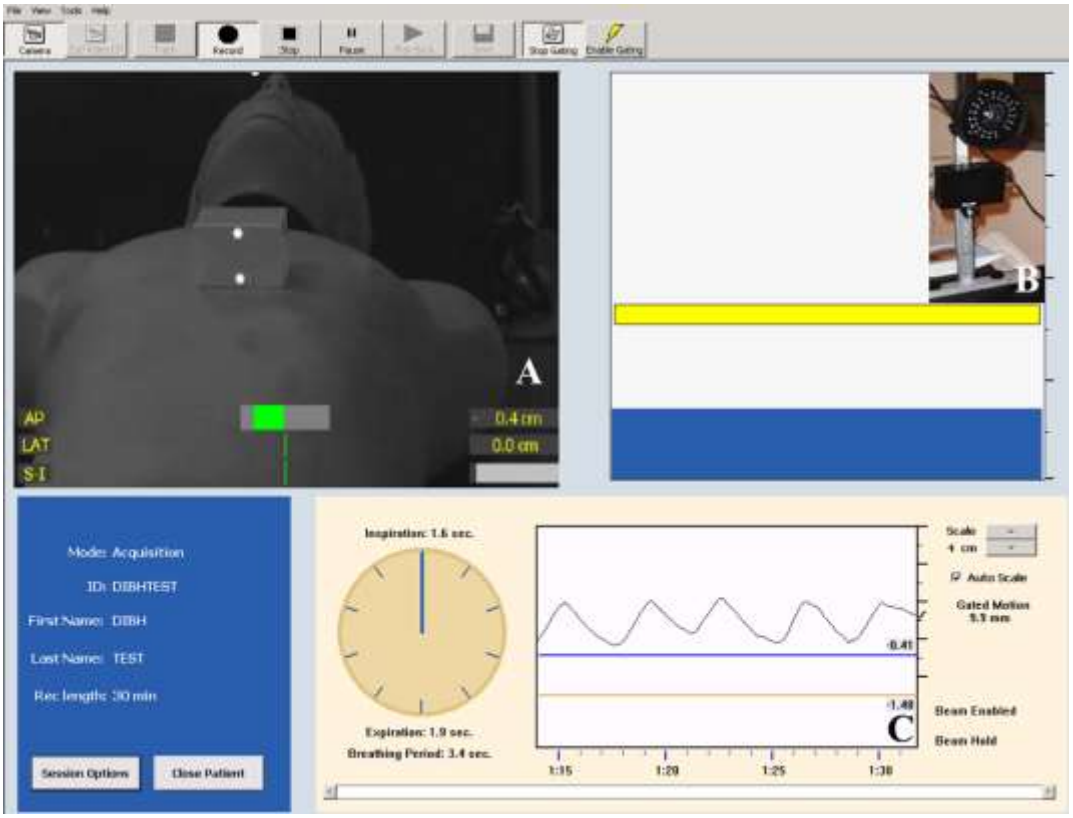

Figure 1.7: Varian's real-time positioning management (RPM) system

Image A showing an infrared marker block placed on the patient's chest and the infrared camera in image B records the real-time breathing trace shown in image C. The breathing trace is saved on a local RPM database and used to segregate the acquired CT data into the required number of bines.

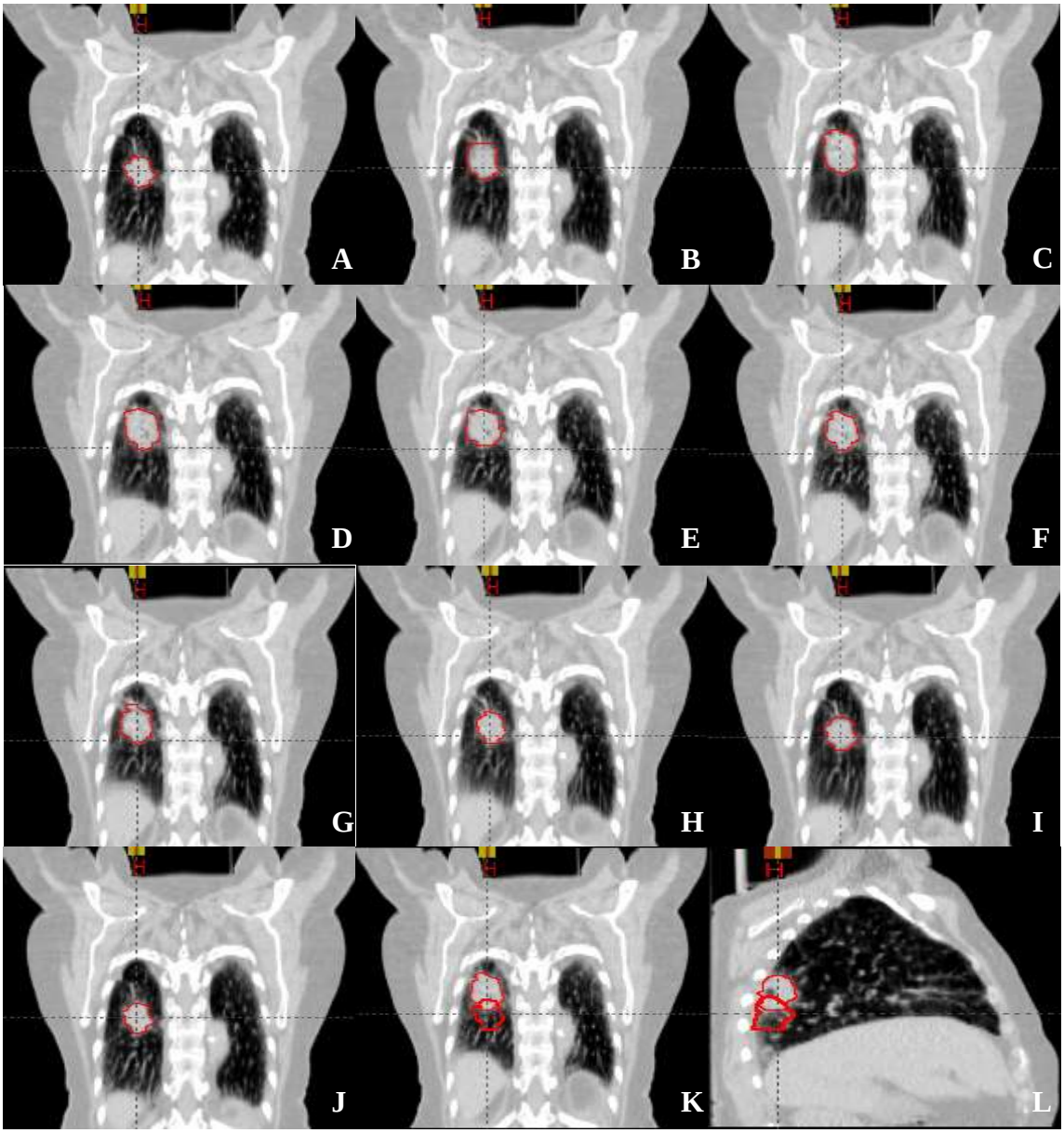

Figure 1.8: Tumour motion in a 4D-CT scan

Images shown are superior and inferior directions around cross-hair. The gross tumour volume (GTV) is shown in red. Locally, 4D-CT images are binned into ten phases, phase 0 to phase 90, images A to J correspond to phase 0 to phase 90 respectively and images K and L show the range of target motion observed in two different image planes within a patient. Images A-J are in coronal plane and Image K is in saggital plane

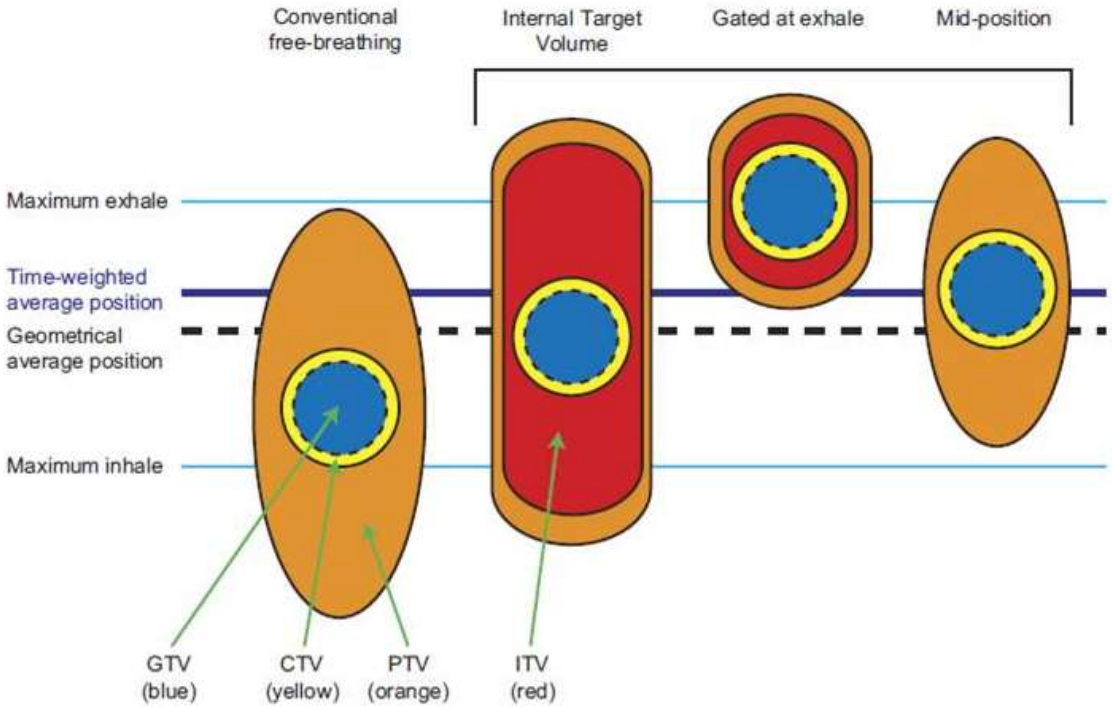

Figure 1.9: Illustration of different PTV volumes constructed following 3D- and 4D-CT scans (Wolthaus *et al.*, 2008)

The PTV volume is generated using a large margin for the patient undergoing a 3D scan to account for unseen target motion. A: conventional free-breathing; B: Internal target volumes (ITV) volume generated taking full target motion into account; C: ITV constructed using exhale phase; D: ITV constructed using mid-ventilation phase images.

Post-radiotherapy toxicities*:* Radiation-induced toxicities are divided into acute (early) and chronic toxicities. Acute toxicities generally occur within the first six months of the treatment, such as radiation-induced pneumonitis (RP). However, chronic (late) toxicities usually develop between six months to several years after treatment, such as lung fibrosis (Common Terminology Criteria for Adverse Events CTCAE v4.0) (p-213, Hoskin, 2012) (National Cancer Institute, 2009; Hoskin, 2012).

Lung toxicities: Patients with RP may present with shortness of breath, cough, congestion and low-grade fever (National Cancer Institute, 2009). Generally, patients with RP respond well to steroids, but severe RP can cause severe respiratory distress, may require hospitalisation and could result in death (p-114, Jeremic, 2011) (Berkey, 2010; Jeremic, 2011). Additional acute toxicities include pleuritic pain due to irradiation of the pleura, and cough due to irradiation to the trachea and bronchus (Berkey, 2010; Jeremic, 2011). These can be treated with anti-inflammatory, pain relief and cough medication (p-588, Jeremic, 2011) (Berkey, 2010; Jeremic, 2011). Pulmonary fibrosis is the most prominent late toxicity of thoracic irradiation (p-611, Jeremic, 2011) (Berkey, 2010; Jeremic, 2011). It causes radiological changes in the majority of patients and, in some patients, it could cause dyspnoea (p-332, Jeremic, 2011) (Berkey, 2010; Jeremic, 2011). Pulmonary fibrosis is irreversible, so the goal of treatment is symptom relief (p-312, Jeremic, 2011) (Berkey, 2010; Jeremic, 2011). This generally includes anti-inflammatory medication, although some patients may need oxygen (Jeremic, 2011). Rarely, the patient may get bronchial stenosis, bronchomalacia, and mediastinal fibrosis with recurrent laryngeal nerve injury (p-611, Jeremic, 2011) (Jeremic, 2011). The occurrence and severity of radiation toxicities are dose-dependent (p-598, Jeremic, 2011) (Jeremic, 2011).

Gastrointestinal (GI) toxicities: Other common toxicities include oesophageal toxicities with severe toxicities (e.g. grade 3 and 4) requiring IV fluids, tube feeding or total parenteral nutrition for more than 24 hours (p-640, 779, Jeremic, 2011) (Bentzen *et al.*, 2010; Jeremic, 2011). Symptoms are mostly managed with supplements, painkillers, or local anaesthesia (Bentzen *et al.*, 2010). In most of these patients, symptoms are relieved after treatment (Bentzen *et al.*, 2010; Jeremic, 2011). Rarely, late effects e.g. oesophageal stricture are seen (p-639, Jeremic, 2011) (Bentzen *et al.*, 2010; Jeremic, 2011).

1.2.5 Immunotherapy

A recent development in the management of lung cancer is the use of immune checkpoint inhibitors that help to reverse cancer immunosuppression and amplify antitumour immunity (Moya-Horno *et al.*, 2018). These include monoclonal antibodies directed against cytotoxic T-lymphocyte associated antigen-4 (CTLA-4) and programmed cell death protein (PD-1) and programmed cell death-ligand-1 (PD-L1) (Antonia *et al.*, 2017; Antonia *et al.*, 2018; Brahmer *et al.*, 2018; Paz-Ares *et al.*, 2020). A recent trial, PACIFIC, reported significant improvement in overall survival for the patients treated with adjuvant durvalumab immunotherapy in addition to concurrent chemo-radiotherapy (Paz-Ares *et al.*, 2020). Durvalumab is a human IgG1 monoclonal antibody that blocks PD-L1 binding to PD-1 and CD 80 (ligand of CTLA-4) allowing T cells to recognize and kill the tumour cell (Antonia *et al.*, 2017; Antonia *et al.*, 2018; Brahmer *et al.*, 2018; Paz-Ares *et al.*, 2020). This has become a new standard of treatment for inoperable advanced-stage NSCLC patients with good performance status (Antonia *et al.*, 2017; Antonia *et al.*, 2018).

1.3 Aims and objective of the thesis

Treatment of lung cancer patients with radiotherapy has evolved significantly, including the use of IMRT/ VMAT (Chan *et al.*, 2011; Abo-Madyan *et al.*, 2014; Diwanji *et al.*, 2017), the development of gated radiotherapy systems (Wolthaus *et al.*, 2008), and development of type B dose calculation algorithms for accurate dose calculation (Knöös *et al.*, 2006). However, personalised optimisation of treatment plans has not developed fully and still has scope for further development. This thesis aims to address some of these gaps in the field, including the themes noted below.

Aim and objectives of the thesis: The key aim of this thesis is to use patient-specific information determined from treatment plans and the knowledge gained from the patient population to personalise optimisation when planning individual patient treatments.

Overarching hypothesis: Data characterising patients can be used to find the most optimal plans for advanced-stage inoperable non-small cell lung cancer patients treated with volumetric modulated arc therapy.

This thesis will examine various ways to personalise and optimise lung cancer radiotherapy, as follows:

1.3.1 Reducing variability in treatment plans: Treatment plans produced by different human planners can increase variability (i.e. variability is the difference between the achieved OAR dose and the minimum dose that could be achieved for an individual patient) in treatment plans. Variability is caused by things such as the planner's experience, subjective plan optimisation preferences and clinical workload. Larger variation in achieved OAR doses could increase toxicities

especially when the achieved doses are significantly larger than the minimum achievable doses. The variability in treatment plans can be reduced using knowledge-based planning (KBP) models (Fogliata *et al.*, 2015b; Chang *et al.*, 2016; Wang *et al.*, 2017). The KBP models can predict minimum achievable OAR doses prior to treatment plan optimisation based on individual patients' anatomy. The planner can aim to achieve the predicted doses during the plan optimisation process. This helps reduce variability in the achieved doses and improves overall treatment plan quality. A reduction in OAR doses could reduce post-treatment toxicities and improve patients' quality of life.

Specific Aim 1*: to reduce variability (i.e. to reduce the difference between the achieved OAR dose and the minimum dose that could be achieved for the individual patient) in treatment plans produced by planners with varying degrees of experience.*

Chapter 3 discuss the method and results of the KBP model developed locally.

1.3.2 Personalising VMAT arc geometry: multimodality treatment has become the standard of treatment for the management of lung cancer patients (Maconachie *et al.*, 2019). Patients with pre-existing co-morbidities are generally not suitable for surgery so radiotherapy with and without chemotherapy is the standard of treatment for these patients (Maconachie *et al.*, 2019). In addition, many chemotherapy drugs have associated pulmonary toxicities (Rancati *et al.*, 2003). Therefore, reducing OAR radiation dose is important to limit toxicities and improve the quality of life of the patient. In addition, advanced radiotherapy techniques such as VMAT increase the OAR volume receiving lower doses and a number of studies have reported that lower doses are also associated with fewer toxicities (Wang *et al.*, 2006; Khalil *et al.*, 2015). Both the rate and severity of

toxicities increase with the volume of OAR receiving lower radiation doses. Therefore, reducing OAR doses is crucial. Numerous alternative planning techniques have been studied to reduce lung doses; these techniques have reduced lung doses but resulted in an increase in heart doses (Mayo *et al.*, 2008; Dumane *et al.*, 2010; Chan *et al.*, 2011). Furthermore, some studies reported increases in treatment time (mainly due to the use of the step-and-shoot IMRT technique). It is, therefore, essential to develop a planning technique that reduces both lung and heart doses and treatment time without compromising target coverage.

Specific Aim 2*: to investigate if OAR doses can be reduced by personalising VMAT arc geometries for treating advanced-stage NSCLC patients, with curative intent, without compromising target coverage. Secondly, to develop and validate a knowledge-based planning model to predict arc geometry based on individual patient geometry.*

Chapter 4 demonstrates a method developed locally and the results.

1.3.3 Personalising adaptive radiotherapy: anatomical changes during radiotherapy treatments are inevitable and significant changes could alter planned dose distribution and affect treatment outcomes. Numerous publications recommend adapting treatment plans halfway through the treatment or twice during the treatment (Guckenberger *et al.*, 2011; Kataria *et al.*, 2014). However, different patients respond differently to treatment and as seen before the treatment regime (i.e. combination of treatments) differs between patients so a 'standard' approach may not be suitable for the patient population. Furthermore, adapting every plan once or twice during treatment may not be necessary and could increase the

clinical workload significantly. It is, therefore, important to investigate methods to identify the patients who would benefit from ART.

Specific Aim 3*: To investigate optimal adaptive strategies for the treatment of inoperable locally advanced NSCLC patients treated with VMAT and to develop knowledge-based models for identifying patients requiring ART.*

Chapter 5 discusses different ART methods and the method developed locally and the results.

1.3.4 Personalised and progressive adaptive dose escalation to adapted GTV: A number of clinical studies have reported that dose escalation improves local control and overall survival (Rengan *et al.*, 2004; Kong *et al.*, 2005; Rosenzweig *et al.*, 2005; Lee *et al.*, 2006; Gillham *et al.*, 2008; Nielsen *et al.*, 2014; Ramroth *et al.*, 2016; Fleming *et al.*, 2016; Fleming *et al.*, 2017; Higgins *et al.*, 2017; Tekatli *et al.*, 2017). However, dose escalation for locally advanced lung cancer patients could be challenging due to the proximity of OAR volumes. The alternate method has been investigated, this includes inhomogeneous dose escalation (i.e., dose escalation to GTV) by (Nielsen *et al.*, 2014). Although this method allows safer dose escalation (i.e., without increasing OAR doses significantly), further methods, e.g. progressive dose escalation to adapted GTV, could significantly increase target doses and improve survival.

Specific Aim 4*: To determine if GTV dose can be escalated continuously during the course of treatment and to develop a knowledge-based planning model to determine achievable dose escalation for inoperable locally advanced stage NSCLC patients treated with curative intent.*

Chapter 6 of this thesis discusses a feasibility study investigating continuous dose escalation to adapted GTV whilst delivering prescription doses to PTV.

2.0 General Materials and Methods

This chapter describes the generic methods used for simulation, contouring, planning, and patient-specific quality assurance testing for advanced-stage non-small cell lung cancer patients in our centre. Methods specific to the different studies have been described in the relevant chapters.

2.1 Patient data background and data storage plan

At the Medical Physics department at Hull University Teaching Hospitals NHS Trust, all studies/projects performed using retrospective patient data do not require additional Health Research Authority (HRA) or ethics committee approval; permission has been granted by our local R&D committee to use this data as long as certain local governance commitments are met. Patients' data security is very important and it is recommended to store the data securely, such as within the hospital network, and all patients' data used in this study were stored securely within the hospital oncology network that operates within the hospital's hardware firewall protection. Patients' CT and CBCT images are stored on Onc-ARIA image network and demographics and plan data are stored on Onc-ARIA DB database. The data is backed up using VEEAM® backup and recovery software. All the test plans produced were saved separately from the clinical course and named clearly so that they can be easily identified.

2.2 Data acquisition, treatment simulation, and contouring

In our clinic, lung cancer patients capable of breathing regularly undergo a four-dimensional computerised tomography scan (4DCT) (as well as a free-breathing (FB) scan). Those with irregular breathing simply undergo the FB (3DCT) scan. The 4DCT scans are binned into ten temporal phases and the gross tumour volume (GTV) is

contoured on at least three binned phases (i.e., max-inhale, max-exhale, and mid-phase) ensuring full tumour motion is captured. These individual phase GTVs are accumulated onto the free-breathing (FB) scan and their union/ combination is used to describe the 4D-GTV. The organs at risk (OAR) volumes are also contoured on FB images. The FB scan is used for treatment plan optimisation and dose calculations. The ITV (4DCT) / CTV (3DCT) are produced by expanding the 4D-GTV/ GTV with isotropic margins (see Figure 1.9), to account for the microscopic spread, of 0.6 cm for squamous cell carcinomas and 0.8 cm for adenocarcinomas respectively. The PTV is produced using a 0.5 cm isotropic margin from ITV for 4D patients, whereas, for 3DCT patients, PTV is produced by applying 0.9 cm circumferential and 1.2 cm superior and inferior margins to the CTV.

2.3 Treatment planning

All patients included in the study were planned with RapidArc®/ VMAT (volumetric modulated arc therapy) using the EclipseTM treatment planning system (Version 13.7, Varian Medical Systems, Palo Alto, CA) with 6MV (flattened) beams. Two partial arcs for both right- and left-sided tumours were used, and direct beam entry through the contralateral lung was avoided in each case to minimise the dose received by it. The planned dose was calculated using the Acuros® algorithm (dose to water) with a uniform dose grid of 0.25 cm. The prescribed dose for patients included in the study was 55 Gy in 20 fractions. Treatment plans were optimised to meet the planning goals as described in Table 2.1.

The normal tissue objective (NTO) function was used to limit the dose to healthy structures with the same priority as the PTV. The NTO has the same purpose as a ring structure when optimising treatment plans. The NTO is a function available in the Eclipse planning system which reduces the dose to healthy tissue surrounding the target volume

as a function of distance from the PTV's outer border (Olofsson, 2012; Indrayani *et al.*, 2022). There are two types of NTO functions available in the Eclipse planning system, automatic/ default setting utilizes vendor-defined formula and the limits, (i.e., distance from target border 1.0 cm, start dose 105 %, end dose 60 % and fall-off 0.05) with priority set to a locally determined value of 300. Whereas in the manual NTO setting, the planner defines the limits. NTO is mathematically defined as a function f(x) at a distance x from the PTV border (Indrayani *et al.*, 2022).

$$f(x) = \begin{cases} -f_o e^{-k(x-x_{start})} + f_\infty(1 - e^{-k(x-x_{start})}), & x \geq x_{start} \\ f_o, & x < x_{start} \end{cases} \qquad \textbf{Equation 2.1}$$

f_o is the start dose - i.e., the upper constraint that should not be exceeded by dose outside the PTV volume; f_∞ is the end dose – i.e., the minimum dose constraint that is accepted by areas outside the PTV region; k is the dose fall off – i.e., the strength of dose decrease and affecting the location of end dose, f_∞,; and x_{start} is the distance from the PTV border (Indrayani *et al.*, 2022).

Table 2.1. Treatment planning clinical objectives and wish-list (planning goals) are used for planning advanced-stage NSCLC patients at our clinic. Wish-list priorities were generated following the recommendations from lung clinicians at HUTH.

	Clinical objective		**Constraints**
	Spinal Cord PRV	Max Dose	≤ 50Gy / 45Gy for 55Gy/20# (Mandatory)
	PTV	$V_{95\%}$	≥ 95%
		Max (1.8cc)	≤ 107% of the prescription dose
	Lungs-GTV	V_{20Gy}	≤ 35%
		V_{5Gy}	≤ 60%
	Heart	Mean dose	≤ 26Gy
		V30Gy	≤ 46%
Wish-list priority	PTV	$V_{95\%}$	≥ 99%
	Lungs-GTV	V_{5Gy}	< 60%
		V_{20Gy}	≤ 30%
	Heart	Mean Dose	≤ 20Gy
		V_{30Gy}	≤ 30%
	Spinal Cord PRV	Max Dose	≤ 45Gy / ≤ 40Gy for 55Gy/20#
	Lungs-GTV	V_{20Gy}	As low as possible
		V_{5Gy}	As low as possible
	Heart	Mean Dose	As low as possible
		V_{30Gy}	As low as possible
	Spinal Cord PRV	Max Dose	Max (As low as possible)

2.4 Data collection

The clinical data for the entire patient cohort is archived daily in our local database. For the studies, retrospective patient data used included planning CT images, structure set, treatment plan data, and treatment images (i.e., CBCT images acquired prior to treatment delivery) for NSCLC patients treated with radical intent between 2015 to 2018. The patient demographics are reported in Table 2.2.

- A total of 80 (40 to build and 40 to validate) patient data sets were randomly selected and used to build and validate knowledge-based planning models.

- 30 patients' data sets were used to develop and validate our knowledge-based planning model to predict optimal arc geometry for inoperable NSCLC patients treated with VMAT.
- 25 patients' data sets were used to determine and verify our knowledge-based planning model triggering adaptive radiotherapy and finally.
- 11 patients' data sets were used to determine personalised and progressive adaptive dose-escalation methodology and knowledge-based planning models estimating dose escalation to adapted GTV.

Table 2.2: Demographics of patients included in this thesis.

	Mean/Frequency/Range
Mean age (SD)	70.37 (6.72) Years
Gender	38 Male/ 42 Female
Laterality	48 right/ 32 left
Location	26UL*/31ML†/23LL‡
Staging	T1N1/T4N3
PTV volume (cc) range	161.0 – 707.0
Lungs volume (cc)# range	1926.7 – 6267.7
Heart volume (cc) range	301.5 – 1110.4

Total lung volumes subtracted from GTV, *UL: upper lobe, †ML: middle lobe, ‡LL: lower lobe.

2.5 Treatment verification

At our clinic, all radical lung patients undergo CBCT imaging prior to every fraction to verify their position. Deviation in the patient's position could lead to geometrical misses and/or could significantly alter the planned dose distribution and affect treatment

outcomes. Deviations in patient position (in the lateral, longitudinal and vertical direction) are corrected prior to treatment delivery.

The pre-treatment CBCT images were processed within the Velocity adaptive radiotherapy software (Varian Medical Systems, Palo Alto, CA) to produce synthetic CT (sCT) images. The sCT images were used to develop a knowledge-based planning model for triggering adaptive radiotherapy (see Chapter 5) and also to study adaptive dose escalation for advanced-stage in-operable NSCLC patients treated with VMAT (see Chapter 6).

2.6 Production of synthetic CT (sCT)

Anatomical changes are inevitable during radiotherapy and could affect the delivered dose distribution, to be significantly different to that planned (and therefore assumed delivered) and therefore treatment outcomes. To overcome this, adaptive radiotherapy is recommended where the planned treatment is updated throughout the course of the treatment to match the anatomical changes and the patients undergo a full re-planning process, (i.e., simulation, based on a planning CT, contouring, treatment plan optimisation, plan check and QA). However, this significantly increases clinical workload especially when anatomical changes are not significant and adaptive radiotherapy may not actually prove beneficial. To avoid the need to acquire a new planning CT and therefore improve efficiency, commercial adaptive radiotherapy software can be used where pre-treatment CBCT images are processed to produce synthetic CT scans (sCT) that include anatomical information from the CBCT images and Hounsfield Units (HU) from the planning CT scan (see Figure 2.1). In this thesis, Velocity (V4.0, Varian Medical Systems) adaptive software was used and sCTs were produced for all the treated fractions for the patients included in the study.

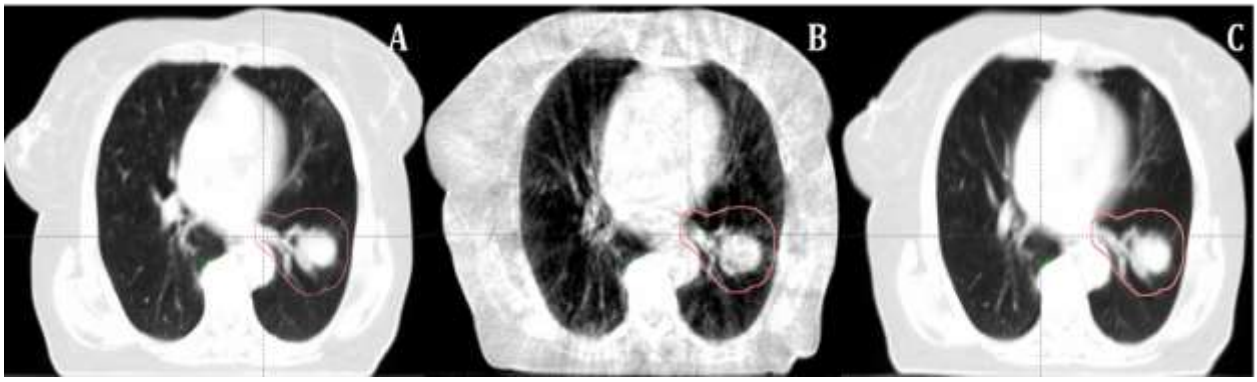

Figure 2.1: Planning CT image (A), cone beam computerised tomography (CBCT) image (B) and a synthetic CT image produced within the Velocity software (C).

The CBCT image (B) includes artefacts due to discrepancies between the mathematical modelling and the actual physical imaging process (Schulze *et al.*, 2011) so the HU are significantly different from the planning CT image (A). Both artefacts and the HU are updated in the synthetic CT image (C). This is required for accurate dose calculations.

To facilitate the image processing within the Velocity software, the following process was undertaken:

1. The planning CT (pCT) and CBCT images were initially rigidly registered using the same transformation obtained during the respective treatment session, to remove the impact of residual setup errors (Wang *et al.*, 2020a).

2. The setup corrected CBCT images were deformably registered to the pCT images excluding the most superior and inferior slices (as these slices do not include full anatomy due to the divergence of the cone beam) to produce a synthetic verification image set (sCT).

3. A secondary structure data set was produced in the sCTs, including GTV and organs at risk (OAR) volumes. The registration and volumes for each sCT were reviewed by experienced physicists and clinical oncologists (any uncertainties with the target and the OAR contours can be reduced by peer-review of the contours as recommended by the RCR (The Royal College of Radiologists, 2022)). The volumes were edited where required, target volumes by clinical oncologists and OARs by a physicist.

2.7 Plan complexity and deliverability

Treatment plan complexity depends on the total number of MU and the level of modulation within a plan. Simpler treatment plans (i.e. lower MU, less modulated with larger leaf pair opening) are preferable as these are relatively less dependent on MLC motion/position accuracy during delivery (Olofsson, 2012). Highly complex plans generally have a higher number of MU, which increase treatment delivery time, increase

the dose to the patient - due to MLC transmission - and are more susceptible to interplay effects (Younge *et al.*, 2016).

A number of treatment plan complexity metrics were calculated both for the original plans as well as the test plans (see Table 2.3).

Small aperture score (SAS: calculated as the ratio of open leaf pairs where the aperture was less than a defined criterion to all open leaf pairs (Crowe *et al.*, 2014)) were calculated using a locally developed script, see equation 2.2. The effect of change in optimisation technique on plan complexity was assessed.

$$SAS(x)beam = \sum_{i=1}^{1} \frac{N(x > a > 0)i}{N(a > 0)i} \times \frac{MUi}{MUbeam} \qquad \textbf{Equation 2.2}$$

where *x* is the aperture criteria, *i* is the number of segments in the beam, *N* is the number of leaf pairs not positioned under the jaw, and a is the aperture distance between opposing leaves (Crowe *et al.*, 2014).

Table 2.3. Plan complexity metrics were calculated for both original clinical plans and the test 'optimal' plans.

Complexity metrics	Description
MUperGy	Number of monitor units per Gy
MUPerDegree	Number of monitor units per degree of the arc
MeanDoseRate	Mean dose rate of the radiation beam
MeanLeafSpeed	Mean speed of multi-leaf collimator (MLC)
MeanLeafTravelPerMU	Mean leaf travel per MU
FractionMUthrough<5cc	Fraction of the total MU delivered through MLC segments less than 5 cc (cubic centimetre) in size
IslandsPerCP	A total number of islands per control points
MeanIslandSize	Mean island size
FractionIslandBelow1cc	A total number of islands below 1 cc as a fraction of total islands
SAS02 **SAS05** **SAS10** **SAS20**	Small aperture score (SAS: calculated as the ratio of open leaf pairs where the aperture was less than a defined criterion to all open leaf pairs (Crowe *et al.*, 2014)); here the defined criteria is 2 mm, 5 mm, 10 mm and 20 mm.

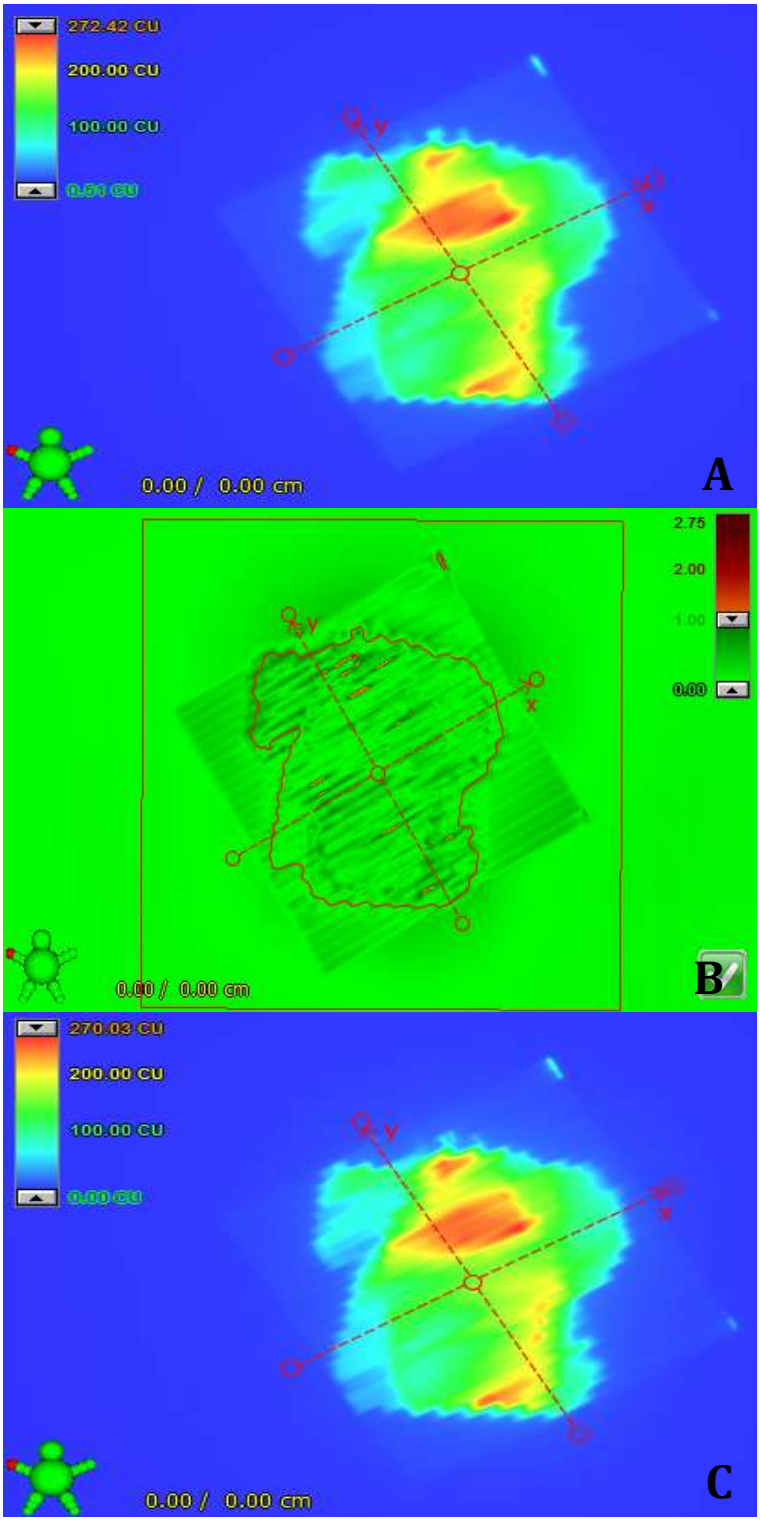

Figure 2.2: Illustrating portal dosimetry predicted (A) and measured (C) images. Image B is a comparison of predicted and measured images using the gamma criteria used locally. Image C is acquired on a TrueBeam linear accelerator using EPID. The image analysis was performed in portal dosimetry software within the Eclipse planning system (V 15.6).

Furthermore, to evaluate the effect of change in optimisation technique on treatment plan deliverability, portal dosimetry measurements were performed on a TrueBeam linear accelerator for all test plans and gamma analysis was performed using our standard clinical criteria (i.e., percentage of pixels where gamma is less than 1 using the criteria of 3%/2 mm with a threshold of 20%) by comparing predicted fluence with the measured fluence. The fluence for each beam was measured using an electronic portal imaging device (EPID) and compared in the portal dosimetry software within the Eclipse™ planning system (see Figure 2.2).

2.8 Statistical analysis

Treatment plans produced using different methods were compared with the original clinical plans and statistical differences between the original and the test plans were calculated using Student's t-test. The normality of data was tested with Kurtosis analysis (p-442, Reinard, 2006) (Reinard, 2006) before the t-test. p values < 0.05 were considered statistically significant. This analysis was performed in Excel (Microsoft office 2016).

3.0 Validation of locally developed knowledge-based planning models for predicting minimum achievable lung dose-volume matrices for patients treated with VMAT

The research in this chapter was published in a peer-reviewed journal and therefore the text presented here is adapted from the article. My contribution consisted in conceptualising the research strategy, performing the research and writing the manuscript with input from my supervisors on designing and planning the work and editing the manuscript. Reference: Tambe, N. S.; Pires, I. M.; Moore, C.; Cawthorne, C.; Beavis, A. W., Validation of in-house knowledge-based planning model for advance-stage lung cancer patients treated using VMAT radiotherapy. Br J Radiol 2020, 93 (1106), 20190535".

3.1 Introduction

Technological advancements in radiotherapy planning and delivery techniques, such as volumetric modulated arc therapy (VMAT), have allowed the reduction of dose to critical structures whilst maintaining target coverage (Mayo *et al.*, 2008; Oliver *et al.*, 2009; Rosca *et al.*, 2012). Nevertheless, achieving the lowest possible organ-at-risk (OAR) doses for a given patient geometry remains challenging as there are large population variations in OAR and target structure geometries (Nelms *et al.*, 2012; Batumalai *et al.*, 2013). Several studies have reported large heterogeneity in treatment plans produced by human planners with different levels of experience (Nelms *et al.*, 2012; Batumalai *et al.*, 2013; Moore *et al.*, 2015; Berry *et al.*, 2016). A treatment plan meeting OAR constraints and with adequate target coverage may still be considered suboptimal if it is possible to reduce OAR doses further without compromising target coverage.

To reduce variability between planners, different knowledge-based planning (KBP) methods have been implemented. KBP utilises prior patients' geometries, plans, and resultant dosimetric coverage to estimate the lowest achievable OAR doses for prospective patients prior to treatment plan optimisation (Fogliata *et al.*, 2014a). KBP offers several benefits including improvements in treatment plan quality, reduction of inter-observer variability and improvement of treatment planning efficiency (Fogliata *et al.*, 2015b; Chang *et al.*, 2016; Wang *et al.*, 2017). In addition to OAR dose prediction, KBP methods have also been used successfully to determine optimal gantry angles for IMRT patients (Pugachev and Xing, 2002; Zhang *et al.*, 2011b).

A number of different metrics have been explored for predicting OAR doses prior to treatment plan optimisation. The most commonly used metric is an overlap volume histogram (OVH: it is a 2-dimensional (2D) curve that describes the geometric relationship, such as distance, shape and relative location between PTVs and OARs volumes. The 2D curve shows the ratio of PTV within and outside OAR volume) to characterise the 3D spatial relationship between an OAR and a target (i.e., PTV) (Wu *et al.*, 2009; Kazhdan *et al.*, 2009; Wu *et al.*, 2013). Other metrics can include an overlap of OAR volume with target structure(s) (Hunt *et al.*, 2006), OAR volume within and outside a target structure (Yuan *et al.*, 2012) and similarity coefficient between retrospective and prospective patients' geometry (Schreibmann and Fox, 2014).

KBP methods have been largely used for prostate and head and neck planning (Zhu *et al.*, 2011; Fogliata *et al.*, 2014a; Tol *et al.*, 2015b; Powis *et al.*, 2017). However, only a limited number of studies have reported its benefit for lung cancer patients (Fogliata *et al.*, 2014a; Cui.W *et al.*, 2015). A study performed by Fogliata *et al* utilised commercial software (Varian's RapidPlan™) for VMAT lung planning and reported that the

RapidPlan™ KBP model facilitated achieving the desired clinical constraints in 4% more patients compared to the plans produced without a model (Fogliata *et al.*, 2014a). Cui *et al* produced an in-house model for predicting lung doses using a line of best fit to the data for patients treated with IMRT fields (Cui.W *et al.*, 2015). In this study, fifteen ring structures from the planning target volume (PTV) were produced and the overlap of lungs with each of the rings was used to determine V_{10} (i.e. volume receiving 10 Gy), V_{20} and V_{30}. Furthermore, Zawadzka *et al* developed an in-house model to predict the minimum achievable mean lung dose (MLD) for a given geometry (Zawadzka *et al.*, 2017). They predicted MLD using the dose calculated from 36 equidistance fields.

At the time of writing, none of the studies in the literature includes predictions of minimum achievable V_5 (percentage of lungs receiving ≥ 5 Gy dose) and minimum achievable V_{20} for lung cancer patients treated with VMAT. V_5 is a valuable metric as it has been widely reported as a predictor of radiation pneumonitis for advanced-stage lung cancer patients, not limited to only mesothelioma patients (Wang *et al.*, 2006; Oh *et al.*, 2009; Zhuang *et al.*, 2014; Ren *et al.*, 2018). V_5 constraints are routinely used at our institution for all advanced-stage lung cancer patients therefore a KBP modelling study involving this metric has been of particular interest to our department and would be a useful addition to the literature.

Therefore, the aim of this study was to reduce variability (i.e. to reduce the difference between the achieved OAR dose and the minimum dose that could be achieved for the individual patient) in treatment plans produced by planners with varying degrees of experience.

3.2 Methodology

In order to do this, in-house KBP models were developed for inoperable advanced-stage NSCLC patients to predict minimum lung dose constraints for V_5, V_{20}, and MLD for a given patient geometry. Combinations of volumes and dose-volume histogram (DVH) were used to build the models on a trial-and-error basis. Of note is the fact that treatment plans optimised using the lower bound model (i.e., a model that predicts the lowest achievable doses for given geometry) to achieve the lowest OAR doses could produce highly modulated plans, thereby increasing uncertainties in treatment delivery as compared to the plan optimised without the model. Furthermore, any error in treatment plan delivery could significantly alter delivered dose distributions, especially within high-dose gradient regions. Therefore, an important objective of our study is to verify the treatment delivery accuracy of plans produced using KBP models and compare it with the respective delivery accuracy of plans optimised without the model so that an optimal trade-off between lower OAR dose and plan delivery can be established. In the present study, the produced treatment plans were verified using treatment planning and measurements on the TrueBeam™ (V2.5 Varian Medical Systems, Palo Alto, CA) linear accelerator which is a novel approach not yet reported in the KBP field.

A total of forty pre-existing, clinically accepted, treatment plan datasets from our database were selected randomly and used to build the models in this study. All plans were calculated with the Acuros algorithm within the same version of the Eclipse planning system. Volumes (in cubic centimetres (cc)) for numerous structures including gross tumour volume (GTV), PTV, lungs (lungs minus GTV), PTV outside lungs, an overlap of lungs with PTV, lungs volume cropped back from the PTV by 1 to 5 cm (with 1 cm increment) and field size were collected. These volumes were selected on a trial-and-

error basis, and additional volumes were added/considered when a poor correlation between the volume and dosimetric metrics was observed. Dosimetric parameters, percentage of lungs volume receiving ≥ 5 Gy (V_5), V_{20}, and MLD were collected from the Eclipse treatment planning system for the above.

3.2.1 Development of KBP Model

To determine suitable volumes (including the ratio of different volumes (e.g. Lungs/PTV)) for our KBP model, correlation coefficients (R^2) of all collected volumes with the dosimetric data (i.e., V_5, V_{20}, and MLD) were determined. The commonly used parameters (i.e., overlap volume histogram) and several volumes (e.g. lungs, PTV, lungs within PTV etc) showed a very poor positive correlation. Finally, the residual lung volume ($Lung_{Residual}$) was calculated using equation 3.1.

$$Lung_{Residual} = \frac{(V_2 - V_1)}{V_2} \qquad \textbf{Equation 3.1}$$

where V_2 is total lung volume excluding GTV and V_1 is the total lung cropped back from PTV by 5 cm (V_1: Lungs5cmCrop – volume was produced by cropping total lung (total lung = lungs-GTV) volume extending inside PTV with an additional margin of 5.0 cm using the crop function within the planning system) demonstrated in Figure 3.1. Furthermore, in this study, a lower bound model was developed (see Figure 3.2) to predict the lowest achievable volume-dose ($Predict_{volume\text{-}dose}$) for a given geometry (i.e., $Lung_{Residual}$) (see Equations 3.1 and 3.2).

$$Predict_{Volume-Dose} = m \times Lung_{Residual} + c \qquad \textbf{Equation 3.2}$$

A lower bound prediction model was developed based on the prescription of 55 Gy in 20 fractions (typically used in our clinic). However, to use the model for different

prescriptions (i.e. 66 Gy in 33 fractions and 60 Gy in 30 fractions), it was normalised using the factor Δ (see equations 3.3 and 3.4) to predict minimum achievable doses. Note: the 55 Gy model data was used in the normalised model.

$$\Delta = \left(\frac{\mathrm{Pr}\, escriptionDose(Gy)}{55Gy} \right) \qquad \textbf{Equation 3.3}$$

$$\mathrm{Pr}\, edict_{Volume-Dose} = \left(m \times Lung_{\mathrm{Re}\, sidual} + c\right) \times \Delta \qquad \textbf{Equation 3.4}$$

3.2.2 Verification of Model Using Treatment Planning

A total of forty previously treated patients (not included in the training data) were re-planned using the values predicted by the models. For re-planning, optimisation objectives for V_5, V_{20} and MLD were set to achieve the model-predicted values, whereas all other objectives were kept the same as the original plans. The difference in dosimetric parameters between 1) predicted and replanned 2) predicted and original, and 3) replanned and original plans were compared.

In addition, the prediction accuracy of the normalised model (see equation 3.4) was assessed by re-optimising ten plans from the test dataset (originally prescribed 55 Gy in 20 fractions but for the validation of the model prescription doses were changed within the planning system). The differences between predicted and achieved doses were calculated for both 60 Gy and 66 Gy prescriptions.

3.2.3 Verification of Model Using Treatment Delivery

All VMAT plans are routinely verified with portal dosimetry measurements on a linear accelerator prior to delivering them to patients. All the plans optimised using the KBP model were verified by measuring the fluence on the electronic portal imaging device

(EPID) panel, without the presence of a patient, and comparing it with the planned fluence in the portal dosimetry image prediction software (PDIP) within the Eclipse planning system. Gamma analysis (criteria 3%/2mm ≥ 98% (optimal tolerances set locally) or ≥ 95% (mandatory tolerance)) results were collected and compared with the original plan results to assess the effect of KBP on plan delivery. Analysis was carried out in absolute dosimetry mode, with doses normalised to the maximum dose. For analysis, a global normalisation was used and the lower dose cut-off threshold was set to 20%, the measured and predicted images were auto-aligned and improved gamma evaluation was used.

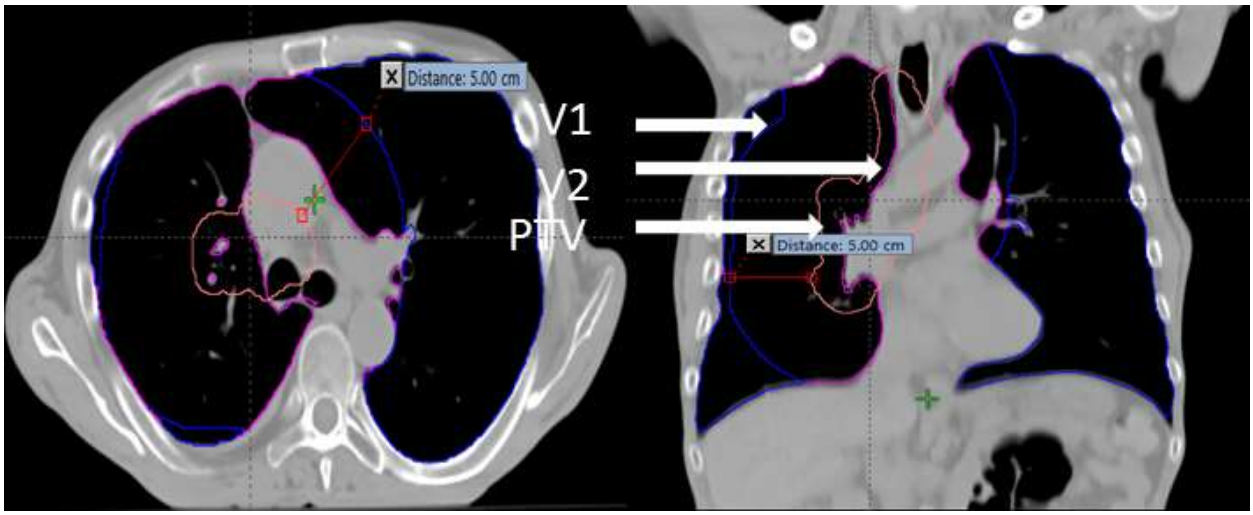

Figure 3.1: Example image showing the construction of residual lung volume ($Lung_{Residual}$)

Displaying the total lung volume excluding GTV (volume V2) in magenta and the volume V1 (i.e. the lung volume cropped back from PTV (pink) by 5 cm (blue).

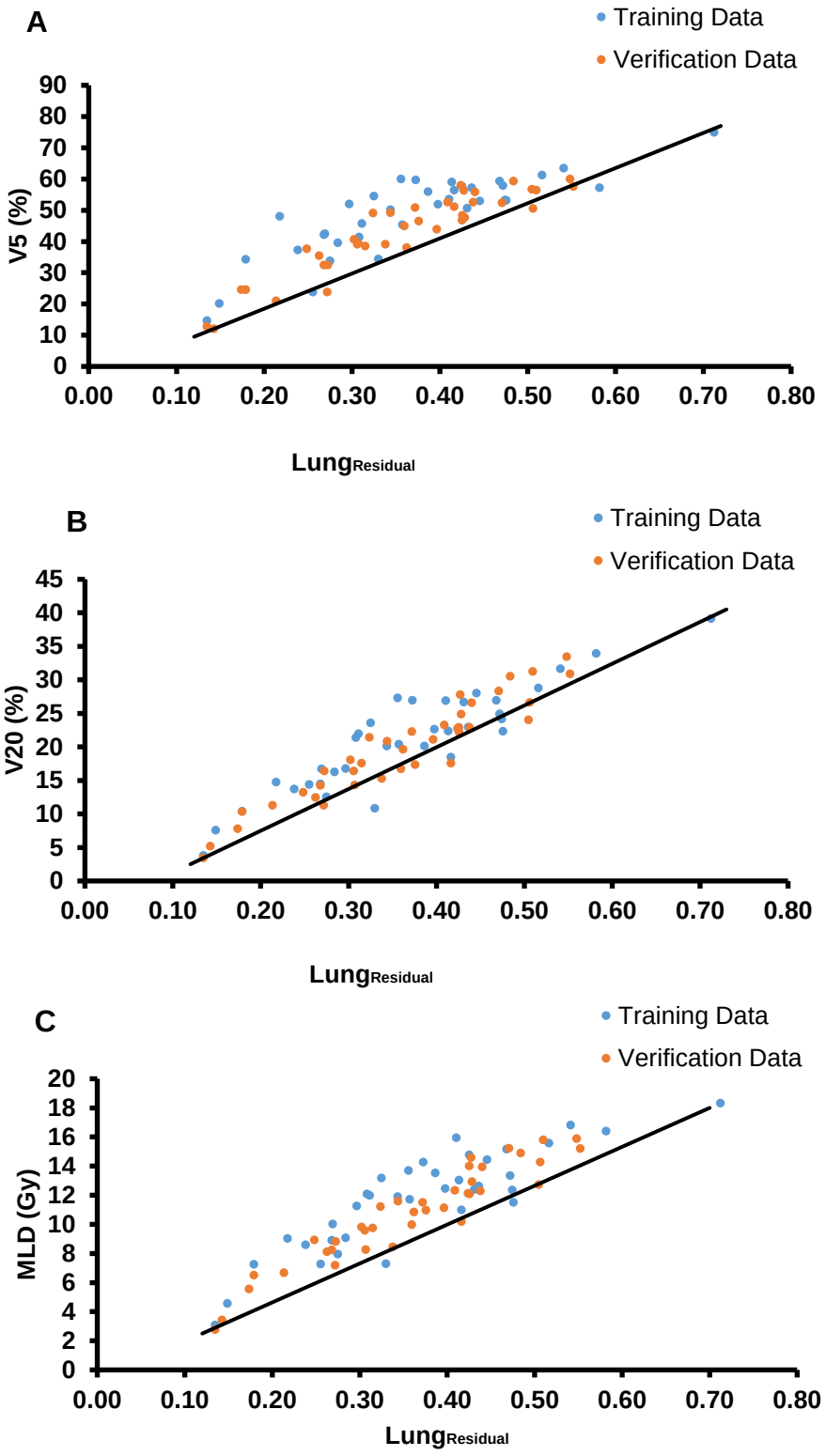

Figure 3.2: Lower bound models developed using $Lung_{Residual}$ volume.

These KBP models were developed using equation 3.2, a total of forty patients' data was used to build the models. Later the models were verified using forty patients' data, the plots showing training and verification data and the linear line showing the lower bound model for V_5 (A), V_{20} (B), and MLD (C). The slope and intersections of the models are shown in Table 3.2.

3.2.4 Plan Complexity Measurements

Treatment plan complexity is dependent on the total number of MU and the level of modulation within a plan. Simpler treatment plans (i.e., lower MU, less modulated with larger leaf pair opening) are preferable as these are relatively less dependent on MLC motion/position accuracy during delivery (Olofsson, 2012). Highly complex plans generally have a higher number of MU, which increase treatment delivery time, increase the dose to the patient - due to MLC transmission - and are more susceptible to interplay effects. A number of treatment plan complexity metrics were calculated both for the original plans as well as the plans produced using the KBP model. The treatment plan complexity parameters, including MU/Gy, MU/Degree, islands below 1cc (i.e. small islands), small aperture score (SAS: calculated as the ratio of open leaf pairs where the aperture was less than a defined criterion (2 mm, 5 mm, 10 mm and 20 mm in this study) to all open leaf pairs (see equation 2.2) (Crowe *et al.*, 2014)) were calculated using a locally developed script.

3.3 Results

The clinical KBP models were developed to determine the minimum achievable dose metrics using the $Lung_{Residual}$ volume (Figure 3.1). $Lung_{Residual}$ volumes calculated using 5.0 cm crop volume showed the highest correlation with all the dosimetric parameters studied (see Table 3.1). The slope and intersection of the KBP models are displayed in Table 3.2.

A significant reduction in variability in treatment plans amongst different planners was observed following the implementation of the model (see Table 3.3 and Figure 3.4).

Table 3.1. Showing correlation coefficients for different structures and three dosimetric metrics.

	Correlation coefficient (R^2)		
	V5	V20	MLD
(Lungs-Lung'1cmCrop)/Lungs	0.73	0.62	0.80
(Lungs-Lung'2cmCrop)/Lungs	0.73	0.61	0.80
(Lungs-Lung'3cmCrop)/Lungs	0.75	0.60	0.79
(Lungs-Lung'4cmCrop)/Lungs	0.77	0.61	0.80
(Lungs-Lung'5cmCrop)/Lungs	0.81	0.64	0.81
(Lungs-Lungs2cmCrop)/Lungs	0.55	0.62	0.77
(Lungs-Lungs3cmCrop)/Lungs	0.71	0.80	0.84
(Lungs-Lungs4cmCrop)/Lungs	0.78	0.87	0.81
(Lungs-Lungs5cmCrop)/Lungs	0.79	0.88	0.81
Lung(cc)	0.08	0.02	0.09
Lung'(cc)	0.52	0.35	0.54
Lung'/Lungs	0.74	0.62	0.80
Lung'/Lungs2cmCropLungs	0.70	0.58	0.73
Lung'/Lungs3cmCropLungs	0.62	0.50	0.68
Lung'/Lungs4cmCropLungs	0.46	0.34	0.54
Lung'/Lungs5cmCropLungs	0.19	0.10	0.27
Lung'1cmCrop	0.52	0.35	0.54
Lung'1cmCrop/Lungs	0.73	0.62	0.80
Lung'2cmCrop	0.53	0.36	0.55
Lung'2cmCrop/Lungs	0.73	0.61	0.80
Lung'3cmCrop	0.55	0.37	0.57
Lung'3cmCrop/Lungs	0.75	0.60	0.79
Lung'4cmCrop	0.58	0.39	0.59
Lung'4cmCrop/Lungs	0.77	0.61	0.80
Lung'5cmCrop	0.62	0.42	0.62
Lung'5cmCrop/Lungs	0.81	0.64	0.81
Lungs/LungsInPTV	0.37	0.30	0.54
Lungs/PTV	0.55	0.40	0.61
Lungs2cmCrop(cc)	0.17	0.08	0.19
Lungs3cmCrop(cc)	0.23	0.14	0.25
Lungs4cmCrop(cc)	0.32	0.22	0.34
Lungs5cmCrop(cc)	0.43	0.33	0.43
LungsInPTV(cc)	0.23	0.33	0.47
Lungs-Lung'(cc)	0.38	0.43	0.39
Lungs-Lungs2cmCrop(cc)	0.39	0.61	0.55
Lungs-Lungs3cmCrop(cc)	0.38	0.60	0.46
Lungs-Lungs4cmCrop(cc)	0.36	0.56	0.38
Lungs-Lungs5cmCrop(cc)	0.33	0.52	0.33
Lungs-PTV(cc)	0.32	0.06	0.16
PTV(cc)	0.27	0.25	0.42

! Lung' volume is defined in figure 3.3.

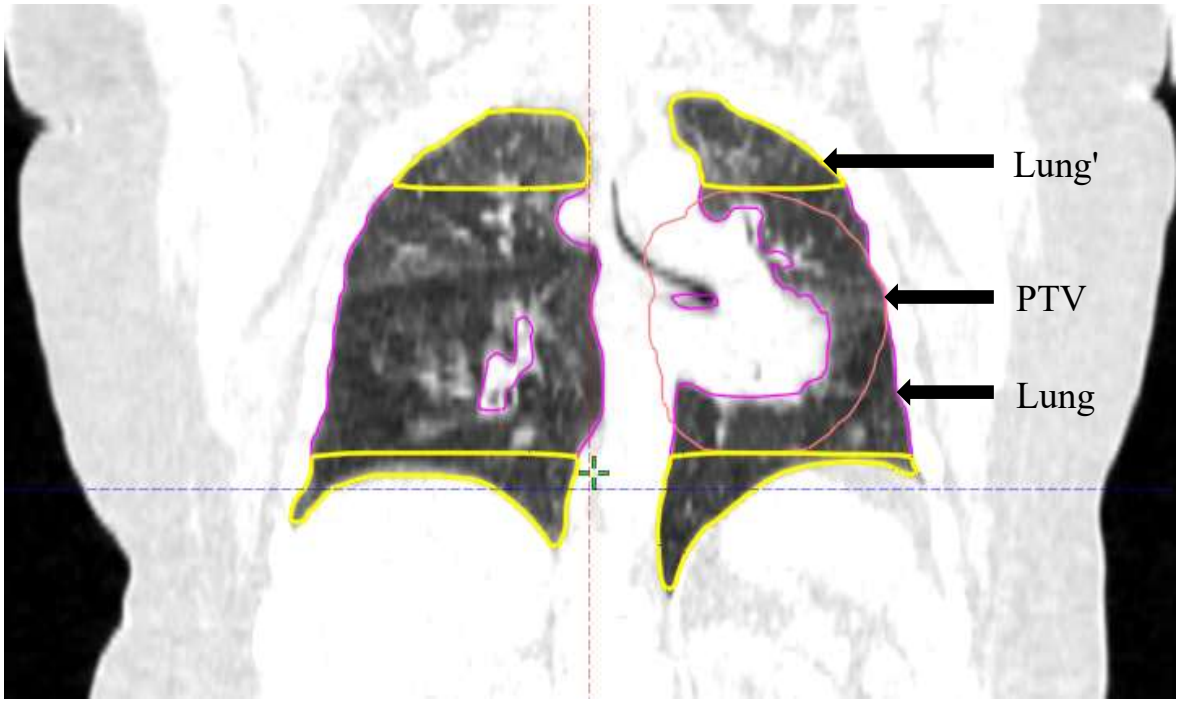

Figure 3.3: Displaying construction of Lung' volume in yellow.

The lung' volume was produced by deleting lungs-GTV volume overlapping axially with the PTV, leaving the superior and inferior parts of the lung-GTV from the PTV as it is. The lung' volume is shown in yellow and the lung-GTV and PTV volumes in magenta and orange respectively.

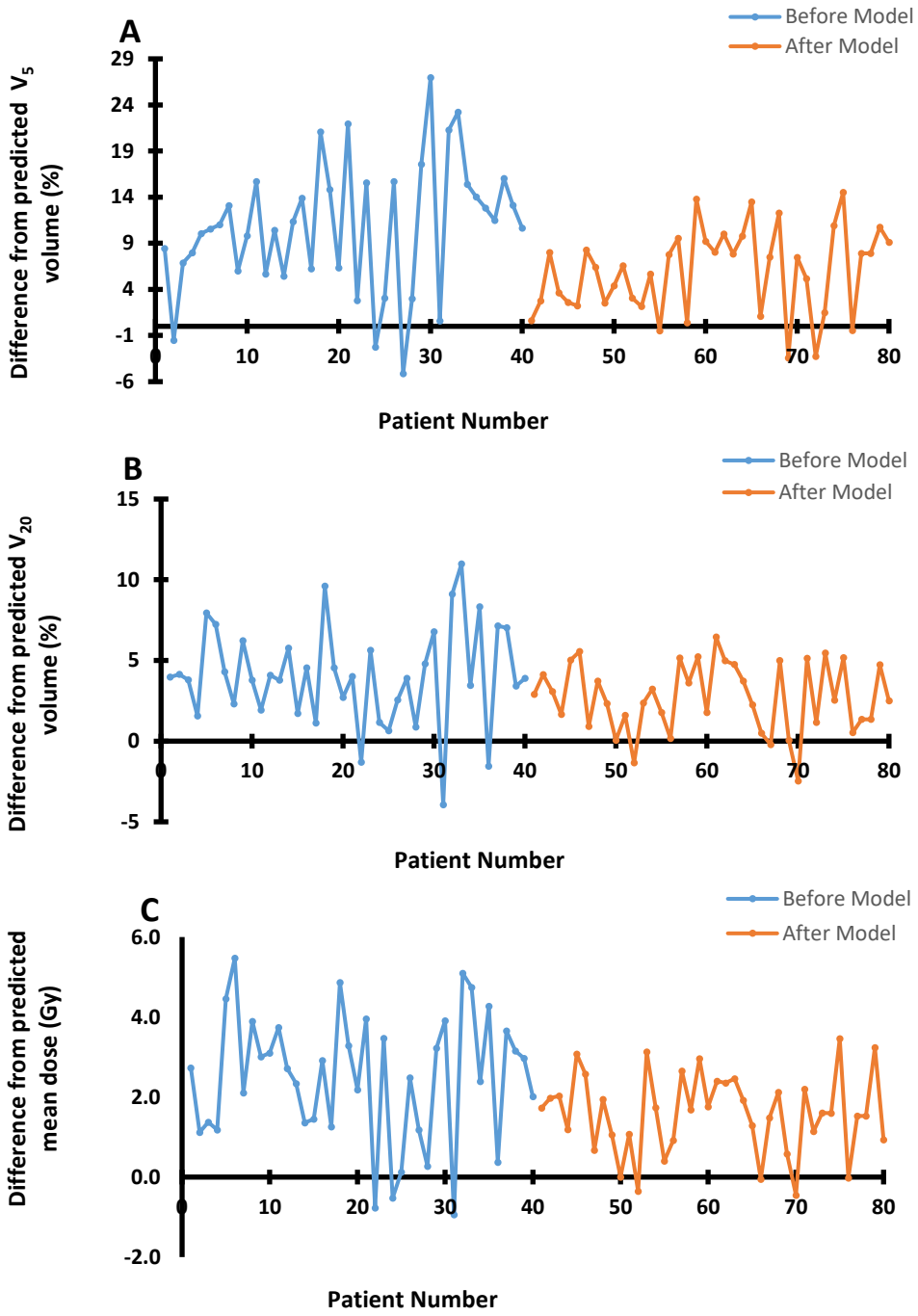

Figure 3.4: Reduction in variability in the plans produced after the model.

Plots A, B and C show a consistent reduction in plan variability in plans produced after the models compared for V_5, V_{20} and MLD respectively. The original plans were planned without model-predicted values, whereas achieved values were obtained by re-optimizing plans with the model-predicted values. Three separate models were produced for each dose-volume parameter shown in Figure 3.2, using residual lung volume. The minimum achievable dose-volume parameters were predicted prior to the plan optimisation and the predicted values for each parameter were entered in the optimiser.

Table 3.2. Showing slope and intersection of the clinical KBP models.

Model	Slope (M)	Intersection (C)
A (V_5)	111.67	-3.4
B (V_{20})	63.33	-5.6
C (Mean Dose)	27.05	-0.98

Table 3.3. Mean and standard deviation of the differences between achieved and predicted dose-volume parameters for lung before and after implementation of the model for 55Gy/20 fractions regime.

Dose-volume parameter	Before model		After model		p-value
	Mean	SD	Mean	SD	
V5	10.8%	7.1%	5.9%	4.6%	0.007
V20	4.0%	3.1%	2.7%	2.1%	0.038
MLD	2.5 Gy	1.6 Gy	1.6 Gy	1.0 Gy	0.012

Furthermore, the plans optimised using the model showed a significant reduction in differences in dose-volume in all three, V_5, V_{20} and MLD, dosimetric parameters (see Figure 3.5). The mean difference between predicted and achieved values was reduced from 10.8% to 5.9%, 4.0% to 2.7% and 2.5 Gy to 1.6 Gy for V_5, V_{20} and MLD respectively using the model (see Table 3.3). In Figure 3.4, it can be observed that negative differences indicate that the model predicted values were higher than the achieved values and positive differences indicate model predicted values were lower.

Furthermore, treatment plans produced using the model-predicted values resulted in a concurrent reduction in all three dosimetric parameters compared to the original plans (Figures 3.5 and 3.6). The average reduction observed in V_5, V_{20} and MLD was 6.6% (range: 0.4% – 19.78%), 1.1% (range: -0.93% – 7.77%) and 0.7 Gy (range: 0.03 Gy – 2.38 Gy) respectively. The reduction in lung doses was achieved (see Figure 3.6) without compromising the overall plan quality. All test plans were evaluated by a clinician and were deemed acceptable for clinical delivery.

In addition, the model developed for the prescription used in our clinic (55 Gy in 20 fractions) was normalised for use with different prescriptions. The normalised model (equation 3.4) was validated for two additional prescriptions (66 Gy in 33 fractions and 60 Gy in 30 fractions) by replanning ten patients. The indicated accuracy of the models was clinically acceptable; the mean difference between predicted and achieved doses at V_5 was 0.5% and 2.3% for 66 Gy and 60 Gy prescriptions respectively and for V_{20} and MLD it was 2.1% and 1.2 Gy for both prescriptions respectively (see Figure 3.7).

It was noted in the KBP model-based plans that the total number of MU increased significantly in the majority of plans compared to the original clinical plans (mean increase = 46.21 MU (range: – 48 MU – 186 MU), $p = 0.011$). Therefore, a number of treatment plan complexity metrics were calculated using a locally developed script for both the original and re-optimised plans. The results are shown in Table 3.4.

Table 3.4. Comparison of treatment plan complexity measurements for the original and re-planned plans.

Parameters	Original Plan*	SD	Re-planned Plan*	SD	p value
MU/Gy	236.6	29.0	253.4	29.4	0.0002
MU/Degree	1.8	0.2	2.0	0.2	0.0001
Fraction of islands < 1cc	0.49	0.2	0.58	0.1	0.0002
Islands/control point	3.9	2.1	4.9	2.3	0.0001
SAS2	0. 19	0.1	0.23	0.1	0.0003
SAS5	0.22	0.1	0. 27	0.1	0.0002
SAS10	0.28	0.1	0.34	0.1	0.0002
SAS20	0.40	0.1	0. 48	0.1	0.0002

* Means of noted parameters; SD = standard deviation

The results show that all studied complexity metrics increased significantly in the re-plans optimised using KBP models when compared to the original plan (see Table 3.4). This indicates that KBP plans were relatively highly modulated compared to the original plans.

Treatment verification measurements performed on linear accelerators showed that both original and KBP plans were delivered as planned. Differences in treatment verification measurements for all parameters were within the optimal tolerance limits set locally (≥ 98% pixels passing with gamma criteria of 3%/2mm) except two arcs from the KBP plans showed slightly higher differences with gamma pass rates at 96.9% and 97.2%. However, these were within the mandatory tolerance limit of ≥ 95%; therefore, these plans were deemed clinically acceptable for treatment delivery.

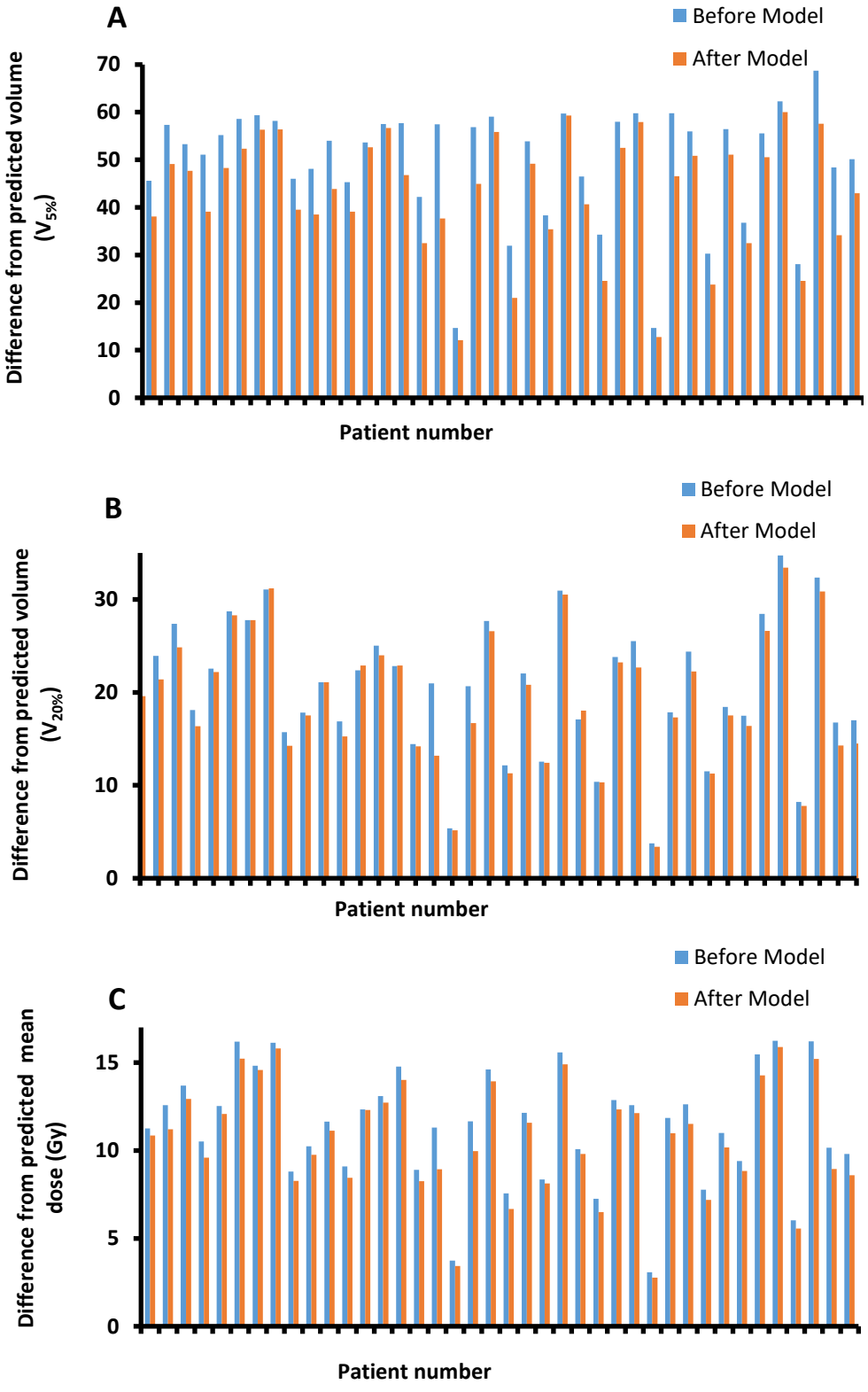

Figure 3.5: Difference in dose-volume parameters before and after the model. The concurrent reduction was seen in all the dosimetric parameters studied V_5 (A), V_{20} (B) and MLD (C) after the model. The achievable dosimetric parameters were determined using the models prior to optimisation and the predicted values were entered in the optimiser.

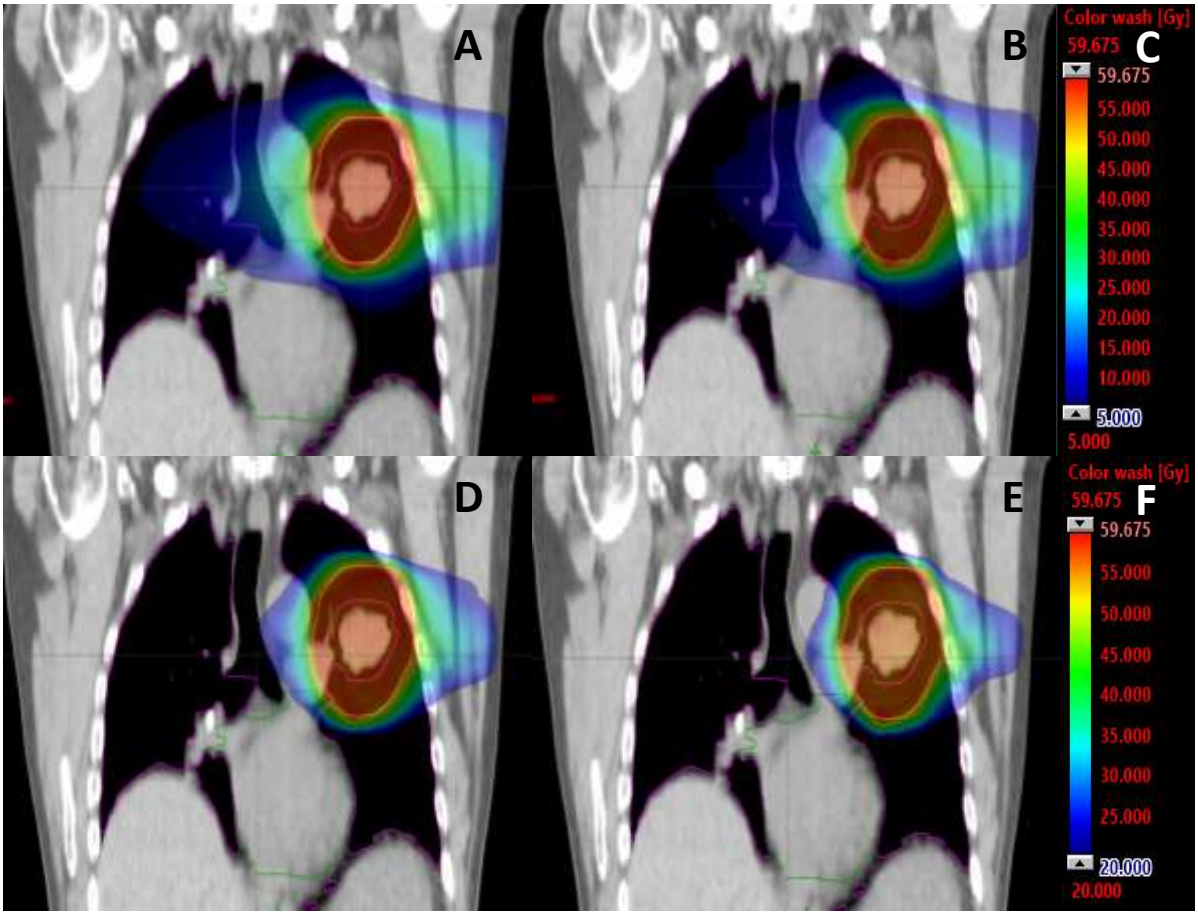

Figure 3.6: Example images displaying dose distribution achieved with and without KBP models.

Higher dose spillage was seen in the plans produced without a model (V_5: compare A and B) and (V_{20}: compare D and E) where the plans without a KBP model are A and D and with a KBP model are B and E. The plans produced using the knowledge-based planning models achieved more conformal dose distribution and low dose spillage in OARs (e.g. lungs) is less compared to the previous/original clinical plans (B and E).

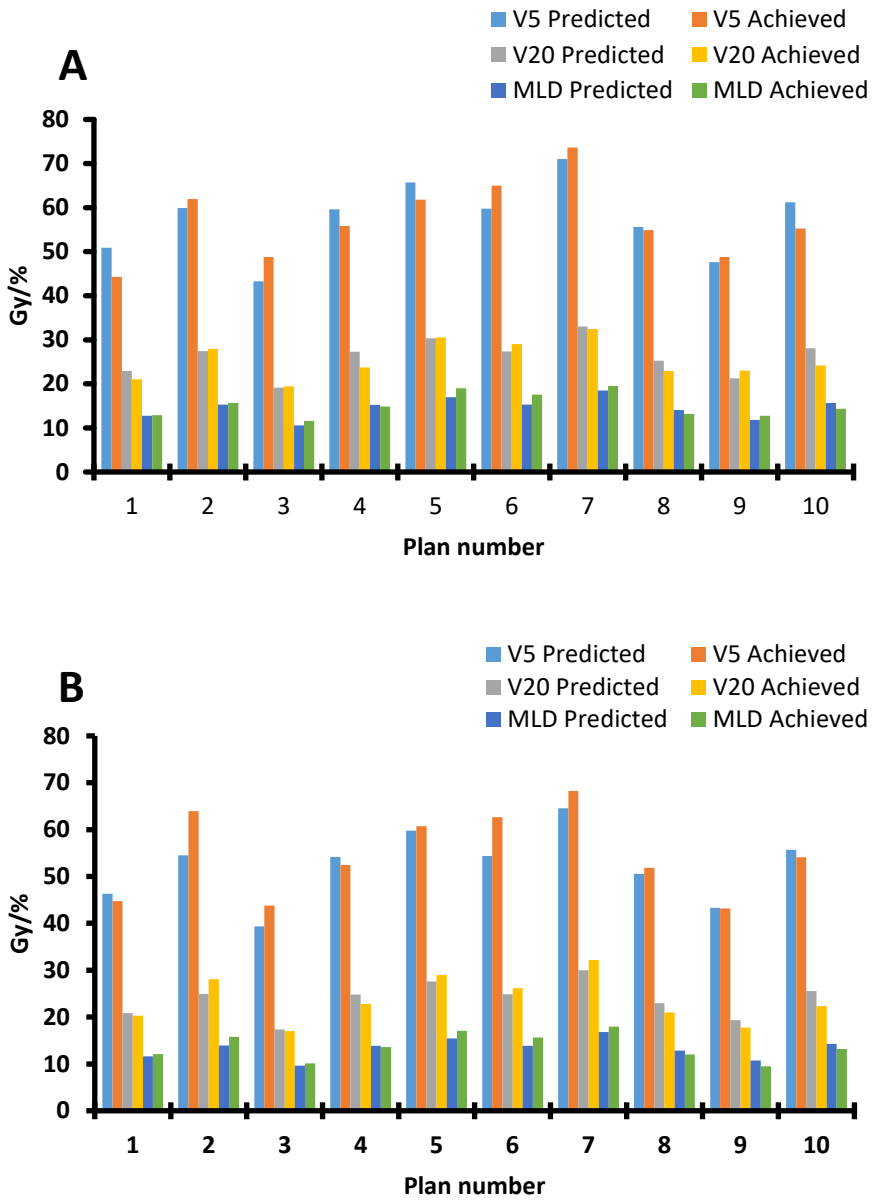

Figure 3.7: Difference in dose-volume parameters before and after the model for 66 Gy in 33 fractions (A) and 60 Gy in 30 fractions (B) prescriptions.

The normalised model was verified using ten plans. The minimum achievable doses were predicted using the normalised model and the predicted values were used during plan optimisation.

3.4 Discussion

The aim of treatment planning is to achieve optimal target coverage whilst reducing OAR doses as low as reasonably achievable without compromising target coverage (Mayles, Nahum and Rosenwald, 2007). However, in routine clinical practice, due to treatment planners' experience and clinical workload, this is not always achieved for all patients (Nelms *et al.*, 2012; Batumalai *et al.*, 2013; Moore *et al.*, 2015; Berry *et al.*, 2016). Furthermore, not all plans meeting target coverage and OAR constraints are optimal if there are opportunities to minimise OAR doses further without compromising target coverage. This balance may be difficult to be achieved efficiently in the absence of KBP methods, especially for relatively inexperienced treatment planners.

3.4.1 Model development

Building KBP models for lung cancer patients could be more complex compared with some other sites (e.g. prostate) as there are large variations in the location, shape, size and orientation of lung tumours with respect to OAR volumes. Several combinations of volumetric parameters (e.g. PTV and OAR volumes, overlap volumes, field size) and their correlation with studied lung dose-volume parameters were evaluated. However, by trial and error, we found that the $Lung_{Residual}$ volume that was calculated using total lung volume and the lungs crop back from PTV by 5.0 cm (equation 3.1) had the highest correlation with all the studied lung dose-volume parameters.

Only two studies have reported on the use of in-house KBP modelling for optimising lung plans (Cui.W *et al.*, 2015; Zawadzka *et al.*, 2017). These studies predicted V_{30}, V_{20} and V_{10}, using the best fit model (Cui.W *et al.*, 2015) and minimum achievable mean lung dose (Zawadzka *et al.*, 2017). However, as none of these models predicts the minimum dose to

V_5 and V_{20} of lungs, we felt it was important to develop local models that predict the minimum achievable dose to these percentages of lung volumes for a given patient's geometry. Furthermore, none of the studies in the literature has investigated the effect of KBP models on the complexity of plans and the deliverability of these plans. In this study, the accuracy of the models was verified using a planning study while the effect of KBP models on plan complexity and delivery was assessed by calculating complexity metrics and performing measurements on a linear accelerator.

3.4.2 Validation of KBP models

Our models were built to predict minimum doses to three lung dose parameters for lung patients treated with VMAT. This study demonstrated that minimum lung dose-volume prediction models can be developed and used in the routine clinical setting. Relatively simple and cost-effective models reduced variability/heterogeneity in treatment plans significantly compared to the original clinical plans, which was the primary aim of this study. Predicting dose-volume parameters prior to optimising a plan could reduce the number of optimisations/iterations required to achieve the optimal plan and reduce the overall planning time.

Additionally, the treatment planning study performed showed that the use of a KBP model led to a larger reduction in V_5 as compared to V_{20} and MLD (Figure 3.4). The moderate reduction observed for the V_{20} (1.4%) and MLD (0.7 Gy) may be attributed to the use of the NTO function in the original and re-optimised plans with the same priority as PTV. Results from a number of commercial auto-planning software platforms showed similar results as our in-house developed model (Zhang *et al.*, 2011a),(Quan *et al.*, 2012; Della Gala *et al.*, 2017). One of the auto-planning studies reported a statistically insignificant increased V_5 whereas our study showed a consistent and significant

reduction in this dosimetric parameter (Quan *et al.*, 2012). The normalised model (see Equation 3.4) shows that the model could be used for different prescriptions.

In addition, we also assessed the accuracy of the model for oesophageal cancer (commonly treated with 45 Gy and 50 Gy in 25 fractions), treated with full-arc geometry but the prediction accuracy of V_5 was not clinically acceptable. Significantly higher differences were seen between the predicted and achieved V_5 values; this could be due to differences in the arc geometry (start-stop angle) used for planning these patients. The full arcs treating through both (right and left) lungs deliver a low radiation dose (e.g. 5Gy) to large lung volume compared to the half arcs used for treating lung patients. However, the prediction accuracy of V_{20} and MLD was clinically acceptable but the difference seen between predicted and achieved doses was higher compared to the lung plan. The mean difference between predicted and achieved values for 50 Gy and 45 Gy prescriptions were V_5 = 29.7% and 30.8%, V_{20} = 1.8% and 3.4% and MLD = 2.3 Gy and 2.1 Gy respectively. This could be due to the difference in the beam geometry and the gradient of the DVH curve at V_5 could be significant and a small shift in the DVH curve could result in higher differences.

Furthermore, it was noted that the largest reduction in all three dosimetric parameters investigated was achieved with the use of KBP models in the subset of plans produced by relatively less experienced planners, compared to experienced planners (see patient numbers 2, 4, 17, 19, 30 and 39 in Figure 3.4), due to not driving the optimiser harder. However, almost all the original clinical plans considered met the planning goals given in Table 1.1 and were therefore acceptable, although some were not classed as 'optimal' as lung dosimetric parameters could be reduced further to some extent without compromising target coverage. Some of these plans were produced by experienced staff

indicating the potential benefits of KBP for all planners. In addition, a relatively smaller reduction in the studied parameters was noted in plans where lung constraints were either exceeding or were very close to the tolerance levels in the original plans as compared with the plans where lung constraints were well within tolerance – potentially due to the fact that the original plans were increasingly optimised to bring doses within tolerance. These results indicate the importance and efficiency of KBP modelling for this type of patients in reducing OAR dose variability in treatment plans produced by planners of variable experience.

3.4.3 Assessment of treatment plan complexity

Webb *et al* and Abdellatif *et al* reported that plan complexity increases with an increasing number of small segments, MU/cGy and the number of MUs per control point (Webb, 2003; Abdellatif and Gaede, 2014). An increase in the total number of MUs seen in the KBP optimised plans warranted further investigation: Treatment plan complexity metrics were calculated and delivery verification measurements were performed on a linear accelerator. Plan complexity metrics indicated a significant increase in smaller islands (i.e., smaller than 1.0 cc), number of MUs per control point and small aperture segments in the KBP plans. These plans were optimised to achieve minimum achievable doses, rather than generic OAR tolerances; therefore, an increase in plan complexity was expected. A study by Crowe et al reported that SAS could be used as an indicator of the level of plan modulation; they showed a positive correlation between quality assurance (QA) results and SAS was set at 0.5 cm (Crowe *et al.*, 2014). In this study, SAS increased for all test plans indicating an increase in modulation in these plans.

3.4.4 Treatment plan deliverability

Although the plan complexity parameters for KBP model-based plans were relatively higher than the ones for clinical plans, their impact on the measured fluence was relatively minimal for the majority of the test plans. Similar results are reported in the literature (Zhen, Nelms and Tome, 2011; Younge *et al.*, 2016). The measurements showed overall good agreement with the planned fluence except for two arcs where differences exceeded the locally determined optimal gamma tolerance limits. These measurements showed that KBP may increase modulation and hence affect delivery therefore the model must be verified using treatment delivery measurements prior to implementing it clinically. Furthermore, in this study, delivery measurements were performed using an EPID panel (without a patient or moving phantom) that does not fully verify the impact of an increase in modulation on the robustness of the plan. Further investigation, using a moving phantom, is needed to quantify the effect of high modulation of the delivery, especially for the treatment of thoracic tumours.

3.4.5 Clinical implementation of KBP models

Finally, the model was implemented clinically in our clinic using the Eclipse scripting tool (ESAPI: Eclipse Scripting Application Plugg-In). Planners produce the structure (Lungs5cmCrop = crop total lung volume extending inside PTV with an additional margin of 5.0 cm) using the crop function and then run the script within the Eclipse planning system prior to proceeding with plan optimisation. The script displays the minimum achievable dosimetric metrics based on the residual lung volume for the selected patient. The predicted values are then manually entered in the optimiser (priorities are set within the clinical protocol template) during the optimisation of the plan.

The reduction of lung dose-volume parameters will not only reduce toxicities and improve the quality of life for NSCLC patients but the reduction in lung doses also provides an opportunity for dose escalation that may improve local control and overall survival. A subsequent dose-escalation study is described in Chapter 6.

3.5 Conclusion

This study showed that a relatively simple knowledge-based planning model can significantly reduce variability in lung planning between planners. The models are implemented clinically and have demonstrated an increase in lung-sparing. It is, however, important to assess plan deliverability prior to the clinical implementation of such models to ensure that the potential increase in plan complexity will not affect the dosimetric accuracy required.

Appendix: Chapter 3

Several volumes were considered to develop the lower bound model, and correlations between the volumes and the dosimetry parameters were assessed (see Table 3.1). However, most of these structures did not show a strong correlation with the dosimetric parameters. The volumes, Lungscrop (lungs crop back from PTV) and Lung' (see figure 3.3), and their ratio to the total lung volumes showed a strong correlation with the dosimetric parameters. To find out the highest correlation, several crop volumes were produced for lung and lung' volumes with a margin of 2 cm to 5 cm from the PTV and correlated with the dosimetric parameters. The planning system did not allow more than 5 cm crop in a single operation so we did not assess the correlation of volumes that are cropped back with a margin > 5 cm. The results showed a higher correlation with the volumes cropped back by 5 cm (see Table 3.1). In this thesis, we decided not to use the Lung' volumes, as the correlation was similar the lung5cmcrop volume and it was time-consuming to produce the lung' structure.

Several KBP models were produced using $Lung_{Residual}$ volume. Initially, the lower bound models were produced with the model line encompassing all the data points shown in Figure 3.2. These models were verified by re-planning patients from the verification data set. The verification results showed that these models were over-ambitious (the slope and intersection of the clinical and the initial model are shown in Table 3.5) as the achieved dose-volume parameters were significantly different from the predicted dose-volume parameters. Any attempts made to achieve the predicted values were significantly affecting the PTV coverage and hence were considered not suitable for clinical use. Furthermore, qualitative assessment from the treatment planners showed that the initial models were not efficient and required additional optimisations/

iterations to achieve clinically acceptable target coverage whilst trying to achieve predicted lung doses.

Table 3.5. Showing slope and intersection of the clinical KBP models.

Model	Slope (M) Clinical	Intersection (C) Clinical	Slope (M) Initial	Intersection (C) Initial
A (V_5)	111.67	-3.4	103.4	-3.6
B (V_{20})	63.33	-5.6	58.0	-8.4
C (Mean Dose)	27.05	-0.98	28.7	-2.5

Therefore, the initial models were revised and some of the data points were excluded from the lower bound model (see Figure 3.2). These models were verified using an independent data set. The results showed a significant reduction in the achieved and predicted dosimetric metrics (see Figure 3.4) compared to the initial models. In addition, these models were efficient (fewer iterations were required to achieve the predicted values) and produced clinically acceptable results (i.e., achieving desired target coverage).

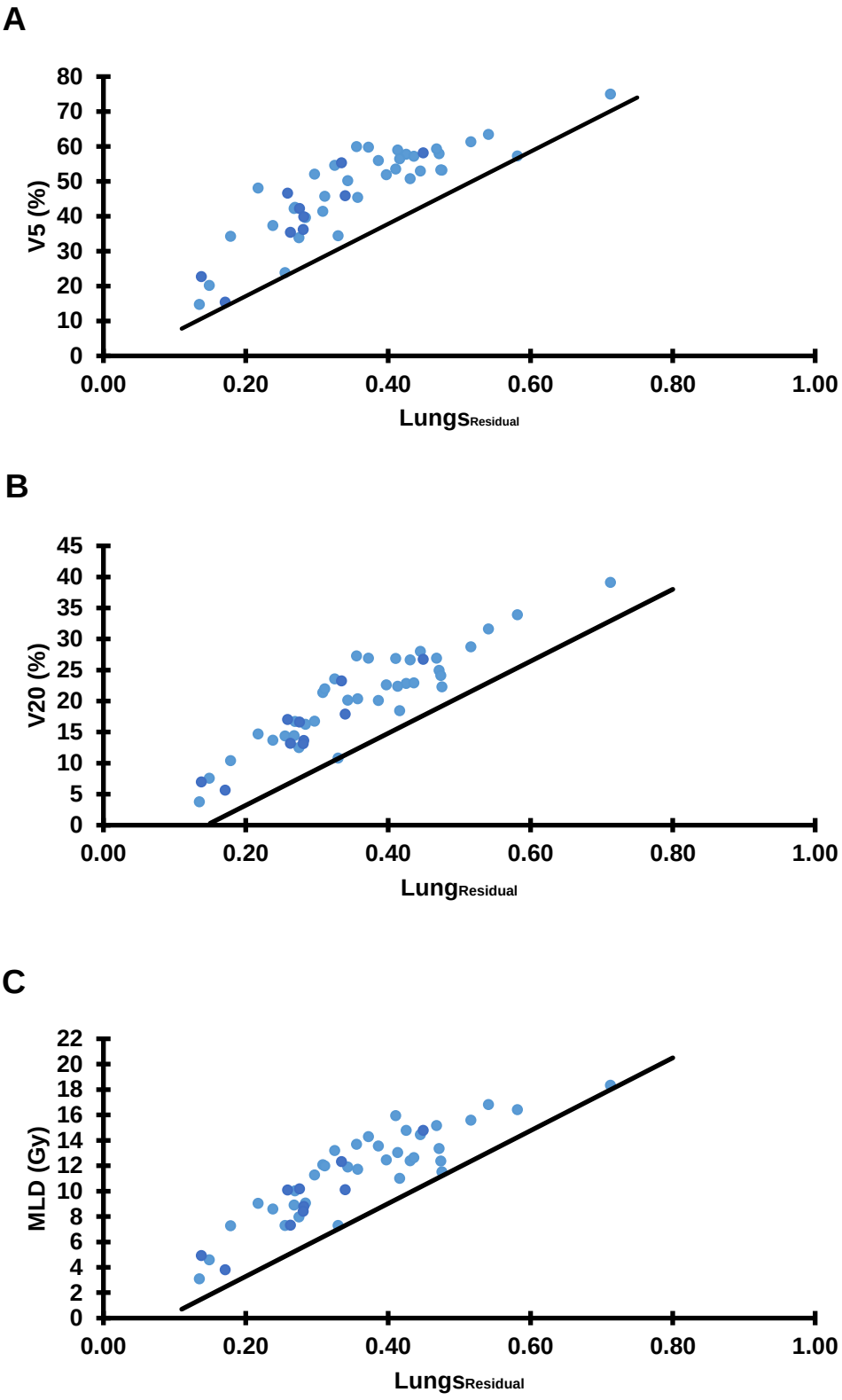

Figure 3.8: The initial lower bound models developed using $Lung_{Residual}$ volume.

The initial KBP models were developed including all the data points. These models were verified using independent data, but the discrepancies between the predicted and the achieved values were not clinically accepted. Therefore, some of the points from the lower bound models were excluded. The slops and intersections of the models are shown in Table 3.8.

4. Predicting personalised optimal arc parameters using knowledge-based planning model for inoperable locally advanced lung cancer patients to reduce organ at risk doses

The research in this chapter was published in a peer-reviewed journal and therefore the text presented here is adapted from the article. My contribution consisted in conceptualising the research strategy, performing the research and writing the manuscript with input from my supervisors on designing and planning the work and editing the manuscript and clinical inputs from clinicians Dr. A Wieczorek, and Dr. S Upadhyay. Reference: Tambe, N. S.; Pires, I. M.; Moore, C.; Wieczorek, A.; Upadhyay S.; Beavis, A. W., Predicting personalised optimal arc parameters using knowledge-based planning model for inoperable locally advanced lung cancer patients to reduce organ at risk doses. Biomed. Phys. Eng. Express, 2021. 7.065002.

4.1 Introduction

Radiotherapy treatment planning aims to maximize the therapeutic ratio, that is, to achieve higher tumour control whilst lowering the risk and severity of associated toxicities (Mayles, Nahum and Rosenwald, 2007). This is achieved by minimizing organ at risk (OAR) doses whilst delivering a prescription dose designed to control tumour cells to the target volumes. Treatment planning and delivery techniques have evolved significantly over the years from parallel opposed fields to multiple conformal fields to advanced techniques such as intensity-modulated radiation therapy (IMRT) and volumetric modulated arc radiotherapy (VMAT), which have improved overall treatment plan quality. This has led to a relatively larger number of patients receiving the intended tumour dose without exceeding OAR doses.

Three-dimensional conformal radiotherapy (3D-CRT) and VMAT/IMRT treatments reduce higher doses to OARs due to the conformity of the high doses to targets. However, due to the nature of VMAT/IMRT techniques, the low-dose bath increases significantly (Marks *et al.*, 2009; Diwanji *et al.*, 2017). Several studies have reported that lower doses to a larger portion of healthy lung volume increased the incidence of grade 3 radiation pneumonitis (Wang *et al.*, 2006; Marks *et al.*, 2009). Additionally, patients undergoing combination chemo-radiotherapy and who have associated co-morbidities are more prone to chemo-associated toxicity (Rancati *et al.*, 2003). Finally, increasing the low-dose bath in IMRT and VMAT plans could also increase the risk of secondary malignancies (Abo-Madyan *et al.*, 2014). Therefore, it is critical to keep doses to the lung as low as possible.

Several studies have reported that IMRT reduces V_{20} (lung volume receiving 20 Gy) but may increase V_5 (the lung volume receiving 5 Gy) when compared to 3D-CRT plans (Li *et al.*, 2018; Yin *et al.*, 2012). Furthermore, lung V_5 and mean lung dose (MLD) increased in VMAT plans for lower and middle oesophageal cancer plans when compared to IMRT plans, whereas V_{20} of lung and V_{30} of heart decreased slightly in VMAT plans with a comparatively lower treatment time (Yin *et al.*, 2012). Recently, a study reported an increase in grade 3 cardiac toxicities for oesophagus patients where the mean heart dose is greater than 15 Gy (Wang *et al.*, 2020b). Therefore, reducing doses to both lungs and heart is important.

Numerous treatment planning methods have been studied to reduce lung doses including the use of avoidance sectors in VMAT, 4 pi, and hybrid planning. Regarding the latter, a study combined 3D conformal fields with IMRT fields and reported that, for lung cancer plans, V_5 increased by 3.7% in the hybrid IMRT plans compared to the 3D conformal plans

and reduced by 4.8% and 9.8% for four/five and nine fields IMRT plans respectively (Mayo *et al.*, 2008). The V_{20}, and MLD were reduced by 4.3% and 0.5 Gy respectively. However, the same hybrid plans increased heart V_{30} dose by 6.3% compared to IMRT and 3D conformal plans (Mayo *et al.*, 2008). Another study demonstrated that lung V_5 can be reduced using a hybrid RapidArc (Varian's VMAT) technique compared to a 240^o RapidArc plan but is still increased compared to the 3D conformal plans (Chan *et al.*, 2011). In addition, an increase in total treatment time was reported in the hybrid RapidArc plans (Chan *et al.*, 2011).

Further studies have reported the benefit of RapidArc with avoidance sectors (the linear accelerator switches the beam off in the defined avoidance segment/sector of the arc treatment) for head and neck, abdomen, pelvic and stereotactic ablative body radiotherapy cases (Dumane *et al.*, 2010; B and ChihYao, 2013; Huang *et al.*, 2015; Rana and Cheng, 2013; Pursley *et al.*, 2017). Furthermore, a study performed by Rosca *et al* (Rosca *et al.*, 2012) demonstrated that restricted arc (i.e. arcs with avoidance sectors) plans reduce lung doses but the heart dose increases compared to full arc plans (Rosca *et al.*, 2012). One of the shortcomings of this evaluation was that it only investigated the restricted arc technique for centrally located tumours. Recently, the use of the 4 pi technique has been investigated for stereotactic ablative body radiotherapy for lung cancers, this study reported a significant reduction in lung V_5, V_{10} and V_{20} (Dong *et al.*, 2013). The 4 pi technique includes non-coplanar IMRT beams distributed on the 4 pi spherical surface; the beam optimisation begins with a pool of 1162 non-coplanar IMRT beams with 6^o separation in the 4 pi solid angle space. The optimiser then eliminates the beams that could collide with the couch/patient and the plan is optimised using the remaining beams (Tran *et al.*, 2017).

All these studies recommended using a single protocolised treatment plan for all patients irrespective of patient anatomy (e.g., fixed restricted arcs or hybrid arcs). However, tumour shape, size and location and its overlap with OAR volumes could vary significantly among patients with locally advanced-stage lung cancer disease. Therefore, a single protocolised, fixed arc parameter approach may not be the most optimal planning method across the patient population. The field size, multi-leaf collimator (MLC) sequencing and the isocentre can be optimised by the planning system for IMRT and VMAT treatments. Here we are addressing arc parameters that are not automatically selected by the planning system or the optimiser, such as start-stop arc angle and avoidance sectors.

The aim of the present study is to investigate optimal arc geometries using a personalised arc parameter approach for planning inoperable locally advanced-stage lung cancer patients treated with curative intent. This strategy hopes to reduce low-dose bath and OAR doses whilst maintaining target coverage. Furthermore, a knowledge-based planning model was developed to predict the optimal arc parameter using patient-specific parameters.

4.2 Methodology

4.2.1 Patients and prescription

In our clinic, all locally advanced-stage lung cancer patients are treated using RapidArc (Varian's solution for VMAT), as previously described (Tambe *et al.*, 2020). Treatment plans were produced using the Eclipse™ treatment planning system (V15.6, Varian Medical Systems). A total of 30 previously treated patients', clinically accepted plans were randomly selected from our database treated between January 2017 and December 2019

(excluding patients/plans used in the previous study), of which 20 were used as baseline 'training' plans and ten reserved for validation of the model. Patient demographics are summarized in Table 2.2. The prescription dose was 55 Gy in 20 fractions (i.e., ≥ 99% of the PTV receives ≥ 95% of the prescription dose (see Table 2.1)). For imaging protocol and contouring protocols see section 2.2, and for planning and treatment delivery please check sections 2.3 and 2.5.

4.2.2 Re-planning with different arc geometries

A total of twenty patients were re-planned, each with the seven different arc parameters illustrated in Figure 4.1; different arc parameters (gantry start and stop angles, see Table 4.1) were selected using trial and error based on clinical experience. The test plans include a range of active treatment angle arc geometries to minimize entry through whole lungs, contralateral lung, or heart, and a range of treatment angles from 360^{o} arcs to 90^{o} arcs. The 90^{o} arc was placed in the same quadrant as the PTV. Optimization objectives were kept the same as the original clinical plans so that the effect of change of arc parameter on lung, heart and spinal cord PRV doses could be assessed. In addition to different arc parameters, five patients were planned with three different collimator angle settings, 30^{o} and 330^{o}, 20^{o} and 340^{o} and 10^{o} and 350^{o} to assess their impact, within the study aims, and all other patients were planned with one collimator angle setting (i.e., the collimator angle that reduced overall OAR doses). All the plans, including the original clinical plans, were blind reviewed (i.e., without knowing arc parameters) by both clinical oncologists, and a preferred plan was selected for each patient following the pre-defined clinical criteria (see Table 2.1), including target coverage and OAR doses at specified dose-volume tolerance level (e.g. lung V_5 or V_{20}). The optimal plans were then compared with the original clinical plans (i.e., arc parameter A). In addition, the conformity index

(CI) and homogeneity index (HI) were calculated as defined in ICRU (International Commission on Radiation Units and Measurements) report 83 ('Preface,' 2017) for clinical and test plans (using equations 4.1 and 4.2) and compared.

$$\text{Conformity Index (CI)} = \frac{V95\%}{Volume\ of\ PTV} \qquad \textbf{Equation 4.1}$$

where V95% is the volume of PTV covered with at least 95% of the prescription dose.

$$\text{Homogeneity Index (HI)} = \frac{D2\%\text{-}D98\%}{D50\%} \qquad \textbf{Equation 4.2}$$

where $D_{2\%}$, $D_{50\%}$ and $D_{98\%}$ are the doses received by 2%, 50% and 98% of the planning target volume.

Table 4.1. Arc parameters used for planning test and clinical plans (arc parameters are displayed in figure 4.1).

Arc parameter	**Start and stop angle**	**Avoidance sector(s)**
A	0^o to ± 180^o	None
B	0^o to ± 180^o	For right-sided tumours: 220^o to 300^o For left-sided tumours: 140^o to 60^o
C	± 30^o to ± 180^o	For right-sided tumours: 220^o to 300^o For left-sided tumours: 140^o to 60^o
D	± 60^o to ± 180^o	For right-sided tumours: 220^o to 300^o For left-sided tumours: 140^o to 60^o
E	181^o to 179^o	220^o to 300^o and 140^o to 60^o
F	181^o to 179^o	For right-sided tumours: 220^o to 300^o and 0^o to 140^o For left-sided tumours: 140^o to 60^o and 0^o to 220^o
G	181^o to 270^o Or 179^o to 90^o Or 90^o to 0^o or 270^o to 0^o	None
H	181^o to 179^o	None

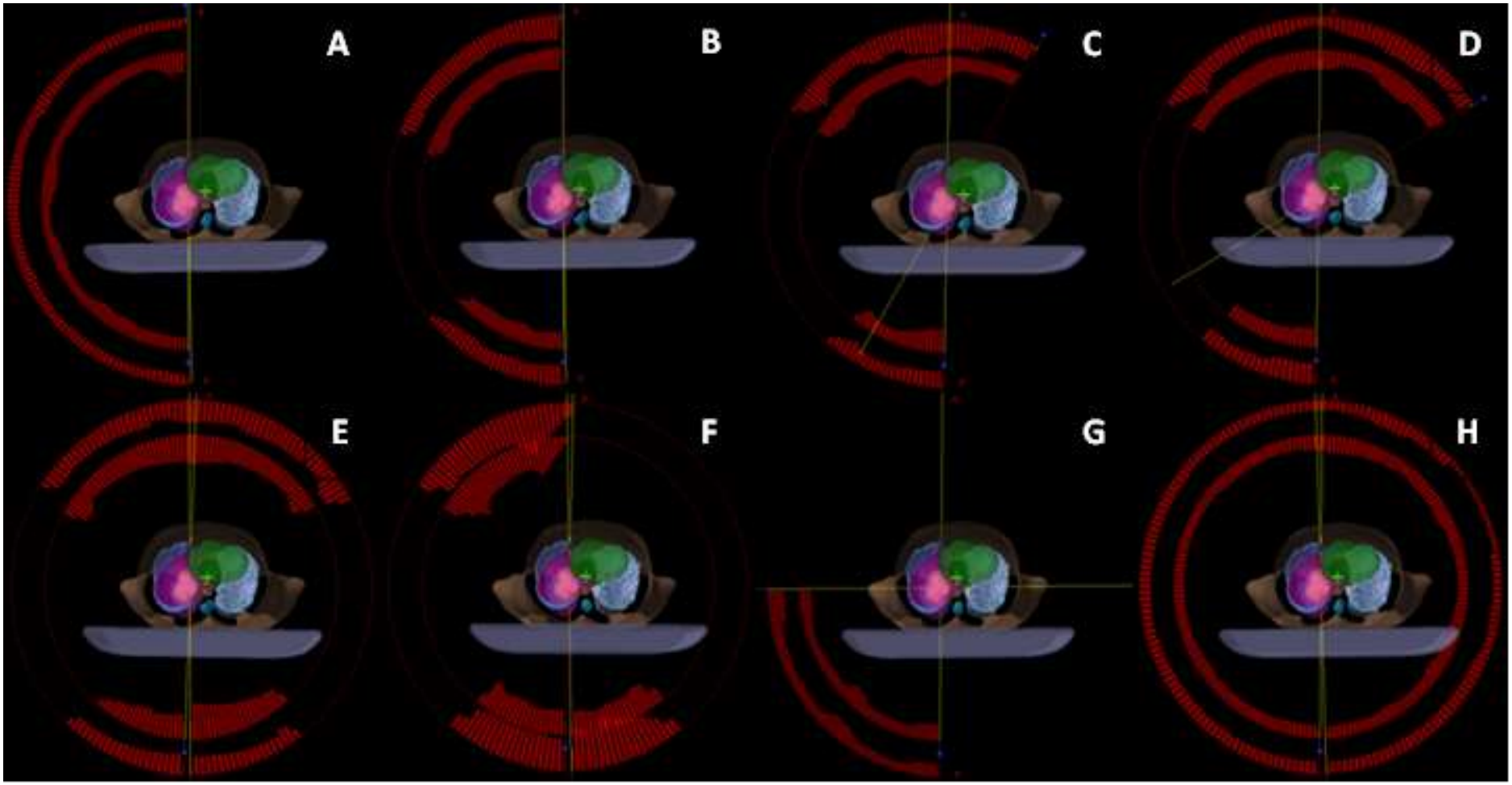

Figure 4.1. Arc parameters for test plans and clinical plans

Different arc parameters can be seen in the figure. A: is the clinical arc parameter, whereas, B to H are the test arc parameters. Start and stop angle and avoidance sectors used for different arc parameters are given in Table 4.1.

4.2.3 Development of knowledge-based planning model

The plans for a training subset of 20 patients were used to develop a knowledge-based planning (KBP) model to predict the optimal arc parameter. A number of patient-specific volumes (i.e., PTV, Lungs, Heart, and overlap of heart with PTV) and the location of the volumes/ structures were recorded and used to develop the KBP model. In addition, each arc configuration was given an identification index (1 to 8) that was used in the correlation analysis to identify/ describe it. Essentially, these indices were used as the predicted arc parameter by the models (see Figure 4.1: 1 to 8, parameters A to H respectively). The KBP model was developed using Multivariate regression analysis in Excel 2016, (see equations 4.3 and 4.4) to predict the arc parameter that will provide the most optimal OAR sparing whilst achieving adequate target coverage for prospective patients. The patient factor was calculated using the patient-specific geometric volumes and the coefficients predicted by the multivariate regression analysis. Several patient factors were produced, firstly using all the patient-specific volumes (see Table 4.2), then the important volumes were identified using the individual *p*-values and the model was refitted using only significant terms. The predicted arc parameter, i.e., geometry number, was rounded to the nearest whole number and compared with the clinician's chosen arc parameter, this was required as the model uses continuous functions to predict a discrete parameter.

$$Arc\ Parameter_{predict} = m\ \times Patient\ Factor \qquad \textbf{Equation 4.3}$$

$$Patient\ Factor = \left[\left(m1 \times \frac{Lungs_{cc}}{PTV_{cc}}\right) + (m2\ \times MSD_{PTV\ and\ Heart}) + \left(m3\ \times MSD_{PTV\ and\ Contralateral\ Lung}\right)\right] \qquad \textbf{Equation 4.4}$$

where MSD: mean square difference in centre of mass between the referenced structures

Table 4.2 Patient-specific volumes and their location used to build different KBP models using multivariate analysis

PTV Vol	Planning target volume (cc)
PTV_X, Y, Z	X, Y and Z coordinate (lateral, vertical and horizontal distance) of PTV centre of mass
Lung Vol	Total lungs subtracted from gross tumour volume (Lungs-GTV) volume (cc)
Heart Vol	Heart volume (cc)
Heart_X, Y, Z	X, Y and Z coordinate (lateral, vertical and horizontal distance) of the Heart centre of mass
CLLung Vol	Contralateral lung volume (cc)
ClLung_X, Y, Z	X, Y and Z coordinate (lateral, vertical and horizontal distance) of Contralateral centre of mass
IlLung Vol	Ipsilateral lung volume (cc)
IlLung_X, Y, Z	X, Y and Z coordinate (lateral, vertical and horizontal distance) of Ipsilateral centre of mass
PTVHeartOverlap	PTV and heart overlap volume (cc)
Body_X, Y, Y	X, Y and Z coordinate (lateral, vertical and horizontal distance) of Body centre of mass
Lungs_2cmCropVol	Lungs-GTV crop back from PTV with a margin of 2 cm (cc)
Lungs_2cmCropVol_X, Y, Z	X, Y and Z coordinate (lateral, vertical and horizontal distance) of lungs crop back 2 cm from PTV centre of mass
Lungs_3cmCropVol	Lungs-GTV crop back from PTV with a margin of 3 cm (cc)
Lungs_3cmCropVol_X, Y, Z	X, Y and Z coordinate (lateral, vertical and horizontal distance) of lungs crop back 3 cm from PTV centre of mass
Lungs_4cmCropVol	Lungs-GTV crop back from PTV with a margin of 4 cm (cc)
Lungs_4cmCropVol_X, Y, Z	X, Y and Z coordinate (lateral, vertical and horizontal distance) of lungs crop back 4 cm from PTV centre of mass
Lungs_5cmCropVol	Lungs-GTV crop back from PTV with a margin of 5 cm (cc) (see Figure 3.1)
Lungs_5cmCropVol_X, Y, Z	X, Y and Z coordinate (lateral, vertical and horizontal distance) of lungs crop back 5 cm from PTV centre of mass
LngHrt_2cmCropVol	Lungs-GTV crop back from Heart with a margin of 2 cm (cc)
LngHrt_2cmCropVol_X, Y, Z	X, Y and Z coordinate (lateral, vertical and horizontal distance) of lungs crop back 2 cm from the Heart centre of mass
LngHrt_3cmCropVol	Lungs-GTV crop back from Heart with a margin of 3 cm (cc)
LngHrt_3cmCropVol_X, Y, Z	X, Y and Z coordinate (lateral, vertical and horizontal distance) of lungs crop back 3 cm from the Heart centre of mass
LngHrt_4cmCropVol	Lungs-GTV crop back from Heart with a margin of 4 cm (cc)
LngHrt_4cmCropVol_X, Y, Z	X, Y and Z coordinate (lateral, vertical and horizontal distance) of lungs crop back 4 cm from the Heart centre of mass
LngHrt_5cmCropVol	Lungs-GTV crop back from Heart with a margin of 5 cm (cc)
LngHrt_5cmCropVol_X, Y, Z	X, Y and Z coordinate (lateral, vertical and horizontal distance) of lungs crop back 5 cm from the Heart centre of mass

4.2.4 Verification of arc parameter prediction model

The model was verified using ten independent patients; a total of 80 treatment plans including original clinical plans were used for verification. All ten patients were re-planned using all seven geometries (i.e., parameters B to H, see Figure 4.1) and the preferred plan was selected for each patient using blind review. These calculations and subsequent selection of clinician preferences were done before the knowledge-based planning model was used to predict which arc parameter should be utilised. This was done to ensure the exclusion of any potential bias of choice by the clinician.

Following the (clinician) selection of the optimal plan, via local protocol/ criteria, the KBP model was used to predict the preferred arc parameter (see equations 4.3 and 4.4) and the prediction accuracy of the model was calculated. Furthermore, the target coverage and OAR doses achieved with the optimal plans (i.e., clinician's selected arc parameters) were compared with the original clinical plans (i.e., plans produced using arc parameter A).

4.2.5 Plan complexity and deliverability

Treatment plan complexity metrics small aperture score (SAS: calculated as the ratio of open leaf pairs where the aperture was less than a defined criterion (2 mm, 5 mm, 10 mm and 20 mm in our study) to all open leaf pairs (see equation 2.2) (Crowe *et al.*, 2014)), MU/Gy, MU/control-point, islands < 1 cc) were calculated using an Eclipse scripting application programming interface (ESAPI) script and compared with those for the original clinical plans.

To evaluate the effect of the avoidance sectors on the deliverability of plans, all plans were measured on a TrueBeam linear accelerator and gamma analysis was performed using

our standard clinical criteria (i.e., percentage of pixels where gamma is less than or equal to unity using criteria of 3%/2 mm (global gamma) with a threshold of 20%) by comparing predicted fluence with the measured fluence. The fluence for each beam was measured using an electronic portal imaging device (EPID) and compared in the portal dosimetry software within the Eclipse™ planning system.

4.3 Results

4.3.1 Effectiveness of personalised arc parameter

The results show that different arc parameters and collimator angles resulted in different dose distributions to OAR volumes, whereas dose to target volume was mostly similar between different arc parameters (see Table 4.3, Figure 4.2). Overall, for all arc parameters, the plans produced using collimator angle of 10^{o} and 350^{o} provided lower OAR doses for similar target coverage. All 240 treatment plans (including the original clinical plans) were reviewed; for each patient, the preferred plans (meeting the local protocol: plans with lowest OAR doses and adequate target coverage) were identified. None of the original clinical plans (i.e., arc parameter A plans) was selected as the preferred optimal plan and, more importantly, different patients required different arc parameters to minimize OAR doses.

The clinician chosen plans were compared with the original clinical plans and the results showed a reduction in OAR doses (see Table 4.4). The reduction in V_5, mean lung dose, mean heart dose and mean body doses were statistically significant whereas the reduction in lung V_{20} and heart V_{30} were not statistically significant. Furthermore, an increase in the total number of MUs was observed, however, this was not statistically significant.

4.3.2 Validation of knowledge-based planning model

The model was validated using 80 plans (n = 10 patients) outside the model. The model developed to predict the optimal arc parameter using equation 4.3, predicted the optimal arc parameter accurately for 80% of patients as compared to clinician-selected (i.e., the total optimal plans) best plans (see Figure 4.3). The m-values (see equation 4.4) are shown in Table 4.5. OAR sparing achieved with the model-predicted arc parameters are displayed in Table 4.6.

4.3.3 Planning complexity and deliverability analysis

A number of complexity metrics were calculated and are presented in Table 4.7. Some of the complexity parameters, (MU/Gy, MU/Degree, mean dose rate and mean leaf speed), suggested the optimal plans were more complex than the original clinical plans. The remaining metrics considered did not indicate an increase in complexity.

The selected (clinician-chosen arc parameters) plans were measured on a Varian TrueBeam linear accelerator. Gamma comparisons of the measured and predicted beam fluences were performed at 3%/2 mm. The results showed overall good agreement with all plans passing the local accuracy standard, which requires ≥ 98 % pixels with gamma less than or equal to unity with a 3%/ 2 mm criteria.

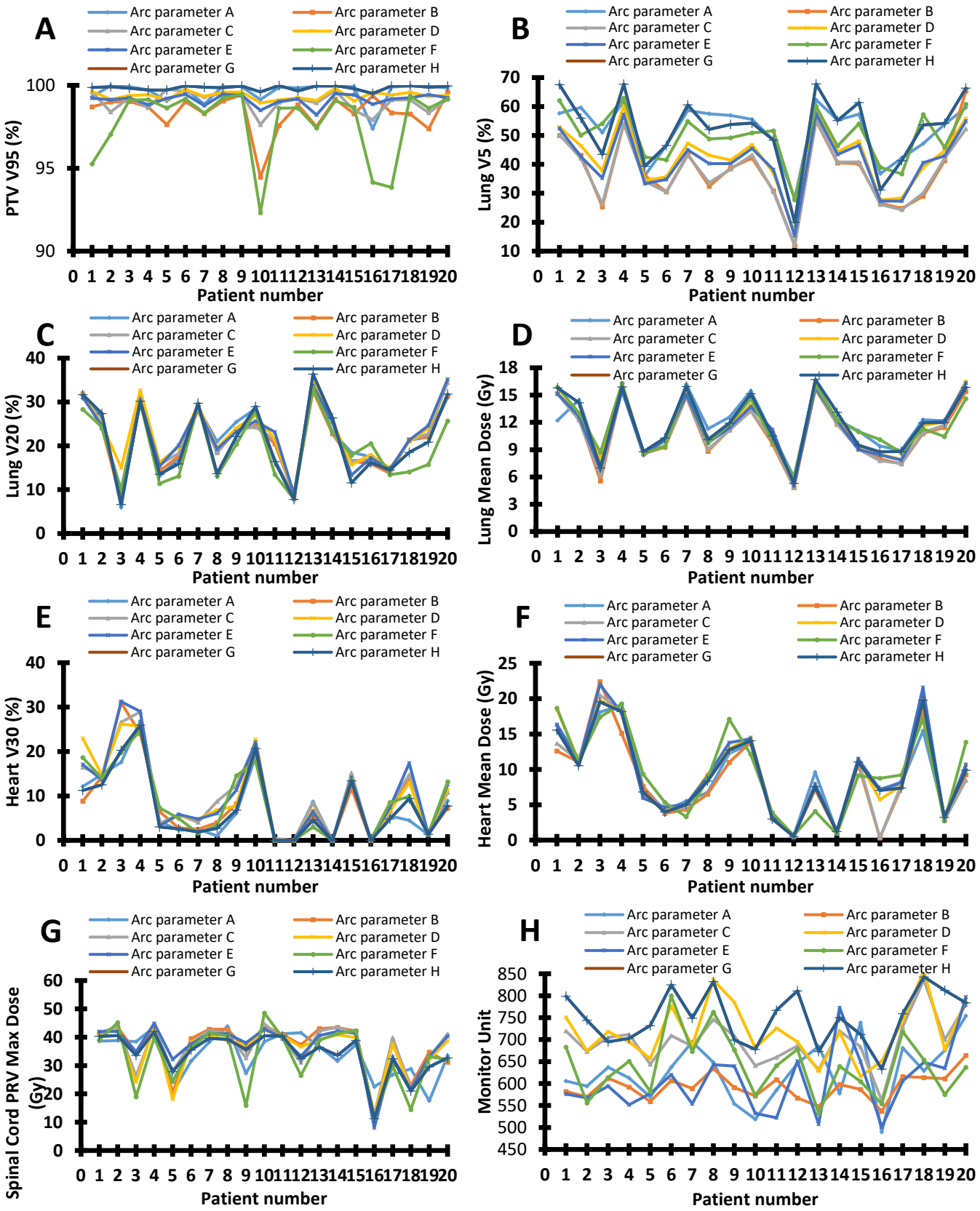

Figure 4.2. Dose distribution achieved with the different arcs defined in Figure 4.1. Different arc parameters resulted in different dose distributions to OAR, whereas the dose to PTV was mostly similar except for five plans from geometry F and one from Geometry B.

Table 4.3. The difference in dose parameters achieved with different arc parameters compared to the half-arc parameter (A) and p values.

Plan Parameters			A	B	p	C	p	D	p	E	p	F	p	G	p	H	p
PTV	V_{95}	≥ 99%	99.6	-1.2	0.000	-0.6	0.001	-0.2	0.145	-0.5	0.002	-1.4	0.000	-1.8	0.000	0.2	0.061
	V_{107}	< 0	0.0	0.1	0.001	0.1	0.001	0.2	0.014	0.1	0.000	0.2	0.030	0.8	0.010	0.0	0.240
Spinal Cord PRV	$D_{0.01cc}$	< 45Gy	33.8	2.9	0.069	2.6	0.158	1.5	0.381	2.7	0.120	4.5	0.009	-0.8	0.694	0.3	0.803
Lungs-GTV	V_{5Gy}	< 60%	51.6	-13.6	0.000	-14.1	0.000	-9.3	0.000	-10.6	0.000	-14.8	0.000	-1.8	0.165	0.4	0.734
	V_{20Gy}	< 35%	21.8	-0.5	0.224	0.2	0.743	1.2	0.064	0.5	0.439	-0.5	0.340	-2.2	0.006	-0.8	0.195
	MLD	< 20Gy	11.9	-1.0	0.001	-0.9	0.005	-0.3	0.173	-0.5	0.062	-1.0	0.003	-0.2	0.432	-0.1	0.821
Heart	V_{30Gy}	< 46%	6.8	1.0	0.283	2.7	0.002	2.2	0.017	2.8	0.011	1.0	0.208	1.6	0.046	0.0	0.938
	MHD	< 26Gy	9.0	-0.8	0.138	-0.4	0.426	0.3	0.388	0.5	0.259	-1.2	0.014	0.5	0.371	0.0	0.991
Total MU			626.8	-33.8	0.017	69.8	0.000	91.3	0.000	-19.5	0.283	27.2	0.035	13.5	0.497	123.2	0.000
Body (mean Gy)			6.9	-0.5	0.000	-0.5	0.000	-0.2	0.002	-0.3	0.004	-0.5	0.000	-0.2	0.010	0.1	0.082

Table 4.4. Dose differences between the original clinical plans (i.e. half-arc plans) and the optimal plans selected for an individual patient.

Structures	Clinical Goals	Clinical	SD	Mean	SD	p
PTV	V95	99.6	0.63	-0.78	0.48	0.000
	V107	0.0	0.02	0.09	0.13	0.003
CI†		1.19	0.05	0.03	0.08	0.028
HI††		0.06	0.02	0.02	0.01	0.000
Spinal Cord PRV	D0.01cc	34.8	6.62	2.31	9.14	0.119
Lungs-GTV	V5Gy	52.2	9.60	-15.05	11.20	0.000
	V20Gy	22.1	7.96	-0.48	7.79	0.348
	MLD	12.1	3.10	-0.97	3.52	0.003
Heart	V30Gy	7.7	7.45	0.53	8.39	0.453
	MHD	9.4	5.30	-1.39	5.23	0.008
Total MU		624.70	69.18	12.10	48.95	0.375
Body (mean Gy)		7.1	1.84	-0.54	1.88	0.000

†Conformity index (CI- calculated using equation 4.1), ††Homogeneity index (HI- calculated using equation 4.2)

Table 4.5. Showing coefficient (m-values) of the knowledge-based planning model developed using patient-specific volumes.

Patient-specific volumes	Coefficient (m-values)
Intercept	9.386
Lungs/PTV	-0.202
MSD! between PTV and Heart	-0.011
MSD! between PTV and contra-lateral Lung	-0.009

! MSD: mean square difference calculated using the centre of the mass of the structures

Table 4.6. Dose differences between the original clinical plans (i.e., arc parameter A) and the optimal plans predicted using the model.

Structures	Clinical Goals	Clinical plan	SD	Optimal plan Mean	SD	p
PTV	V95	99.9	0.63	-0.81	0.08	0.000
	V107	0.0	0.02	0.23	0.02	0.003
CI†		1.19	0.05	0.03	0.08	0.028
HI††		0.06	0.02	0.02	0.01	0.000
Spinal Cord PRV	D0.01cc	30.3	6.62	-1.11	6.19	0.119
Lungs-GTV	V5Gy	49.3	9.6	-13.51	12.36	0.000
	V20Gy	19.3	7.96	1.00	6.73	0.136
	MLD	11.1	3.1	-0.83	2.78	0.033
Heart	V30Gy	5.5	7.45	1.02	7.91	0.090
	MHD	7.4	5.3	-0.41	5.25	0.031
Total MU		662.75	69.18	14.60	57.40	0.559
Body (mean Gy)		6.0	1.84	-0.66	1.70	0.077

†Conformity index (CI- calculated using equation 4.1), ††Homogeneity index (HI- calculated using equation 4.2)

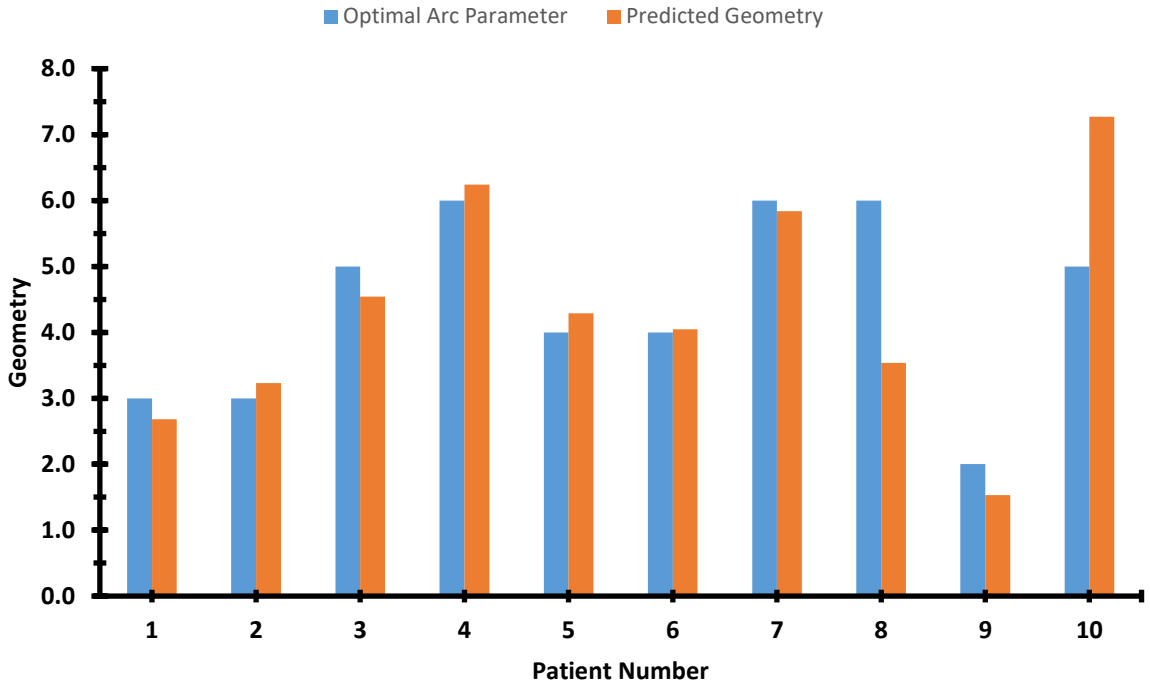

Figure 4.3: **Optimal arc parameter and predicted arc parameter for the test plan.**

Arc parameters were calculated using equation 4, and the predicted arc parameter number was rounded to the nearest number and compared with the optimal arc geometries to validate the model.

4.4 Discussion

Modern arc-based intensity-modulated radiotherapy treatment planning and delivery techniques enable the reduction of the volume of critical structures (OARs) receiving higher doses but increase the volume receiving lower doses (Marks *et al.*, 2009; Diwanji *et al.*, 2017), which remains a concern. In view of the new knowledge (Wang *et al.*, 2006; Marks *et al.*, 2009; Wang *et al.*, 2020b), both dose to the lungs and the heart needs consideration, which means the planning or radiotherapy treatment is considerably more difficult and hence the need for new/ individualized approaches. This study investigated the use of full-arcs (i.e., arc parameter H), short-arcs (i.e., arc parameter G), and arcs with multiple avoidance sectors for treatment planning of inoperable locally advanced lung cancer patients, aiming to reduce OAR dose without compromising target coverage.

The technique presented here separates continuous, half and full, arcs into segmented ones with avoidance sectors, in order to avoid direct (incident) irradiation of normal tissues. Whereas from a dose reduction perspective this follows a simple maxim of conventional radiotherapy, in the context of intensity modulation it also reduces the degrees of freedom available to the optimizer to deliver the required dose to the target. Under these circumstances, an unwanted coincidental effect may be a reduction in the control of the dose to the target or larger contributions from 'allowed' directions which may increase the complexity of delivery, possibly significantly.

Table 4.7. Plan complexity metrics calculated for both the original clinical plans and the test plans.

Complexity metrics	Mean Original clinical plans	SD	Mean Test plans	SD	p-value
MUperGy	224.65	21.93	242.01	9.95	0.001
MUPerDegree	1.73	0.17	2.36	0.10	<0.001
MeanDoseRate	483.27	38.94	521.97	8.08	<0.001
MeanLeafSpeed	10.82	0.48	7.53	0.39	<0.001
MeanLeafTravelPerMU	0.97	0.09	1.00	0.06	0.144
FractionMUthrough<5cc	0.00	0.00	0.00	0.00	0.056
IslandsPerCP	3.62	1.54	3.66	0.44	0.911
MeanIslandSize	1433.82	694.14	1317.52	201.73	0.410
FractionIslandBelow1cc	0.47	0.18	0.49	0.04	0.674
SAS02	0.17	0.04	0.17	0.02	0.813
SAS05	0.20	0.05	0.20	0.02	0.582
SAS10	0.25	0.07	0.26	0.02	0.292
SAS20	0.36	0.09	0.37	0.03	0.376

In this study, we report that deliverable, clinically acceptable VMAT with 'optimised avoidance sectors' plans can be produced using different arc parameters and collimator angles. Treatment plans produced with different arc parameters and collimator angles provided different amounts of OAR sparing. A clinical review of all plans produced for each patient indicated that, although meeting (OAR dose) acceptability criteria, when using the KBP prediction model more optimal plans were always found in preference to original clinical plans. OAR sparing was relatively higher for collimator angles of 10^{o} and 350^{o} compared to other collimator angles used but this was not significant compared to the OAR sparing achieved with the arc parameters.

It was also noted that patient-specific arc parameters provided the highest OAR sparing without clinically significantly compromising target coverage. This shows the importance of the personalization of arc geometries based on each patient's anatomy. A standardized (i.e., arc parameter A or H) arc parameter may not be the optimal solution for treating these patients especially when there are larger variations in target size, shape and location with respect to the OARs volume. The reduction in lung doses is significantly higher in our study compared to other studies (Chan *et al.*, 2011; Mayo *et al.*, 2008), but more notably, our study also reports a reduction in heart doses (significant reduction in mean heart dose), whilst the other studies (Chan *et al.*, 2011; Mayo *et al.*, 2008) reported a systematic increase in heart dose. Additionally, it was noted that the personalization of arc parameters also resulted in a reduction in the mean dose delivered to a patient, despite a small increase in MUs.

Various arc geometries were tested and compared to the original clinical plan. These included full arcs (i.e., arc parameter H), short arcs (i.e., arc parameter G) and arcs with different avoidance sectors (i.e., arc parameter B to E) except for three arc geometries (i.e., arc parameter A (the original clinical arc parameter), G and H). For these arc parameters, avoidance sectors were not used. The 90^{o} arcs were placed in the same quadrant as the tumour.

It was interesting that the original clinical plans (i.e., the plans produced using arc parameter A) or plans produced using arc parameters G and H were not selected as the optimal plans for any of the patients. These arc parameters resulted in significantly higher OAR doses compared to the other test plans. A difference in the target coverage in the plans produced using different arc parameters was not clinically significant, except

for the four plans produced using arc parameter G where the target coverage dropped below 95.0 %.

Moreover, a number of relatively simple knowledge-based planning models were developed to predict arc parameters using OAR volumes, target volume and their centre of mass location. The KBP model developed using, lungs, PTV and mean square difference in the centre of mass of PTV, heart and contralateral lung predicted optimal arc parameter accurately for 80 % of the patients. This model will improve planning efficiency by predicting optimal arc parameters and help reduce OAR doses whilst maintaining target coverage. For two patients, the predicted arc parameters did not match those selected by the clinician, we considered this likely due to the difference in the tumour geometry for these patients compared to the other test patients and the model may be improved in any further work. Furthermore, fine-tuning the arc geometry (start angle, stop angle, avoidance sector span) may provide further benefit in optimal OAR sparing, however, prediction of the 'baseline' arc parameter will potentially save many initial 'iterations' in the planning process. For the patients where the model predicted arc parameter did not match the one selected in the blind review, the predicted plan had lower OAR doses compared to arc parameter A, but the doses were slightly higher compared to the plan with optimal arc parameter.

The conformity and homogeneity indices were calculated and compared for the clinical and the test plans. The results showed statistically significant differences between the clinical and the test plans, but differences were clinically not significant. The mean difference in CI and HI was 0.03 and -0.02 respectively compared to plans with arc parameter A. The CI for the test plans was clinically similar to the original clinical plans (arc parameter A plans) as doses outside the PTV structure were controlled by using a

ring structure. At HUTH, the dose outside the PTV is controlled using the NTO function and a ring structure (an optimisation structure: produced by adding an inner margin of -0.5 cm and an outer margin of 1.5 cm). During plan optimization, an upper limit of 0% of the ring structure receiving < 5Gy less dose than 95% of the prescription dose was used.

Furthermore, the results from the clinical review showed that arc parameter F was chosen more frequently than the other arc parameters: this arc parameter consists of two full arcs with avoidance sectors (see Figure 4.1), so it is important to verify gantry clearance prior to treatment delivery to avoid collision issues. In our experience, this will not be a problem for the majority of patients, but for those where the lateral shift is ≥ 10 cm from the midline, verification will be required prior to treatment delivery.

A number of studies reported that plan complexity is dependent on the number of small segments, MU/Gy and number of MU per control point (MU/Degree) and reduction in these parameters could reduce the plan complexity and reduce errors in delivery (Webb, 2003; Abdellatif and Gaede, 2014). An increase in the total number of MU seen in the optimal plans could mean that these plans are more complex to deliver. In order to test this hypothesis, treatment plan complexity metrics were calculated for both plans. The deliverability was assessed by measuring plans on a TrueBeam linear accelerator. The results showed a significant increase in MU/Gy, MU/degree, mean dose rate and mean leaf speed in the test (i.e., optimal) plans, however, the plans were shown to be deliverable within our 'challenging' accuracy acceptable requirements.

The results show significant reductions in lung V_5 with mean lung V_5 reduced below 42 % (a threshold reported by Wang *et al*). Therefore, this approach should significantly limit lung toxicities below grade 3 for these patients. Furthermore, our study reported significant reductions in mean heart dose; this approach would help reduce mean heart

dose below 15 Gy, where severe cardiac toxicities are reduced significantly (Wang *et al.*, 2020b). A reduction in toxicities may improve the quality of life for these patients. Also, reductions in OAR doses can facilitate dose escalation for these patients.

The current version/license of the planning and delivery system at our clinic does not allow the use of non-coplanar arc geometries. Therefore, this was not investigated in this study. Further evaluation would be required to assess if non-coplanar arcs can help reduce OAR doses for inoperable advanced-stage NSCLC patients.

4.5 Conclusion

Overall, treatment plans produced using personalized arc parameters were superior compared to the clinical plans. This method not only utilizes the benefits of the VMAT planning technique (reducing the volume of healthy lungs receiving higher doses without compromising target coverage) but also reduces OAR doses. This could reduce toxicities and improve the quality of life for locally advanced-stage lung cancer patients treated with VMAT radiotherapy. The model has been implemented clinically for lungs where doses to healthy lung volume are either close to tolerance or exceeding the tolerance values (approximately 30% of the total radical lung cancer patients are planned using the model) and all oesophagus patients and we will report the toxicity data in future.

5.0 Validation of in-house knowledge-based planning model for predicting change in target coverage during VMAT radiotherapy to in-operable advanced-stage NSCLC patients

The research in this chapter was published in a peer-reviewed journal and therefore the text presented here is adapted from the article. My contribution consisted in conceptualising the research strategy, performing the research and writing the manuscript with input from my supervisors on designing and planning the work and editing the manuscript and clinical inputs from clinicians Dr. A Wieczorek, and Dr. S Upadhyay. Reference: Tambe, N. S.; Pires, I. M.; Moore, C.; Wieczorek, A.; Upadhyay S.; Beavis, A. W., Validation of in-house knowledge-based planning model for predicting change in target coverage during VMAT radiotherapy to in-operable advanced-stage NSCLC lung cancer patients. Biomed. Phys. Eng. Express, 2021. 7.065002.

5.1 Introduction

Adaptive radiotherapy (ART) is an interactive process where treatment plans are modified to account for internal and/or external anatomical changes observed on volumetric images acquired prior to treatment delivery (Berkovic *et al.*, 2015; Li, 2011; Yan *et al.*, 1997; Britton *et al.*, 2007; Juhler-Nottrup *et al.*, 2008; Fox *et al.*, 2009). Anatomical changes, such as atelectasis, tumour baseline shift (0.5 cm (Tennyson *et al.*, 2017) to 1.5 cm (Mao *et al.*, 2017)), infiltrative changes, tumour progression, and pleural effusion, are inevitable during radiotherapy (Bosmans *et al.*, 2006; van Zwienen *et al.*, 2008; Fox *et al.*, 2009; Britton *et al.*, 2009; Britton *et al.*, 2007; Juhler-Nottrup *et al.*, 2008; Kwint *et al.*, 2014; Moller *et al.*, 2016). Significant anatomical changes could alter the planned dose distribution to an unacceptable level that could affect treatment outcomes (Kataria *et al.*, 2014; Langendijk *et al.*, 2008). Work performed by Britton et al reported an average reduction in the dose to 95% of the planning target volume (PTV) and internal

target volume (ITV) by – 11.9% ± 12.1% and – 2.5% ± 3.9% respectively compared to the original clinical plan distribution (Britton *et al.*, 2007; Britton *et al.*, 2009). Furthermore, several studies have also reported an increase in organs at risk (OAR) doses as a result of a change in internal anatomy (Britton *et al.*, 2007; Britton *et al.*, 2009; Kataria *et al.*, 2014). These studies have shown that ART improves treatment outcomes (Kataria *et al.*, 2014) for advanced-stage non-small cell lung cancer (NSCLC) patients as prescription doses are delivered as planned, OAR doses are reduced and it allows dose escalation (Yan *et al.*, 1997; Britton *et al.*, 2007; Juhler-Nottrup *et al.*, 2008; Fox *et al.*, 2009; Li, 2011; Kataria *et al.*, 2014; Berkovic *et al.*, 2015; Sibolt *et al.*, 2015; Ramella *et al.*, 2017).

Different thresholds have been used to initiate adapting planning, including an increase in OAR doses and/or reduction in ITV and PTV V_{95} coverage compared to the original clinical plans (V_{95}: volume of PTV or ITV receiving ≥ 95% of the prescription dose). Treatment plans were adapted for the patients where PTV and/or ITV volume(s) receiving 95% of the prescription dose reduced by ≥ 3% and/or ≥ 1% respectively (Britton *et al.*, 2007; Britton *et al.*, 2009; Spoelstra *et al.*, 2009; Moller *et al.*, 2016). In addition to the target coverage threshold, Moller et al investigated if ART could be triggered using surrogate volumes, using ring structures around the gross tumour volume (GTV) and lymph nodes with margins of 2 mm and 5 mm respectively. ART was considered for the patients where the target volumes move outside the ring structures. They reported that 98% of the patients were identified correctly for adaptive planning using the reported trigger criteria (Moller *et al.*, 2016).

However, implementing ART clinically is challenging, especially in identifying the patients who may benefit from ART in a timely manner. Some may not benefit where anatomical changes or tumour baseline shift is not sufficient enough to warrant plan

adaption. The typical processes used for identifying the patients for adaptive planning are time-consuming and require the patients to undergo the full planning process (i.e., rescanning, re-contouring and re-optimising). This could significantly increase the clinical workload and also increase the radiation burden on these patients. Therefore, it is important to develop alternative methods to accurately identify patients for ART, without sending the patients through the full re-planning process for efficiency and convenience.

This study aims to investigate different adaptive strategies for inoperable advanced-stage NSCLC patients treated with VMAT and to develop in-house knowledge-based planning (KBP) models to identify patients requiring adaptive radiotherapy (i.e., models predicting changes in planning target volume coverage). A combination of patient-specific parameters and the change in PTV V_{95} coverage were used to build the models. Finally, the models were verified by comparing their prediction accuracy with the ones calculated on synthetic computerised tomography (sCT).

5.2 Methodology

5.2.1 Data collection

A total of twenty-five pre-existing patients' data were collected from the Eclipse treatment planning system and Lorenzo™ electronic patient record databases. A number of parameters, including, patient demographics, histopathology, tumour staging, immune histology, PTV volume in cubic centimetres (cc), and dose-volume histogram for PTV for each treated fraction were collected. The original clinical plans were produced as described in section 2.3. This study was performed with prior approval from the local research and development department.

5.2.2 Assessment of adaptive planning

Production of synthetic CT (sCT): the cone beam computerised tomography (CBCT) images acquired prior to each treatment fraction were imported in the Velocity 'adaptive radiotherapy' software (Velocity 4.0, Varian Medical Systems, Palo Alto, CA). To facilitate image processing within Velocity, the following was undertaken. The CBCT images are reconstructed with a slice thickness of 0.3cm to match the planning CT images.

1) The treatment planning CT (pCT) and CBCT images were initially rigidly registered using the same transformation obtained during the respective treatment session, to remove the impact of residual setup errors (Wang *et al.*, 2020a).

2) The setup corrected using translational corrections only (6 degrees of freedom correction is not available in our clinic). CBCT images were deformably registered to pCT images excluding the most superior and inferior slices to produce a synthetic image set (sCT).

3) A secondary structure data set was produced in the sCTs, including GTV and organs at risk (OAR) volumes. The registration and volumes for each sCT were reviewed.

Evaluation dosimetric variations*:* sCTs produced within the Velocity software platform were imported into the Eclipse treatment planning system. The GTV for each fraction was reviewed and edited where required by the experienced clinical oncologist to account for tumour baseline shift and anatomical changes. Furthermore, clinical and planning target volumes were produced on each sCT by applying the same margin as the clinical plan. Then, doses were calculated on each synthetic CT (daily) using the same monitor units

(MU) as the original clinical plan and the difference in PTV V_{95} coverage ($\Delta V95^{PTV}$) for each fraction was calculated (equation 5.1) and used to build the models.

Dose calculations in Eclipse V15.6: The planning system was upgraded to V15.6 prior to the experiment, so all the original clinical plans were recalculated in V15.6 using the same MUs as the original clinical plan (i.e. V13.7). Doses were calculated on sCT in V15.6 and compared with the clinical planned dose distribution calculated in V15.6. The PTV coverage by 95% of the prescription dose is denoted $V95^{PTV}$; the coverage planned on the planning scan is given a subscript 'planned' and the delivered dose calculated on the synthetic scan is given a subscript 'delivered'.

$$\Delta V95^{PTV} = (V95^{PTV}_{Delivered} - V95^{PTV}_{Planned}) \qquad \textbf{Equation 5.1}$$

Target volume baseline shift: the baseline shift of the centre of the mass (CoM) between the planned PTV (i.e. PTV from the original clinical plans) location and the adapted PTV (i.e. PTV produced on each sCT) was recorded. The mean square difference (MSD) of the CoM shift was calculated for each fraction, being $[\frac{1}{3}\sum \Delta Xi^2]$ where *i* represents the x, y, and z components of the shift vector.

Immune-histology: Recent clinical trial results showed significant improvement in overall survival in patients who received consolidation treatment with Durvalumab (immunotherapy) (Antonia *et al.*, 2017; Brahmer *et al.*, 2018; Antonia *et al.*, 2018; Paz-Ares *et al.*, 2020). Durvalumab is a human monoclonal antibody that selectively binds to programmed death ligand-1 (PD-L1), blocking its interaction with its receptor, PD-1 (programmed death-1) (Antonia *et al.*, 2017; Antonia *et al.*, 2018; Paz-Ares *et al.*, 2020). In the trial, Durvalumab was administered to patients who have had stable disease or treatment response following chemo-radiotherapy (Antonia *et al.*, 2017; Brahmer *et al.*,

2018; Antonia *et al.*, 2018; Paz-Ares *et al.*, 2020). In our clinic, immune histological testing for PD-L1 expression in NSCLC patients started in 2017. Cell samples taken at biopsy were sent to immune-histology labs to assess PD-L1 expression using the Dako PD-L1 IHC 22C3 pharmDx test. These data were stored in the electronic patient record-keeping system, Lorenzo™ and available for this study.

5.2.3 Development of model

Four knowledge-based planning models were developed using multivariate analysis. Twenty patients' data were used to develop the models and that for five patients were retained for verifying the model predictions. PTV V_{95} coverage was calculated for each fraction; PTV volume, lungs-GTV (total lungs volume subtracted from GTV) volume, Heart (cc) volume, as contoured at planning in cubic centimetres (cc) and MSD, for each fraction, were calculated and used to develop the models. Three models were developed using MSD, PD-L1 and PTV volume parameters to predict the change in PTV V_{95} coverage for each fraction. The PD-L1 parameter was readily available for all the patients included in this study, the initial intention was to assess if it can predict tumour response, and hence help trigger ART. No correlation was observed so later it was included to develop the models. Model 1 was developed using MSD (fraction term) and planning PTV (patient term) (see equation 5.2), Model 2 using all three parameters, fraction term (MSD) and patient term (PD-L1 and PTV) (see equation 5.3) and the Model 3 was developed using MSD and PD-L1 (see equation 5.4) and Model 4 was developed using PTV and PD-L1 (see equation 5.4). The prediction accuracy of each model was calculated using equation 5.6 (where j refers to the model index) and assessed.

$$Model\_1 = [(m_{MSD} \times MSD) + (m_{PTV(cc)} \times PTV_{cc})] \quad \textbf{Equation 5.2}$$

$$Model\_2 = [(m_{MSD} \times MSD) + \left(m_{PTV(cc)} \times PTV_{cc}\right) + (m_{PDL1} \times PD - L1)] \quad \textbf{Equation 5.3}$$

$$Model\_3 = [(m_{MSD} \times MSD) + (m_{PDL1} \times PD - L1)] \quad \textbf{Equation 5.4}$$

$$Model\_4 = [(m_{PTV} \times PTV) + (m_{PDL1} \times PD - L1)] \quad \textbf{Equation 5.5}$$

$$Predict\ \Delta V95^{PTV} = m \times Model\_j \quad \textbf{Equation 5.6}$$

5.2.4 Verification of the models

The models were verified by predicting a change in PTV V_{95} coverage ($\Delta V95^{PTV}$) for five patients that were independent of those used for creating the models. The predicted change for each fraction (using all three models) was compared to the dose coverage calculated on each fraction's synthetic CT.

5.3 Results

5.3.1 Development of models

The knowledge-based planning models were developed to predict the change in PTV V_{95} coverage ($\Delta V95^{PTV}$) using combinations of PD-L1 expression as a biomarker, MSD: tumour baseline shift, PTV, lungs-GTV, and heart size (Figure 5.1). However, the models developed using OAR volumes did not improve prediction accuracy. A total of 400 fractions (n = 20 patients) were used to develop the models (see Table 5.1 for patient demographics). The observed range of the data was: MSD 0.0 to 20.23 mm, PD-L1 0.0% to 100.0% and difference in PTV V_{95} coverage -11.8% to 10.1%.

Table 5.1: Patient demographics for the patients included to build and verify the models.

	Mean/Frequency/Range Within Models	Mean/Frequency/Range Verification (outside models)
Age mean (+/- SD)	70.37 (6.72) Years	69.42 (7.32) Years
Gender		
Male	9	3
Female	11	2
Staging	T1aN0/T4N3	T1aN0/T4N3
PTV volume (cc)	325.6/164.0 – 507.2	269.7/97.8 – 476.41
Histology		
Adenocarcinoma	10	2
Squamous cell carcinoma	10	3

5.3.2 Accuracy of models

$\Delta V95^{PTV}$ was predicted using all three models for 100 fractions (n = 5 patients) (Figure 5.2). Model 1 showed statistically significant differences (i.e. model 1 did not model the change in PTV coverage volume well) between the prediction and calculated PTV V_{95} coverage with p = 0.018, whereas models 2 and 3 did not show significant differences with p = 0.163 and 0.509 respectively.

Furthermore, the percentage of fractions with $\Delta V95^{PTV}$ between ± 0.5% and ± 1.0% was calculated (Table 5.2). The results show that model number three, developed using PD-L1 and MSD, predicted 77% of the total fractions within ± 1.0%. The percentage of such fractions was lower for models 1, 2 and 4, 48%, 59% and 29% respectively. The coefficients (m values) for all three models are shown in Table 5.3.

Table 5.2. Percentage of total fractions of the test plans within the different trigger limits.

	±0.5%	±0.6%	±0.7%	±0.8%	±0.9%	±1.0%
Model1	24%	28%	34%	37%	43%	48%
Model2	32%	39%	42%	45%	53%	59%
Model3	58%	65%	71%	74%	75%	77%
Model4	14%	16%	19%	22%	29%	29%

Table 5.3. Coefficients of the models developed for predicting change in target coverage.

	Model1	Model2	Model3	Model4
Patient factor		**Coefficients**		
Intercept	-2.228	-1.342	0.237	-3.890
MSD	-0.577	-0.669	-0.727	N/A#
PD-L1	N/A#	-0.012	-0.017	-0.002
PTV Vol (cc)	0.005	0.004	N/A#	0.005

the volumes were not included in the models so do not have a coefficient.

These data are depicted over a broader range of comparison thresholds in Figure 5.1 and plots of individual fraction prediction against measured difference, for all the test fractions, are shown in Figures 5.2A-C.

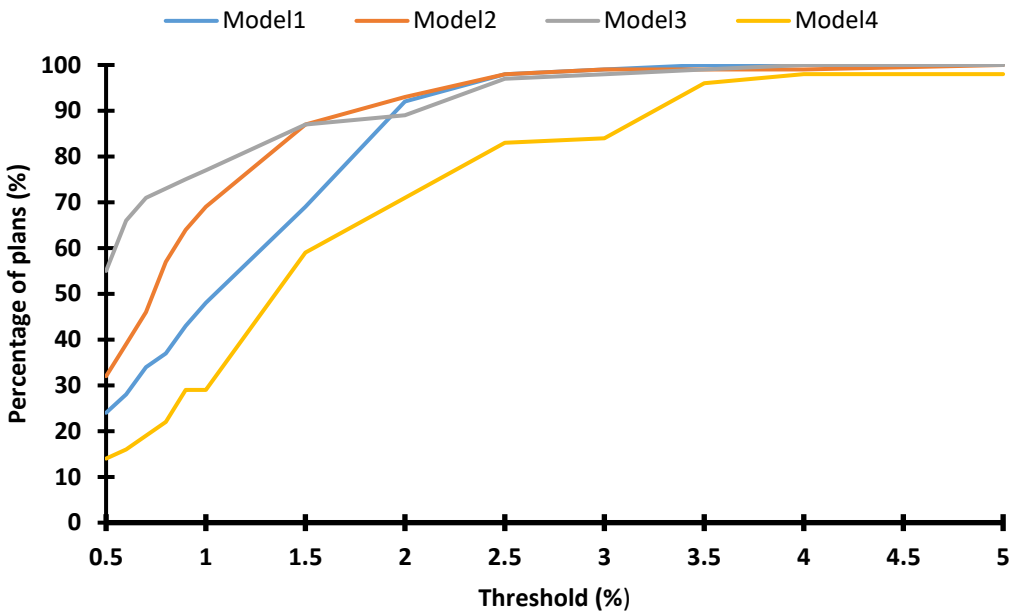

Figure 5.1: Percentage of total fractions within plus and minus the defined threshold.

The models were developed using equations 5.2, 5.3, and 5.4. The results illustrated that model 3 had superior accuracy compared to models 1 and 2, 4, especially at stricter tolerances.

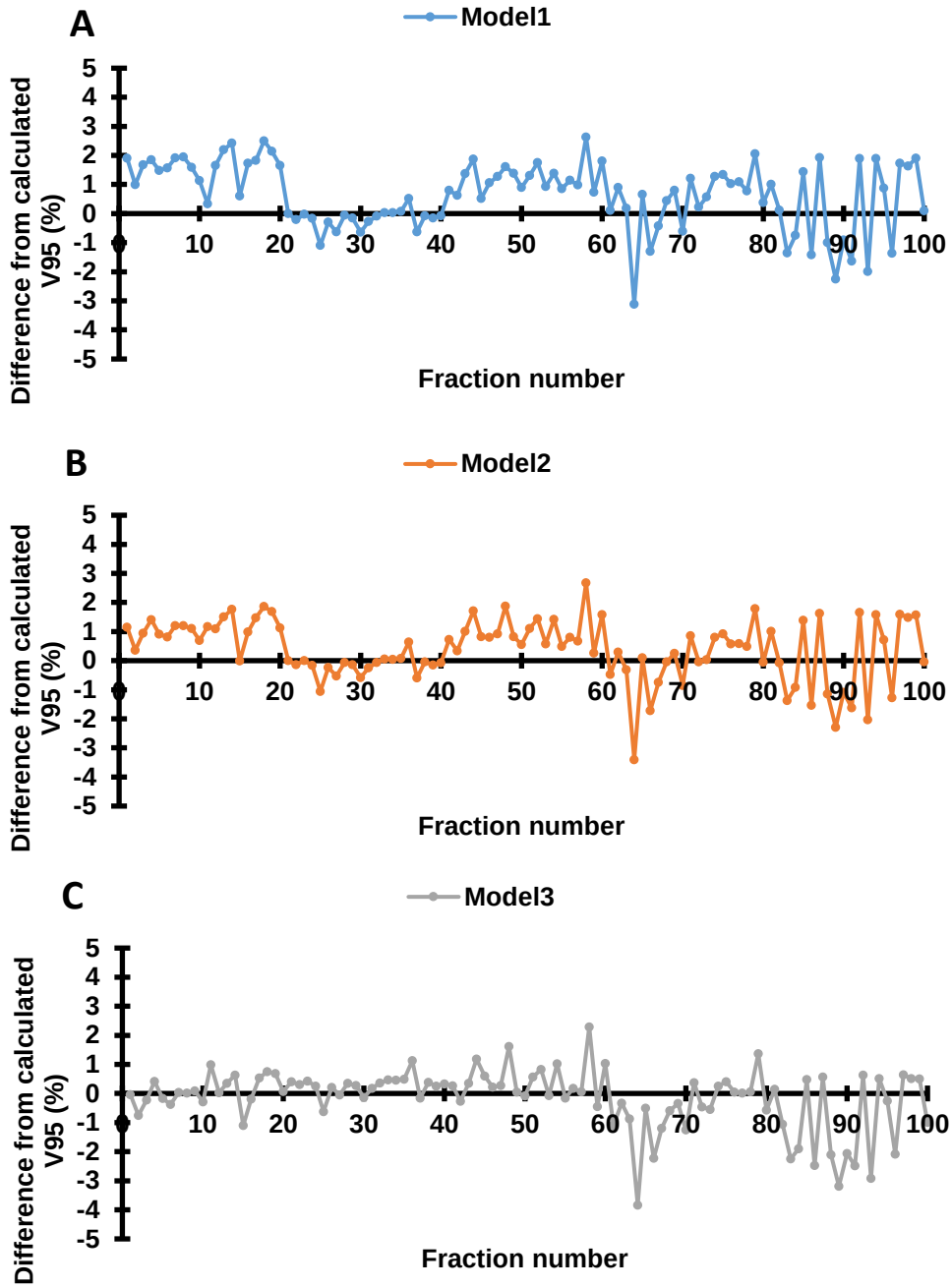

Figure 5.2: Verification data for all three models.

A) Results from the model developed using mean square difference (MSD) and PTV volume (cc); B) Results from the model developed using MSD, PTV volume and PD-L1; C) Results from the model developed using PD-L1 and MSD.

5.4 Discussion

Anatomical changes, either internal (e.g. atelectasis, tumour shrinkage or growth, or shift tumour location) and/or external (patient weight loss), commonly occur during the course of radiotherapy for inoperable advanced-stage NSCLC patients. Significant changes in anatomy could alter planned dose distribution and affect treatment outcomes for patients if treatment plans aren't adapted. Several studies have demonstrated the benefits of adaptive radiotherapy.

Furthermore, the frequency of adaptations is important especially when the patients are treated with fewer numbers of fractions (hypo-fractionated radiotherapy, e.g. 55 Gy in 20 fractions) as compared to conventional fractionated radiotherapy (66 Gy or 60 Gy in 33 or 30 fractions respectively). Volumetric imaging and time-consuming re-planning are required to assess and make treatment management decisions. This could significantly increase clinical workload and also increase the radiation burden due to additional planning CT (over and above the daily CBCT) to the patients who do not benefit from adaptive planning. Therefore, more efficient methods are required to assess if the patients would benefit from adaptive planning or not and to assess the optimal time for adaption.

A percentage drop in PTV V_{95} coverage has been commonly used to trigger ART planning (Britton *et al.*, 2007; Britton *et al.*, 2009; Spoelstra *et al.*, 2009; Moller *et al.*, 2016). To efficiently estimate PTV coverage we felt it was important to develop in-house KBP models using patient-specific parameters with/without data available from patient set-up at the beginning for the fraction. The 'fraction data' considered were PTV characteristics, specifically the difference between the planned PTV and the PTV at the treatment fraction as represented by the MSD of the shift between their respective

centres of mass. The results showed that relatively simple models can predict change in PTV V_{95} coverage efficiently *and* accurately, as compared to recalculations based on original clinical plans, which was the primary aim of this study. The models will be implemented clinically at HUTH using ESAPI scripting. The script can obtain PTV size from the planning system, whereas the PD-L1 value will have to be entered manually as this data is stored outside the planning system. The script can calculate PTV coverage and compare it with the local trigger value of 3%.

It was interesting to observe that the model developed using both PTV characteristics and PD-L1 data (patient term) combined had higher predictions than the model developed using the PTV characteristics or MSD only. Higher PD-L1 values were associated with a higher drop in PTV coverage (i.e., patients with higher PD-L1 values will require more adaption compared to the patients with lower PD-L1 values). However, the model built with PD-L1 data and the single 'fraction' PTV characteristic representing the relative change between plan and fraction presentation had higher accuracy compared to the model produced using these along with the 'planning' PTV size (patient term). This points towards the necessity or importance of having a term that represents the physical changes between the plan and the delivery fraction. A fourth model was investigated that used the planning PTV data and PD-L1 data, however, extremely poor correlation or predictive potential was noted and this option was discarded early in our study.

Validation of the models indicated a superiority of the predictive benefit of a combination of the PD-L1 data and the shift of PTV centre of mass at very exacting comparison criteria (≤ 1%); we note that for more forgiving thresholds (i.e., ≥ ± 2.0%) the three models converged. Compared to the study by Moller (Moller *et al.*, 2016), the prediction accuracy of models 1 and 2 was higher at a locally used trigger level of 3% for adaptive planning

(i.e., a 3% reduction in PTV coverage triggering the decision) whereas it is the same for the model 3. However, the approaches in that study and ours were very different; our study does not require to produce any additional structures which is the basis of their methodology, as described by Moller (Moller *et al.*, 2016). At a 5% trigger level (Britton *et al.*, 2007; Britton *et al.*, 2009; Spoelstra *et al.*, 2009; Moller *et al.*, 2016), the prediction accuracy is 100% for all three of the models presented here. Furthermore, unlike other studies, the models presented in our study can predict trends and could help manage workload.

The parameters used in this study are readily available for all advanced-stage inoperable lung cancer patients. The patient-specific (PTV volume and PD-L1) parameters are available before starting radiotherapy: PD-L1 is acquired for all advanced-stage NSCLC patients to decide if the patient is suitable for immunotherapy and the PTV volume is contoured for all radical lung patients prior to starting treatment (a new PTV will be generated for patients requiring adaptive radiotherapy and the new PTV size will be used in the models for succeeding prediction). The treatment fraction-specific information is available (in some form) for all patients who undergo volumetric image-guided radiotherapy and is obtained prior to delivering each treatment fraction. This means that our models can trigger adaptive radiotherapy using readily available information and more importantly prior to the delivery of each fraction. We continue to consider and explore models that will help predict the likelihood a patient may benefit from an adaption strategy, based on characteristics independent of radiotherapy planning/treatment.

In this study (reflecting our clinical capability) we only considered the use of 3 Degrees of Freedom (3DOF) registration and corrections. This requires that a greater translation

in the registration may be needed, to offset the lack of rotational correction, and would be represented by a larger MSD term in our calculations. In our models, this leads to a larger estimate of the predicted change in PTV coverage which, if greater than the trigger level for re-planning, may lead to a replan (adaption) that wouldn't have been required should a 6DOF correction have been available. However, we do not consider this to be a limitation of our methodology since the replanning is triggered in response to the capabilities of the treatment system under consideration.

5.3 Conclusion

This study showed that relatively simple KBP models can accurately *and* efficiently predict change in the PTV (V95) dose coverage without the need for full-dose calculations. We found that a model based on a parameter (MSD) representing the spatial shift of the PTV between planning and treatment verification scan and a patient-specific parameter (PD-L1) resulted in better accuracy of prediction. The application of such methodologies will help to streamline the adaptive radiotherapy planning process for advanced-stage inoperable non-small cell lung cancer patients. These models could be used in the context of on-table adaption or in a more conservative approach where a trend over 'fractions to date' are considered to predict a likely need for adaption on a 'near future fraction'. More importantly, in this study, a patient-specific biomarker (PD-L1), which is independent of the radiotherapy planning or treatment (verification) parameters, has been used for the first time and shown to be valuable in developing a model for predictively triggering Adaptive Radiotherapy.

Appendix Chapter 5

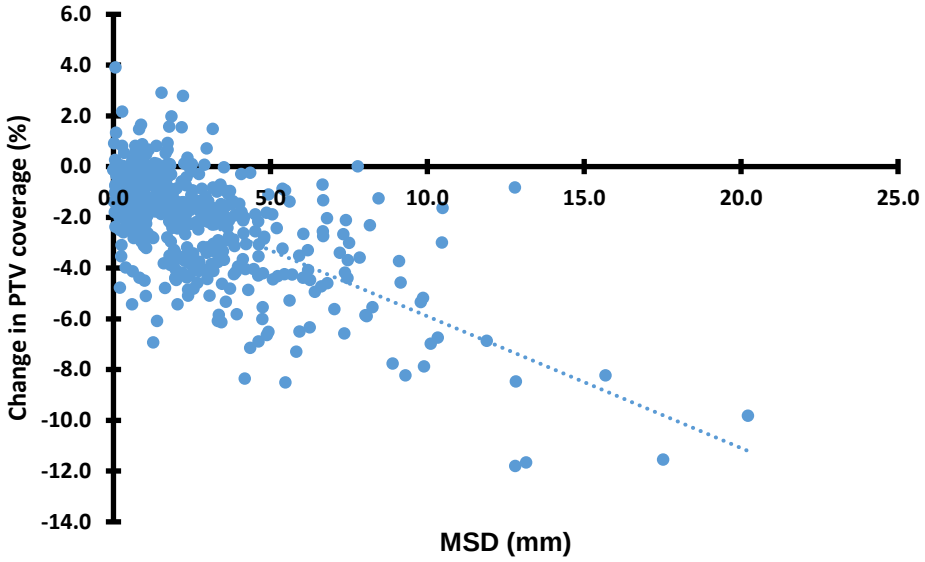

Figure 5.3: Showing a correlation between MSD and change in PTV coverage.
A correlation value of -0.65 was found between MSD and PTV coverage.

6.0 Predicting personalised and progressive adaptive dose escalation to gross tumour volume using knowledge-based planning models for inoperable advanced-stage non-small cell lung cancer patients treated with volumetric modulated arc therapy

The research in this chapter was published in a peer-reviewed journal and therefore the text presented here is adapted from the article. My contribution consisted in conceptualising the research strategy, performing the research and writing the manuscript with input from my supervisors on designing and planning the work and editing the manuscript and clinical inputs from clinicians Dr. A Wieczorek, and Dr. S Upadhyay. Reference: Tambe, N. S.; Pires, I. M.; Moore, C.; Wieczorek, A.; Upadhyay S.; Beavis, A. W., Predicting personalised and progressive adaptive dose escalation to gross tumour volume using knowledge-based planning models for inoperable advanced-stage non-small cell lung cancer patients treated with volumetric modulated arc therapy Biomed. Phys. Eng. Express, 2022. 8. 035001.

6.1 Introduction

Several studies have reported that high radiation doses could improve local control and hence the overall survival compared to low-dose radiotherapy for NSCLC patients (Rengan *et al.*, 2004; Kong *et al.*, 2005; Rosenzweig *et al.*, 2005; Lee *et al.*, 2006; Gillham *et al.*, 2008; Nielsen *et al.*, 2014; Ramroth *et al.*, 2016; Fleming *et al.*, 2016; Fleming *et al.*, 2017; Higgins *et al.*, 2017; Tekatli *et al.*, 2017). However, dose escalation is often restricted by the presence of critical healthy structures in close proximity to the target volume. A significant increase in radiation dose to these organs at risk (OAR) could increase toxicities to an unacceptable level, especially when treating inoperable advanced-stage tumours (Cho *et al.*, 2009; Bral *et al.*, 2010). Additionally, it has been suggested that dose escalation could stimulate immune checkpoint inhibitors (ICI) that

could considerably increase pneumonitis (Zehentmayr *et al.*, 2020). Therefore, it is crucial to limit OAR doses as low as possible whilst escalating the tumour doses.

A number of methods have been proposed to escalate doses for advanced lung cancer patients, including conventional fractionation or hypo-fractionated regimes. However, dose escalation with conventional fractionation increases overall treatment time allowing tumour repopulation (Withers, Taylor and Maciejewski, 1988; Maciejewski and Majewski, 1991; Withers *et al.*, 1995; Petereit *et al.*, 1995; Kim and Tannock, 2005). This has a detrimental effect on local control and overall survival (Withers, Taylor and Maciejewski, 1988; Maciejewski and Majewski, 1991; Withers *et al.*, 1995; Petereit *et al.*, 1995; Kim and Tannock, 2005). Therefore, dose escalation with standard-dose fractionation cannot be considered a standard of care (Yom, 2015) and it is recommended to shorten the overall treatment time to improve survival (Rengan *et al.*, 2004; Kong *et al.*, 2005; Rosenzweig *et al.*, 2005; Nakamura *et al.*, 2008; Gillham *et al.*, 2008; Baumann *et al.*, 2011; Nielsen *et al.*, 2014; Fleming *et al.*, 2016; Fleming *et al.*, 2017; Higgins *et al.*, 2017; Tekatli *et al.*, 2017). Additionally, stereotactic ablative radiotherapy studies reported significant improvement in survival for limited-stage peripheral NSCLC patients (UK SABR Consortium, 2016; UK SABR Consortium, 2019).

Different methods have been proposed for dose escalation, such as using positron emission tomography (PET) scans for contouring boost volume (Gillham *et al.*, 2008) whilst other studies used inhomogeneous dose escalation to GTV contoured on planning CT images (Nielsen *et al.*, 2014; Fleming *et al.*, 2017). Furthermore, Higgins *et al* (Higgins *et al.*, 2017) and Doyen *et al* (Doyen *et al.*, 2018) studied combinations of conventional fractionation radiotherapy with stereotactic ablative body radiotherapy. Higgins *et al* reported that 20 Gy in two fractions following 44 Gy in 22 fraction regime was a tolerable

dose (Higgins *et al.*, 2017) as no grade 3 or higher toxicities were reported, whereas Doyen *et al* reported that three fractions of 11 Gy were safe following 46 Gy in 23 fraction chemo-radiotherapy (Doyen *et al.*, 2018).

Several methods have been used for dose escalation (Rengan *et al.*, 2004; Kong *et al.*, 2005; Rosenzweig *et al.*, 2005; Lee *et al.*, 2006; Gillham *et al.*, 2008; Nielsen *et al.*, 2014; Fleming *et al.*, 2016; Ramroth *et al.*, 2016; Fleming *et al.*, 2017; Higgins *et al.*, 2017; Tekatli *et al.*, 2017), however, none of the studies have evaluated the possibility of multiple adaptive dose escalation to the adapted GTV during the course of radiotherapy for inoperable advanced-stage NSCLC patients. In this study, a personalised progressive dose escalation to adapted GTV was studied without increasing OAR doses compared to the original clinical (i.e., 'homogeneous' – no dose escalation plan). Furthermore, knowledge-based planning models were developed to predict the dose for the initial dose escalation and the adapted (during treatment) dose escalation whilst maintaining OAR doses similar to the non-dose escalation plans and hence, without having to go through a full planning process, to enable prediction of whether adaption was worth taking forward or not. If so, then re-planning could be carried out.

6.2 Methodology

6.2.1 Data collection

Twenty-five previously treated patients' data were curated from our Eclipse treatment planning system database; patient's demographics (see Table 5.1, chapter 5), histopathology, tumour staging, PTV volume in cubic centimetres (cc), $GTV_{Clinical}$ volume, adapted GTV ($GTV_{Adaptive}$) volume and dose-volume histogram (DVH) for target structures were collected.

6.2.2 Assessment of adaptive planning

Production of synthetic CT (sCT): the sCT images were produced using the method described in section 5.2.2.

Evaluation of dosimetric variations: The sCT datasets were imported into the treatment planning system. The associated GTV for each fraction was reviewed and edited where required by experienced clinical oncologists to account for tumour baseline shift and anatomical changes. Furthermore, clinical and planning target volumes were produced on each sCT by applying the same margin as the clinical plan. The GTV contoured on each fraction was evaluated and the fractions where the GTV volume reduced compared to the original $GTV_{Clinical}$ were noted and considered for dose escalation.

6.2.3 Dose escalation strategies

For this planning study, two dose-escalation strategies were considered for each patient:

1. Personalised Dose Escalation (PDE); where dose to the $GTV_{Clinical}$ was escalated, beyond the conventional prescription dose, within the constraints of the individual patient's delineated anatomy.

2. Adaptive Dose Escalation (ADE); where dose escalation was considered for individual 'fractions' when the $GTV_{Adaptive}$ volume seen on the sCT was reduced in comparison to the previous fractions.

For both PDE and ADE plans, the dose to GTV was allowed to be increased/escalated until the OAR doses reached a similar level to those obtained in the original clinical plan and constraining the PTV dose to that intended in the clinical protocol (see Table 2.1, chapter 2). A mixture of traditional and bespoke prescriptions within the PTV (depending on the

patient's anatomy) were used, we characterise this prescription configuration as being heterogeneous.

Adapted dose-volume histogram: The dose to 99% (D_{99}) of $GTV_{Clinical}$, $GTV_{Adaptive}$, $PTV_{Clinical}$, and $PTV_{Adaptive}$ volumes were recorded from the PDE plan (#0) and for the ADE fractions and the total estimated dose was calculated for target structures and OARs by summation over all fractions. The distribution for an adapted fraction was used for subsequent fractions until a new adaption was made, to estimate the total dose to the GTV, PTV and OAR volumes using this technique.

The OARs doses for each metric (see Table 2.1, chapter 2) were calculated and compared with the original clinical plan.

Biological equivalent dose (BED)*:* BED was calculated for $GTV_{Clinical}$, $GTV_{Adaptive}$, $PTV_{Clinical}$, and $PTV_{Adaptive}$, volumes using $D_{99\%}$ statistics for the original clinical (no dose escalation) plans and dose escalation plans (PDE: $GTV_{Clinical}$ and $PTV_{Clinical}$; ADE: $GTV_{Adaptive\_Total}$ and $PTV_{Adaptive\_Total}$). BED was calculated using equation 1.1 with an α/β value of 10 (this is referred to as BED_{10} below). Finally, a total BED was calculated by summing BED over all fractions.

Tumour control probability (TCP): TCPs for $GTV_{Clinical}$ and $GTV_{Adaptive}$ and $PTV_{Clinical}$ and $PTV_{Adaptive}$ structures were calculated using the Linear Quadratic (LQ: this is referred to as TCP_{LQ} below) model within the Biosuite software (Uzan and Nahum, 2012) for clinical plans, fraction '0' plans and for total plans using the parameters identified by Nahum et al for non-small cell lung cancer. These are, an α/β = 10 Gy, α = 0·307 Gy^{-1}, a clonogen density of 10^7 and a clonogen doubling time of 3·7 days (Nahum *et al.*, 2011). Note: here

we acknowledge the use of the generic parameters for TCP_{LQ} calculations and that the TCP values are used for relative comparison only in this study.

6.3 Development of knowledge-based planning (KBP) Model

Knowledge-based planning models were developed to predict achievable D_{99} of $GTV_{Clinical}$ and $GTV_{Adaptive}$ without increasing OAR doses. Two KBP models were developed to predict achievable dose-escalation, first to the $GTV_{Clinical}$ and the second for $GTV_{Adaptive}$. The process to develop the model consists of finding plan signatures (volumes) that show a strong correlation to the achieved dose metrics of interest. The (best-fit) relationship describing the correlation is then used as the predictive function. Initially, a number of patient-specific volumes were considered including, $GTV_{Clinical}$, $GTV_{Adaptive}$ $PTV_{Clinical}$, $PTV_{Adaptive,}$ $PTV\text{-}GTV_{Clinical\ and\ Adaptive}$, Lungs-GTV and Heart to develop the models. Initially, a number of patient-specific volumes were considered including, $GTV_{Clinical}$, $GTV_{Adaptive}$ $PTV_{Clinical}$, $PTV_{Adaptive,}$ $PTV\text{-}GTV_{Clinical\ and\ Adaptive}$, Lungs-GTV and Heart to develop the models. Their correlation with the achieved doses in the clinical plans were assessed. Doses achieved to the $GTV_{Clinical}$ and $GTV_{Adaptive}$ structures were correlated with the $GTV_{Clinical}$, and $GTV_{Adaptive}$ volumes to develop the models.

PDE: The model was developed using fifteen patients' plans and verified using ten independent patients' plans. For the verification, the test plans were optimised to achieve the predicted D_{99} to $GTV_{Clinical}$ whilst ensuring the OARs did not exceed the doses achieved in the original clinical plan and the $PTV_{Clinical}$ received the originally intended (prescribed) dose. Differences between predicted and achieved doses were calculated.

ADE: A total of seven patients (n = 20 plans) data were used to develop a model. The model was then verified using four independent patients' (n = 11 plans) data. Finally, differences between the predicted and the achieved doses to $GTV_{Adaptive}$ were calculated.

6.4 Results

6.4.1 Personalised and Adaptive dose escalation: A total of twenty-five patients were initially included in this study; however, only eleven patients demonstrated a reduction in GTV volume 'during' their treatment and were therefore considered for adaptive dose escalation.

6.4.2 Development of KBP models: A number of volumes (i.e., $GTV_{Clinical}$, $GTV_{Adaptive}$ $PTV_{Clinical}$, $PTV_{Adaptive,}$ $PTV\text{-}GTV_{Clinical\ and\ Adaptive}$, Lungs-GTV and Heart) and their combinations were considered to develop the models. For the PDE model, the $GTV_{Clinical}$ size in cubic centimetres showed the strongest correlation with the achieved D_{99} of $GTV_{Clinical}$ (see Figure 6.1A). Whereas, for ADE, the percentage change in $GTV_{Adaptive}$ compared to the $GTV_{Clinical}$ had the strongest correlation with the percentage increase in D_{99} of the $GTV_{Adaptive}$ (see Figure 6.1B).

The average dose escalation results are given in Table 6.1 and Figure 6.2. The average total dose to GTV can be increased by 15.1 Gy (28.0%) compared to the original clinical plans with personalised and adapted dose escalation methods (i.e, PDE and ADE) compared to the original plans (without dose escalation). Whereas, it was increased by 8.7 Gy (16.1%) with a single personalised dose escalation (i.e., PDE). Neither statistical nor clinical differences were seen in the OAR doses between dose-escalated and clinical plans (Table 6.1 and Figure 6.2).

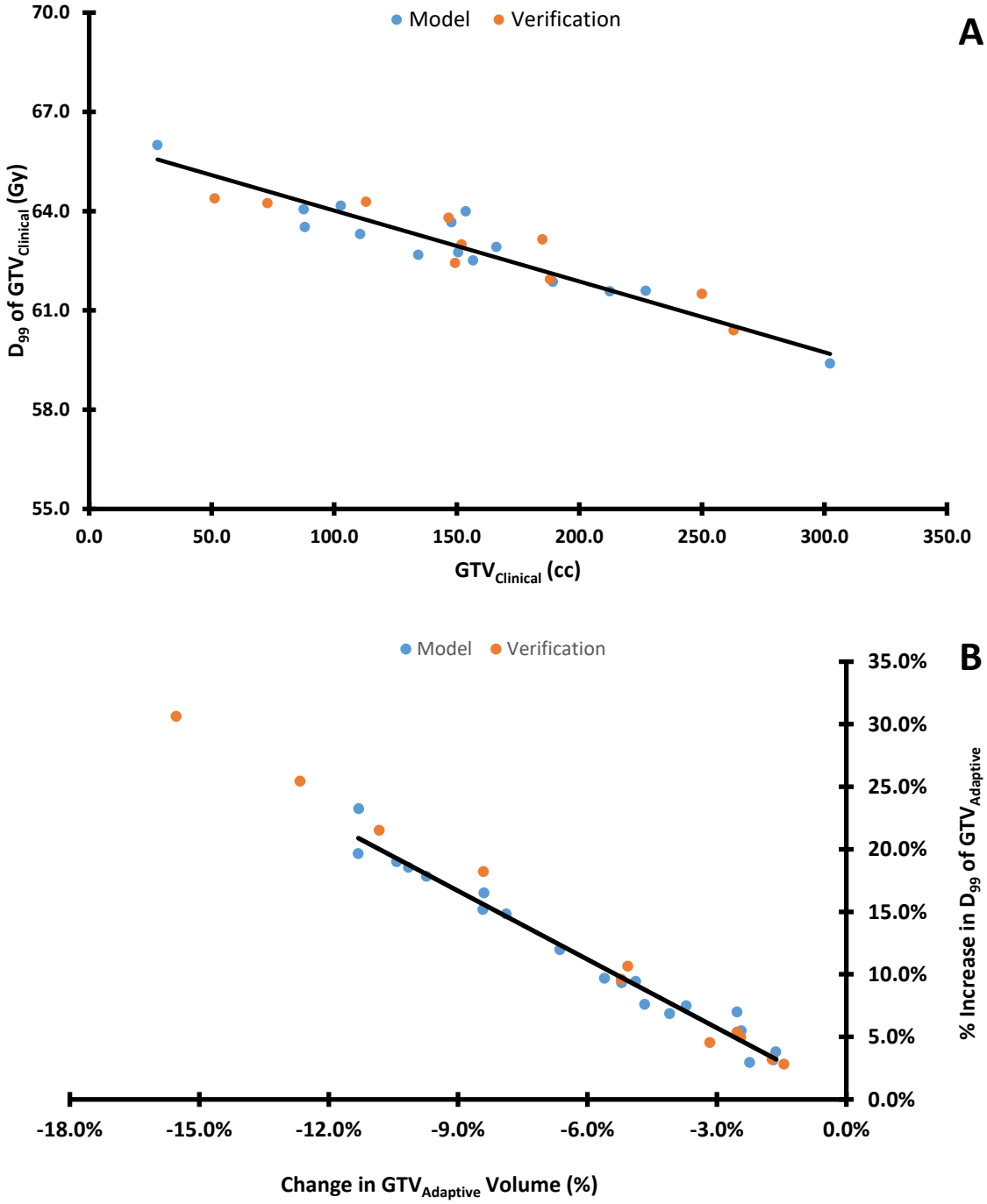

Figure 6.1: Verification of models produced to predict the achievable D_{99} of $GTV_{Clinical}$ (A) and $GTV_{Adaptive}$ (B) without exceeding OAR doses achieved in the non-dose escalated plans. The models were verified using the independent data set and the results are shown in the plots. The variable, constant and the R^2 values for model A were -0.0214, 66.159 and 0.886 and for model B, -1.826, -0.003 and 0.974 respectively.

Table 6.1: Mean dose-volume statistics for the original clinical plans and mean difference in target and OAR dose-volume compared to the original clinical plans. DE_#0 shows the average dose difference between the original clinical plans and the PDE plans and Total_DE shows the mean dose difference between the original clinical plans and the total estimated escalation doses (PDE and ADE).

Parameters		Original Clinical Plans	DE_#0	p	Total_DE	p
PTV_DVH‡	$D_{99\%}$ (Gy)	51.3	2.3	0.045	3.3	0.010
GTV_DE‡‡	$D_{99\%}$ (Gy)	54.0	8.7	0.000	15.1	0.000
Lungs-GTV	V_{5Gy} (%)	46.0	-0.3	0.959	0.4	0.929
	V_{20Gy} (%)	17.8	-0.7	0.761	-0.6	0.785
	Mean Dose (Gy)	10.5	0.2	0.886	0.4	0.721
Heart	V_{30Gy} (%)	6.4	-0.5	0.848	0.1	0.969
	Mean Dose (Gy)	9.5	-0.2	0.924	0.2	0.950
Spinal Cord PRV	$D_{0.01cc}$ (Gy)	32.8	-2.7	0.509	-2.3	0.590
PTV_DVH	BED10 (Gy_{10})	64.5	3.4	0.044	5.0	0.009
GTV_DE	BED10 (Gy_{10})	68.6	13.9	0.000	24.5	0.000
PTV_DVH	TCP_{LQ} (%)	35.0	25.0	0.000	36.0	0.000
GTV_DE	TCP_{LQ} (%)	36.5	48.0	0.000	57.1	0.000

‡ PTV_DVH = PTV – GTV + 0.5cm, ‡‡ GTV_DE = GTV + 0.5cm

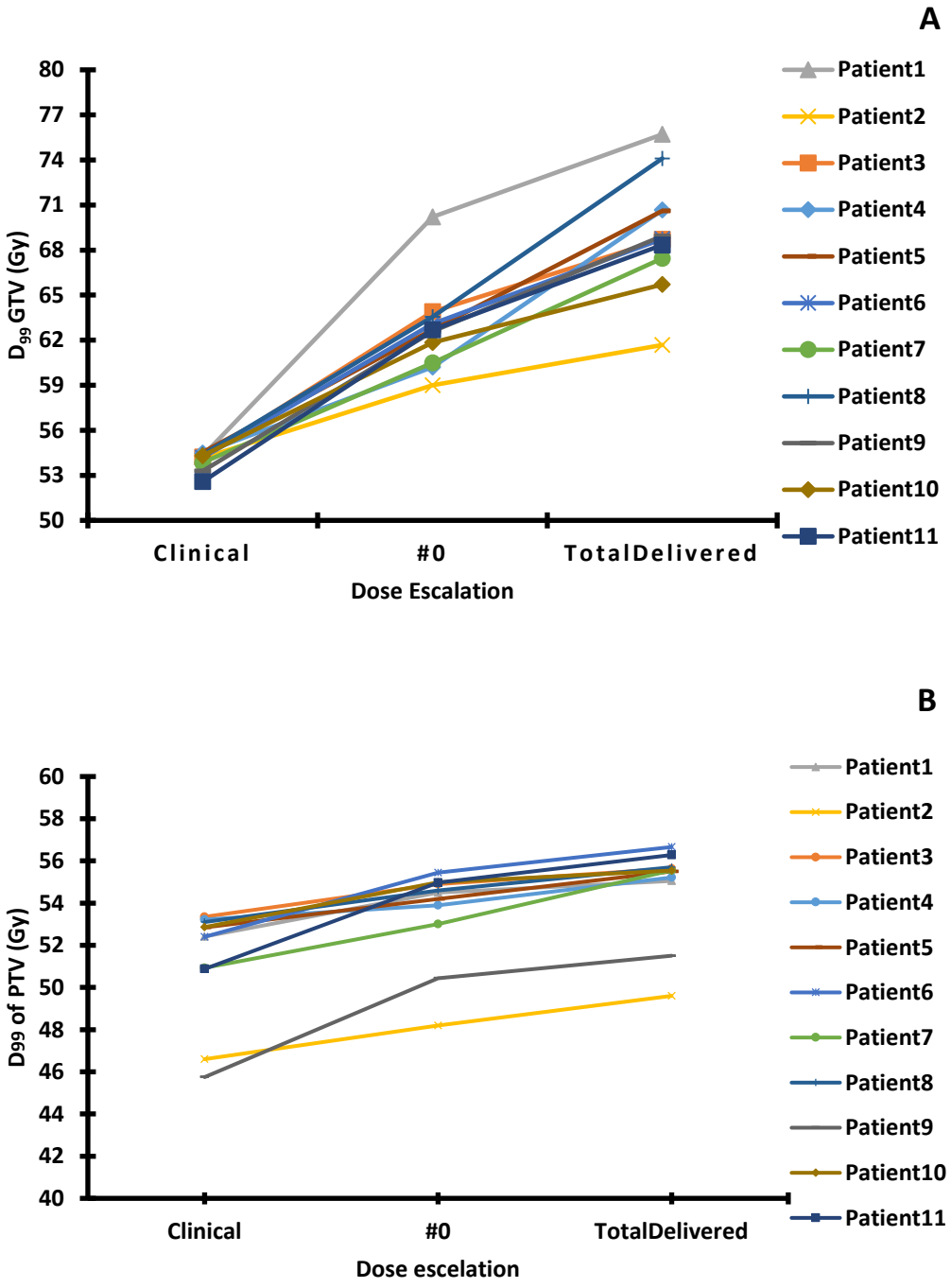

Figure 6.2: Adaptive dose-escalation comparison.

Plots depict doses escalated to GTV volume (A) and doses received by PTV volume (B) in fraction 0 and total plan compared to the original clinical plans (B). Doses reported here are to the 99.0 % of target volumes. Target coverage had to be compromised for patients 2 and 9 (image B) due to its proximity of PTV to the spinal cord. Doses were compromised to respect the spinal cord tolerance limit; PTV volume was cropped back from spinal cord PRV and the cropped volume was used for optimising the plan.

6.4.3 BED and TCP: The BED_{10} and TCP_{LQ} were calculated and were seen to increase significantly for both $GTV_{Clinical}$, $GTV_{Adaptive}$, $PTV_{Clinical}$ and $PTV_{Adaptive}$ volumes, compared to those for the original clinical plans. BED_{10} for GTV_{DE} and PTV_{DVH} increased by 20.3% and 5.3% for PDE plans and 35.7% and 7.7% respectively for adapted plans (i.e., PDE + ADE) based on a comparison of the accumulated doses against the original clinical plans. TCP_{LQ} values increased from 36.5% to 84.5% and 35.0% to 60.0% for PDE plans and 36.5% to 93.9% and 35.0% to 71.0% for accumulated plans for $GTV_{Adaptive}$ and $PTV_{Adaptive}$ volumes respectively (see Table 6.1).

6.4.4 Validation of knowledge-based planning models: The prediction accuracy of the models was verified using independent data sets. PDE, the mean difference between predicted and the achieved D_{99} $GTV_{Clinical}$ was 0.4% (range = 1.3% to -0.7%) (Figure 6.3A) and for ADE, the average difference was 0.7% (range = 2.5% to – 1.6%) (Figure 6.3B). The OAR doses achieved in the adapted plans were not statistically significantly different compared to those in the original clinical plans whereas $PTV_{Clinical}$ and $PTV_{Adaptive}$ coverage improved compared to the clinical plans (Figure 6.2 and Table 6.1).

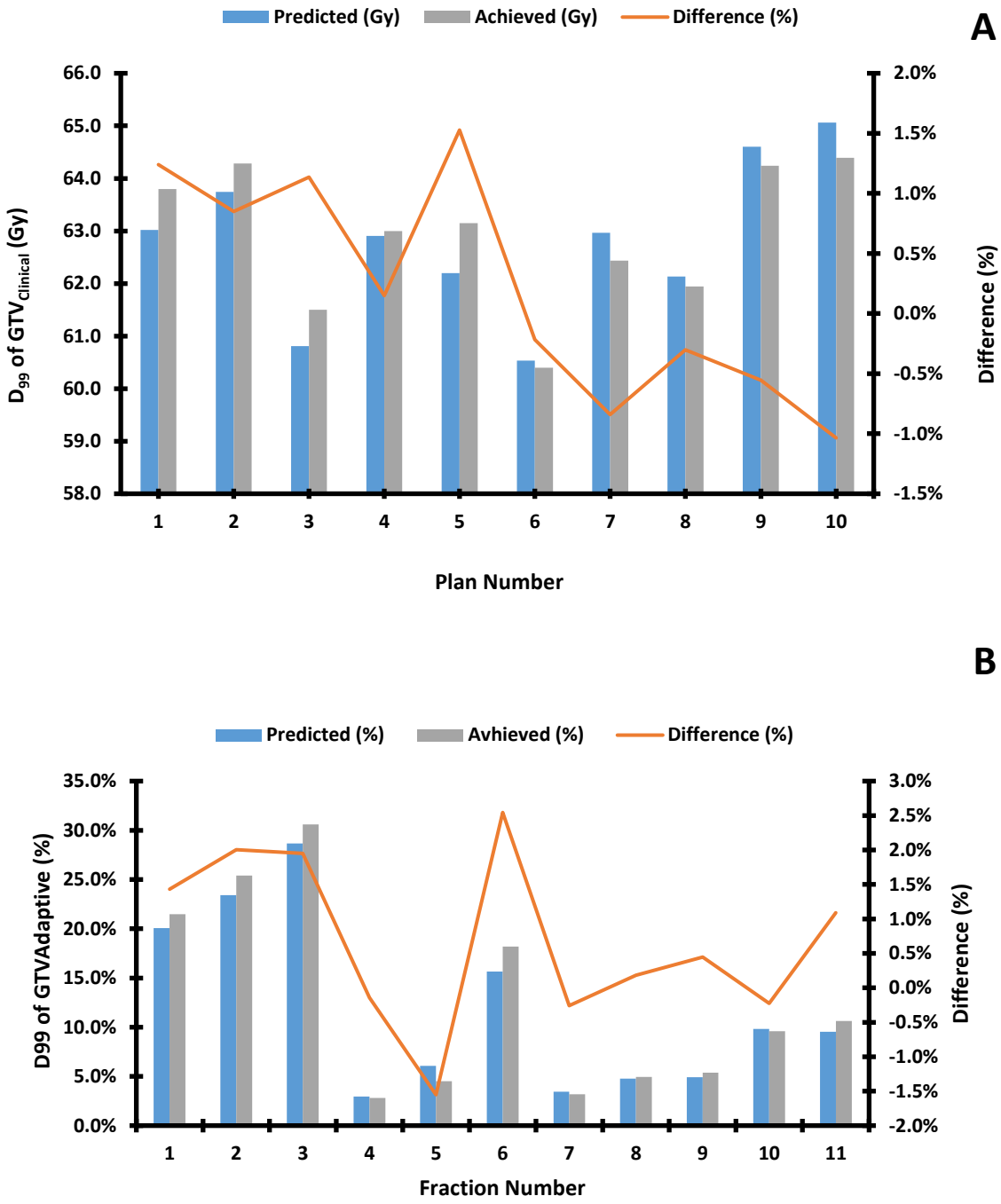

Figure 6.3: Verification of KBP models developed using patient-specific parameters. Images A and B, showing predicted and achieved doses for $GTV_{Clinical}$ and $GTV_{Adaptive}$ and the percentage difference between achieved and predicted doses.

The model was developed for predicting maximum $D_{99\%}$ of $GTV_{Clinical}$ (PDE) and $GTV_{Adaptive}$ (ADE) respectively whilst keeping the OAR dose similar to the original clinical plans.

6.5 Discussion

Several studies have demonstrated that increasing prescribed doses can lead to an increase in the overall survival in NSCLC patients, including those with inoperable advanced-stage disease (Rengan *et al.*, 2004; Kong *et al.*, 2005; Rosenzweig *et al.*, 2005; Lee *et al.*, 2006; Gillham *et al.*, 2008; Nielsen *et al.*, 2014; Fleming *et al.*, 2016; Ramroth *et al.*, 2016; Fleming *et al.*, 2017; Higgins *et al.*, 2017; Tekatli *et al.*, 2017). However, an increase in organs at risk doses can adversely affect patients' quality of life and, potentially, survival. It is therefore important to investigate methods for dose escalation that increase the therapeutic ratio by increasing the probability of disease control and by reducing the probability of toxicity.

Single inhomogeneous 'personalised' dose escalation was studied by Nielsen et al (Nielsen *et al.*, 2014), optimising prescription dose to the pre-treatment imaging. They reported an increase of 3.6 Gy (from 64.8 ± 0.9 Gy to 68.4 ± 2.9 Gy) dose to the $GTV_{98\%}$ whereas, in our study dose to GTV $D_{99\%}$ increased by 8.7 Gy (from 54.0 ± 0.6 Gy to 62.8 ± 2.9 Gy). However, the present study reports personalised progressive adaptive dose-escalation where, following personalisation, the opportunity to dose-escalate was continually assessed prior to each fraction. In this method, OAR doses and PTV (see Figure 6.2B and Table 6.1) dose coverage were kept very similar to the original (non-dose escalated) plans that had been used clinically. Doses were escalated whilst keeping the total number of fractions the same, with the dose per fraction to the adapted GTV increased in each escalated plan.

A number of patients in this study had treatment volumes comprising of primary plus nodal volumes and some had volumes in close proximity to the spinal cord volume, nevertheless, adaptive dose escalation was achievable whilst keeping the OAR doses

similar to the original clinical plans for all patients. We noted that patients with apical tumours were able to receive higher doses compared to the patients where the tumour appears on the same slices as the heart and tumours near the spinal cord.

The application of our method to identify patients that would benefit from progressive dose escalation following the initial personalisation of prescription dose increased their mean $GTV_{Adaptive}$ dose and TCP_{LQ} by 10.2% and 10.8% respectively compared to those receiving personalised dose (escalated) prescription only, without increasing OAR doses or compromising PTV coverage. Thereby demonstrating that personalised progressive adaptive dose escalation is feasible and may lead to significantly increased tumour control probability compared to the standard or personalised prescription plans for inoperable advanced-stage NSCLC patients.

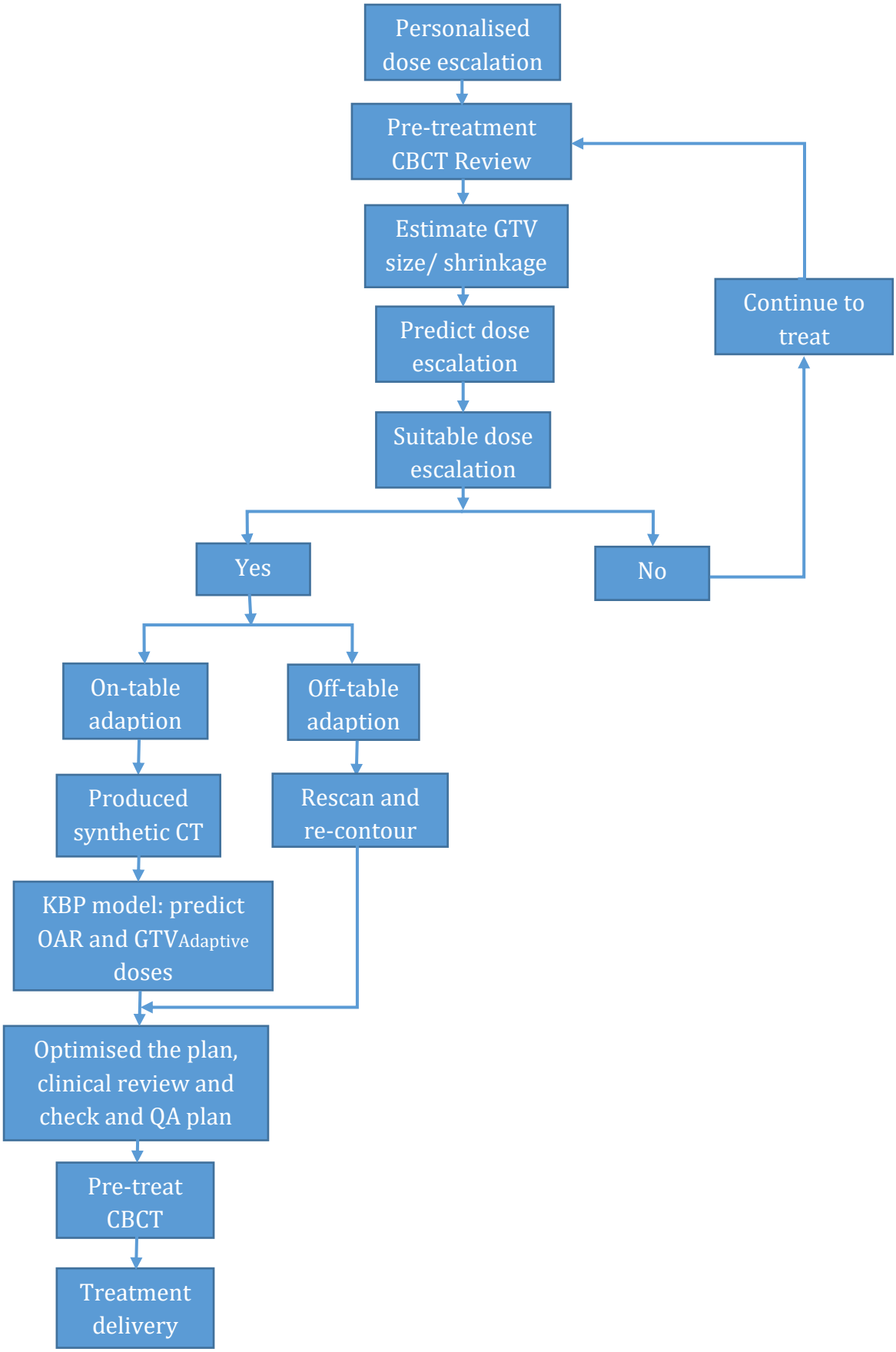

Chart 6.1: Showing steps from the initial dose escalation (PDE) to the adaptive dose escalation (ADE), including online and offline adaption.

A knowledge-based planning model was successfully developed in this study to predict the maximum achievable doses to $GTV_{Adaptive}$ using our approach. Model accuracy was assessed and prediction accuracy for PDE (initial plan personalisation) plans was observed to be superior compared to ADE plans (i.e., subsequent adaption), this could be due to the relatively small number of the training dataset. However, the model was deemed acceptable to use clinically and could therefore be used as an efficient tool to predict if spending time performing additional plans, either in the planning stage or at the Linac to consider 'on-table adaption' would be worthwhile. From a pragmatic perspective, the benefit afforded by the use of the KBP planning prediction of which patients may benefit is the streamlining of the decision-making process for on-table adaption. Without requiring a full dose calculation, appropriate patients can be quickly identified and in the case that a beneficial adaption is not predicted the planned treatment can continue without any further time-consuming interruption. The steps requiring adaptive dose escalation are shown in chart 6.1.

One of the objectives of this study was to assess if the dose to $GTV_{(Clinical\ and\ Adaptive)}$ can be increased without increasing OAR doses compared to the original clinical plans (i.e., the homogeneous plan) so that tumour control probability can be increased without increasing toxicities or reducing the quality of life; our results showed this to be possible. Furthermore, potentially significant increases in TCP, over the standard or personalised prescription plans were demonstrated by the personalised progressive adaption strategy. Whilst such calculations may be considered subjective, we considered the results of the Biosuite software to at least indicate relative probabilities for the structures considered.

This objective was set to ascertain if we could achieve personalisation and progressive adaptive dose-escalation within (potential) treatment toxicities that we are clinically comfortable with. We consider this to be an experience-based isotoxicity regime, however, we acknowledge that further and potentially more beneficial dose escalation might be achievable if we extended our isotoxicity considerations to literature-based tolerance doses. However, although increased dose to target volume could improve local control, increases in OAR doses could significantly affect survival (Bradley *et al.*, 2005; Brower *et al.*, 2016) and so we considered such as approach outside the scope of our study.

In this study, we assumed that the adaptive GTV contoured sCT (produced using CBCT) represents the 'true' GTV (i.e., similar to the one contoured on 4DCT scans – including the full extent of motion). The CBCT image is acquired over a period of few breathing cycles and hence should demonstrate full tumour motion as seen on the 4DCT images. Furthermore, we did not investigate if the CBCT slice thickness used locally has any impact on the quality of the sCT images and the target delineation. Whereas these might be considered as limitations of the study, however for clinical implementation, a 4DCT scan and/ or PET-CT scan will be required to accurately delineate target and OAR volumes thus removing the impact of these observations. However, the model should help identify patients for dose escalation based on GTV contoured on CBCT images.

6.6 Conclusion

We demonstrated that a Personalised Progressive adaptive dose-escalation strategy could significantly increase the dose to adapted GTV and relative TCP_{LQ} without increasing OAR doses. This may improve local control and overall survival of the patients with inoperable advanced-stage NSCLC without an increase in toxicities compared to the

non-dose escalated plans. Limiting OAR dose will also help these patients maintain their quality of life and we based our dose levels on our clinical experience. In this study, we present the first report of the development of a knowledge-based planning model for rapidly predicting D_{99} of the GTV, whilst maintaining OAR doses and PTV coverage similar to our current clinical protocol requirements, thus remaining within our experience bounds. The model can be used as a predictive tool to assess the potential for adaption prior to performing the treatment planning itself and therefore to streamline the adaptive planning decision-making processes.

7.0 Discussion and conclusions

Radiotherapy plays a very important role in the treatment of advanced-stage non-small-cell lung cancer. A large number of patients (27% to 42%) with advanced-stage disease receive radiotherapy with curative or palliative intent compared to surgery (National Cancer Registration & Analysis Service and Cancer Research UK, 2017). Until recently, radiotherapy with and without chemotherapy was a standard of care for inoperable advanced-stage NSCLC patients. The recent clinical trials reported a significant increase in overall survival in the patients who received immunotherapy (Antonia *et al.*, 2017; Antonia *et al.*, 2018; Brahmer *et al.*, 2018; Yoneda *et al.*, 2019; Paz-Ares *et al.*, 2020).

Furthermore, radiotherapy treatment planning and delivery techniques have evolved significantly over the past few years, including the development of intensity modulation radiotherapy and volumetric modulated radiotherapy. The outcomes of treatment plans produced using these techniques are highly dependent on the optimisation parameters/objectives used during optimisation or the beam/arc geometry. If the same or similar optimisation objectives or arc geometries are used for planning all patients, then it could result in suboptimal dose distribution (i.e., higher OAR doses or inadequate target coverage) due to large variations in patients' anatomy.

7.1 Key findings of the thesis

This thesis aimed to extract patient-specific information that could facilitate the prediction of personalised optimisation parameters to limit OAR doses whilst achieving optimal target coverage and/ or whilst using dose escalation. This thesis developed four personalised solutions for optimising plans for advanced-stage non-small cell lung cancer patients treated with VMAT.

Chapter 3. The aim of this study was to reduce variability in treatment plans produced by planners with varying degrees of experience. The knowledge-based planning models were developed using patient-specific factors to predict minimum achievable doses to lung V_{5Gy}, V_{20Gy} and mean lung dose. The results showed that the models can predict the doses accurately for a range of prescriptions. However, the model predictions were unacceptable for oesophageal patients as these are planned with significantly different arc geometries (two full-arcs as compared to two half-arcs). Furthermore, the plans produced using the models showed a concurrent reduction in lung doses and reduced variability between planners. The delivery measurements performed on a linear accelerator showed that the plans produced using the model can be delivered as expected, except for two arcs where gamma results exceed the optimal tolerance but were within the mandatory tolerance level. Therefore, these plans would have been considered acceptable for clinical delivery. In conclusion, the patient-specific anatomy can be used to predict minimum achievable lung doses accurately for different prescriptions and improve the inter-patient consistency of treatment plans.

Chapter 4. The aim of this study was to investigate optimal arc geometries using a personalised arc parameter approach for planning inoperable locally advanced-stage lung cancer patients treated with VMAT. Target volume geometry can significantly vary between patients and if these patients are planned with the same arc parameter then it could result in a suboptimal dose distribution (i.e., higher OAR doses or reduced target coverage). In this chapter, we studied the personalised arc parameter approach to produce optimal plans (i.e., the plans achieving minimal OAR doses whilst maintaining adequate target coverage). Eight arc parameters were studied, and these resulted in different dose distributions to OAR volumes whereas target coverage was similar for

most of the geometries. Furthermore, the 'optimal' plan for each patient was selected using a blind review following local clinical protocol. The optimal plan resulted in a significant reduction in OAR doses compared to the original clinical plan whilst maintaining adequate target coverage. Additionally, a knowledge-based planning model was developed using patient-specific factors to identify optimal arc parameters for prospective patients. The accuracy of the model was assessed by predicting optimal arc parameters for the patients outside the model (i.e., these patients were not included to develop the model), and the prediction accuracy was 80%. In conclusion, the patient-specific factor can help predict an optimal arc parameter for advanced-stage NSCLC patients and reduce OAR doses significantly compared to the plans produced using standard arc parameters. Reducing the dose to healthy tissues can reduce toxicities and help improve patients' quality of life.

Chapter 5. The aim of this study was to investigate different adaptive strategies for inoperable advanced-stage NSCLC patients treated with VMAT and to develop in-house knowledge-based planning models to identify patients requiring adaptive radiotherapy. Following the personalised treatment plan optimisation (discussed in chapters 3 and 4), the next stage is to ensure/monitor that the doses are delivered as planned and anatomical changes do not alter the planned dose distribution significantly, as a significant anatomical change could alter the planned dose distribution and affect treatment outcome. If the anatomical changes can be identified using pre-treatment CBCT imaging and shown to be significant, the treatment plan can be adapted to the changes seen. Adaptive radiotherapy is becoming a new standard of treatment and has been proven beneficial when treating these patients. Recent technological developments, for example, magnetic resonance imaging (MRI) linear accelerators (MR-Linac) allow real-

time anatomical visualisation and facilitate online/ on-table adaption. The method used widely (Yan *et al.*, 1997; Britton *et al.*, 2007; Juhler-Nottrup *et al.*, 2008; Fox *et al.*, 2009; Li, 2011; Kataria *et al.*, 2014; Berkovic *et al.*, 2015; Sibolt *et al.*, 2015; Ramella *et al.*, 2017) requires the patient to undergo a full planning process (i.e., CT simulation, target delineation, treatment plan optimisation, treatment plans check and QA), which is a time-consuming process and could increase workload and patient stress, especially for the patients who do not require adaptive planning. In this chapter, we developed knowledge-based planning models to trigger adaptive radiotherapy, allowing quick and accurate assessment to identify patients who may benefit from adaptive radiotherapy. Three different models were developed using patient (i.e., PTV size and PD-L1) and a fraction (i.e., the mean square difference in centre of mass between PTV at planning and delivery) specific factors. Importantly, we identified a biomarker (i.e., PD-L1), currently being used as a target for immunotherapy, which can be used to identify patients for adaptive replanning. In conclusion, the patient-specific factors evaluated in this study accurately identify patients for adaptive radiotherapy without increasing patients' stress (i.e., sending the patient through the whole planning process) and increasing the overhead of a busy clinical service.

Chapter 6. The aim of this study was to investigate personalised and progressive dose escalation without exceeding OAR doses (compared to the non-dose-escalation plans) for advanced-stage NSCLC patients treated with VMAT and to develop knowledge-based planning models predicting GTV doses. Several studies have shown that higher radiotherapy doses could improve local control and overall survival for NSCLC patients (Rengan *et al.*, 2004; Kong *et al.*, 2005; Rosenzweig *et al.*, 2005; Gillham *et al.*, 2008; Nielsen *et al.*, 2014; Fleming *et al.*, 2016; Fleming *et al.*, 2017; Higgins *et al.*, 2017; Tekatli

et al., 2017). However, dose escalation could be very challenging and limited for advanced-stage NSCLC patients especially when the tumour is in proximity to critical/ dose-limiting structures (e.g. spinal cord). In this chapter, we have identified an alternate method for dose escalation. A personalised and progressive dose escalation to the visible/adapted gross tumour volume was studied whilst keeping the OAR dose and PTV coverage similar to the original clinical plan, i.e., non-dose escalation plans, treated PTV 'homogeneously' with 55Gy in 20 fractions. The dose-escalation strategies (personalised and adaptive dose escalation) developed in this thesis could increase tumour control probability by 1.5 times higher compared to the non-dose escalation plans (clinical plans). More importantly, this was achieved without increasing organs at risk doses. Thus, higher tumour control could be achieved without increasing toxicities. Furthermore, we developed knowledge-based planning models using patient-specific factors to predict the maximal dose to the visible/adapted GTV without increasing OAR doses or affecting PTV coverage. The models can predict personalised doses and will reduce variability in the achieved doses as seen in chapter 3. In conclusion, the method used allowed a significant increase in dose to GTV and most importantly the reports that dose escalation can be performed without increasing OAR doses or toxicities. The KBP models could accurately predict 'safe doses' (i.e., without increasing OAR doses) for escalation.

7.2 Impact of these findings

The knowledge-based planning model developed to predict minimal lung doses (Chapter 3) has been implemented in our clinic following discussion and approval from the treatment planning medical physics expert (MPE). An ESAPI script was developed by a colleague that predicted lung doses using the patient-specific geometry before starting

plan optimisation. The predicted values can be entered in the optimisation with the appropriate priority.

The personalised arc parameters study (Chapter 4) results were discussed with the radiotherapy planning MPE and also with the oesophageal and lung cancer clinicians. It is initially implemented clinically in our centre for planning oesophagus patients as the lung doses were significantly higher with the arc parameter (arc parameter H: see Figure 4.1) used for planning these patients previously. For these patients, the tumour is located centrally so most of the treatments for these patients are planned using arc parameter E (see Figure 4.1). For the patients where the heart dose exceeds the tolerance limit, other geometries are used to achieve the optimal plan. Whereas for NSCLC patients, the model is currently being used only for the patients where lung and/or heart doses exceed the tolerance limits due to the clinical workload and resource issues, however, we are in the process of implementing the arc geometry model for all the NSCLC patients. A script will be developed to predict the best arc parameter for planning and treating these patients routinely. A number of quality documents will be produced (protocol and guidance documents) will be uploaded to the quality system. This technique has allowed us to treat patients (oesophagus and NSCLC) without compromising (or reducing overall dose) to the target volume whilst limiting OAR doses below tolerance level. This means that the use of the methodology has potentially extended the survival of these patients.

Similarly, the ART models (Chapter 5) will be implemented locally for NSCLC patients following approval from an MPE and clinical oncologist. The method and the results of the study will be presented and discussed with physicists (including MPE) and clinicians and the relevant staff will be trained to perform and check the tasks. The dose-escalation study (Chapter 6) demonstrated that significant dose escalation can be achieved and

implemented safely for inoperable advanced-stage NSCLC patients. However, it would require ethical approval from the health and research authority (NHA) as this would change the management of these patients and would need validation through a clinical trial. The primary endpoints of the clinical trial would be to assess local control, early and late toxicities and overall survival following personalised and progressive dose escalation.

7.3 Caveats of the studies

A knowledge-based planning model was developed for predicting minimal achievable doses to lung volume (Chapter 3). Similarly, several patient-specific volumes, such as heart size, heart overlap with PTV, and the difference in centre of mass of the heart and PTV were studied to develop knowledge-based planning to predict minimal achievable doses to the heart and spinal cord volumes but could not find the patient-specific volumes that correlate with dose-volume parameters. Furthermore, the model could not accurately predict minimal achievable doses to lung volume for oesophageal cancer patients. This could be due to the difference in arc geometry used for planning oesophagus patients.

Similarly, the personalised arc geometry model (Chapter 4) that was developed, included co-planar arc geometries but non-coplanar geometries were not studied as the current version of the planning system does not allow the use of non-coplanar arcs. The non-coplanar geometries may help reduce OAR doses further but this may significantly increase the risk of gantry collision. This will be explored when the planning system allows using non-coplanar geometries clinically. The arcs delivered with the couch rotation will reduce radiation dose exiting through the contralateral lungs and heart and help reduce the dose to these structures.

The knowledge-based models (Chapter 5) developed for triggering adaptive planning used the CBCT images registered using 3 degrees of freedom only as it is reflecting our clinical capability. The rotational (i.e., pitch, roll and rotation) corrections were not considered, therefore the models may not be optimal for the patients where the 6 degrees of freedom registration is being used for matching and treating patients. This could be considered to be a limitation of the study; however, in this study, the replanning is triggered in response to the capabilities of the treatment system used locally.

Furthermore, the adaptive dose escalation (Chapter 6) was evaluated using sCT (produced using CBCT) images. The GTV contoured on the sCT images was assumed to be the 'true' GTV (i.e., includes full tumour motion similar to the 4DCT images), since the CBCT images are acquired over a period of few breathing cycles and could represent full tumour extent similar to the 4DCT images. However, for clinical implementation 4DCT images and/ or PET-CT images would be required for accurate delineation of target and OAR volumes.

7.4 Future work

The models developed in this thesis will be implemented clinically using ESAPI scripts. and their benefits, such as reducing variability in treatment plans, OAR doses, efficiency-saving, and clinical outcomes will be reported. Then the clinical benefits of the techniques developed to personalise treatment plan optimisation will be studied by collecting clinical follow-up information and assessing the impact of the studies on local control, OAR toxicities and the quality of life of the patients. The outcome data will be correlated with the delivered dose as it was seen that there could be a significant difference in the planned and delivered dose. These results will be published when available.

In addition, the current KBP model (Chapter 3) only predicts minimum achievable lung doses. New models will be developed to predict minimum achievable heart and spinal cord doses, using new patient-specific parameters like the distance between the OARs and target volume, an overlap with target volume etc. Currently, the non-coplanar VMAT delivery technique is not available clinically; once this is available, we will evaluate if non-coplanar arcs can help reduce OAR (lung, heart and spinal cord) doses without affecting target coverage and if the treatment can be delivered safely.

The use of machine learning in radiotherapy planning has increased in recent years (Meyer *et al.*, 2018); including target volume delineation (Boon, Au Yong and Boon, 2018), radiotherapy patient-specific quality assurance (Chan, Witztum and Valdes, 2020), adaptive radiotherapy (Tseng *et al.*, 2018). Future work will involve developing a machine learning model to automate the personalised treatment planning optimisation process (i.e., predict minimal OAR doses and optimal arc-geometry based on patient-specific factors). Furthermore, 'big data' includes patients' age, gender, histology, staging, weight (before, during and after treatment), biomarkers, radiomics parameters, treatment combinations, delivered radiation dose, change in tumour volume during treatment, change in densities (e.g. tumour, lungs, patient), CT scan, standardized uptake volume (SUV) from positron emission tomography (PET) imaging will be collected using machine learning scripts to develop models predicting clinical outcomes such as, toxicities, local control, local recurrence, metastasis, and overall survival based on tumour and patient-specific information. The patient who may have higher chances of local recurrence could be treated using progressive adaptive dose escalation to achieve superior local control.

This thesis showed simple and cost-effective KBP models can be very beneficial in planning for advanced-stage NSCLC patients treated with VMAT. The methodology developed here can be used to develop KBP models for other sites, such as brain, head and neck, prostate, and gynaecological cancers. In this thesis, we noted that the personalised arc geometry model reduced OAR doses significantly compared to the clinical plans, so it would be interesting to assess if it can be beneficial for these other sites and if KBP models can be developed to predict optimal arc parameters for them.

In addition to personalising treatment planning, efforts can be made to reduce variations in delineated target volume(s) with the help of functional imaging such as PET-CT images. However, a 3D PET-CT is not optimal for delineating target volumes for patients with significant tumour motion (e.g. lungs and oesophagus), as the motion can degrade image quality. For these patients, 4D PET-CT might be beneficial and could help reduce uncertainties in target delineation. A 4D PET-CT protocol could be developed and implemented clinically for these patients.

7.5 Conclusions

In conclusion, the studies performed in this thesis showed that patient-specific information could be used to personalise treatment planning optimisation. The knowledge-based planning models developed can be used clinically for predicting OAR doses, arc parameters, triggering adaptive radiotherapy, and personalised and adaptive dose-escalation accurately and effectively. Additionally, the models can be used to make predictions that can make the ART decision more efficient and practical.

8.0 References

1.0 Abdellatif, A. and Gaede, S. (2014) 'Control point analysis comparison for 3 different treatment planning and delivery complexity levels using a commercial 3-dimensional diode array', *Med Dosim,* 39(2), pp. 174-9.

2.0 Abo-Madyan, Y., Aziz, M. H., Aly, M. M., Schneider, F., Sperk, E., Clausen, S., Giordano, F. A., Herskind, C., Steil, V., Wenz, F. and Glatting, G. (2014) 'Second cancer risk after 3D-CRT, IMRT and VMAT for breast cancer', *Radiother Oncol,* 110(3), pp. 471-6.

3.0 Antonia, S. J., Villegas, A., Daniel, D., Vicente, D., Murakami, S., Hui, R., Kurata, T., Chiappori, A., Lee, K. H., de Wit, M., Cho, B. C., Bourhaba, M., Quantin, X., Tokito, T., Mekhail, T., Planchard, D., Kim, Y. C., Karapetis, C. S., Hiret, S., Ostoros, G., Kubota, K., Gray, J. E., Paz-Ares, L., de Castro Carpeño, J., Faivre-Finn, C., Reck, M., Vansteenkiste, J., Spigel, D. R., Wadsworth, C., Melillo, G., Taboada, M., Dennis, P. A., Özgüroğlu, M. and Investigators, P. (2018) 'Overall Survival with Durvalumab after Chemoradiotherapy in Stage III NSCLC', *N Engl J Med,* 379(24), pp. 2342-2350.

4.0 Antonia, S. J., Villegas, A., Daniel, D., Vicente, D., Murakami, S., Hui, R., Yokoi, T., Chiappori, A., Lee, K. H., de Wit, M., Cho, B. C., Bourhaba, M., Quantin, X., Tokito, T., Mekhail, T., Planchard, D., Kim, Y. C., Karapetis, C. S., Hiret, S., Ostoros, G., Kubota, K., Gray, J. E., Paz-Ares, L., de Castro Carpeño, J., Wadsworth, C., Melillo, G., Jiang, H., Huang, Y., Dennis, P. A., Özgüroğlu, M. and Investigators, P. (2017) 'Durvalumab after Chemoradiotherapy in Stage III Non-Small-Cell Lung Cancer', *N Engl J Med,* 377(20), pp. 1919-1929.

5.0 Appelt, A. L., Vogelius, I. R., Farr, K. P., Khalil, A. A. and Bentzen, S. M. (2014) 'Towards individualized dose constraints: Adjusting the QUANTEC radiation

pneumonitis model for clinical risk factors', *Acta Oncologica (Stockholm, Sweden),* 53(5), pp. 605-612.

6.0 B, R. S. and ChihYao, C. (2013) 'Investigating VMAT planning technique to reduce rectal and bladder dose in prostate cancer treatment plans', *Clinical Cancer Investigation Journal,* 2(3), pp. 212-217.

7.0 Balcı, A. E. (2013) *Lung Cancer: Clinical and Surgical Specifications.* Bentham Science Publishers.

8.0 Barrett, A., Dobbs, J. and Roques, T. (2009) *Practical Radiotherapy Planning Fourth Edition.* Taylor & Francis.

9.0 Battista, J. (2019) *Introduction to Megavoltage X-Ray Dose Computation Algorithms.* CRC Press.

10.0 Batumalai, V., Jameson, M. G., Forstner, D. F., Vial, P. and Holloway, L. C. (2013) 'How important is dosimetrist experience for intensity modulated radiation therapy? A comparative analysis of a head and neck case', *Pract Radiat Oncol,* 3(3), pp. e99-e106.

11.0 Baumann, M., Herrmann, T., Koch, R., Matthiessen, W., Appold, S., Wahlers, B., Kepka, L., Marschke, G., Feltl, D., Fietkau, R., Budach, V., Dunst, J., Dziadziuszko, R., Krause, M., Zips, D. and studygroup, C.-B. (2011) 'Final results of the randomized phase III CHARTWEL-trial (ARO 97-1) comparing hyperfractionated-accelerated versus conventionally fractionated radiotherapy in non-small cell lung cancer (NSCLC)', *Radiother Oncol,* 100(1), pp. 76-85.

12.0 Beets-Tan, R. G. H., Oyen, W. J. G. and Valentini, V. (2020) *Imaging and Interventional Radiology for Radiation Oncology.* Springer International Publishing.

13.0 Bentzen, S. M., Constine, L. S., Deasy, J. O., Eisbruch, A., Jackson, A., Marks, L. B., Ten Haken, R. K. and Yorke, E. D. (2010) 'Quantitative Analyses of Normal Tissue Effects in the Clinic (QUANTEC): an introduction to the scientific issues', *Int J Radiat Oncol Biol Phys,* 76(3 Suppl), pp. S3-9.

14.0 Bergsma, D. P., Salama, J. K., Singh, D. P., Chmura, S. J. and Milano, M. T. (2017) 'Radiotherapy for Oligometastatic Lung Cancer', *Frontiers in oncology,* 7, pp. 210.

15.0 Berkey, F. J. (2010) 'Managing the adverse effects of radiation therapy', *American Family Physician,* 82(4), pp. 381-8, 394.

16.0 Berkovic, P., Paelinck, L., Lievens, Y., Gulyban, A., Goddeeris, B., Derie, C., Surmont, V., De Neve, W. and Vandecasteele, K. (2015) 'Adaptive radiotherapy for locally advanced non-small cell lung cancer, can we predict when and for whom?', *Acta Oncologica (Stockholm, Sweden),* 54(9), pp. 1438-1444.

17.0 Berry, S. L., Boczkowski, A., Ma, R., Mechalakos, J. and Hunt, M. (2016) 'Interobserver variability in radiation therapy plan output: Results of a single-institution study', *Pract Radiat Oncol,* 6(6), pp. 442-449.

18.0 Bertelsen, A., Schytte, T., Bentzen, S. M., Hansen, O., Nielsen, M. and Brink, C. (2011) 'Radiation dose response of normal lung assessed by Cone Beam CT - a potential tool for biologically adaptive radiation therapy', *Radiother Oncol,* 100(3), pp. 351-5.

19.0 Boon, I. S., Au Yong, T. P. T. and Boon, C. S. (2018) 'Assessing the Role of Artificial Intelligence (AI) in Clinical Oncology: Utility of Machine Learning in Radiotherapy Target Volume Delineation', *Medicines,* 5(4), pp. 131.

20.0 Boon, I. S., Marsden, J. E., Tambe, N. S., Wieczorek, A. and El-Mahdawi, N. (2017) 'Initial outcome and toxicity of stereotactic ablative body radiotherapy (SABR) for early stage lung cancer in a single UK centre', *Clinical Oncology,* 29(11), pp. e204-e205.

21.0 Bortfeld, T. (2006) 'IMRT: a review and preview', *Phys Med Biol,* 51(13), pp. R363-79.

22.0 Bosmans, G., van Baardwijk, A., Dekker, A., Öllers, M., Boersma, L., Minken, A., Lambin, P. and De Ruysscher, D. 2006. Intra-patient variability of tumor volume and tumor motion during conventionally fractionated radiotherapy for locally advanced non-small-cell lung cancer: A prospective clinical study. *International Journal of Radiation Oncology*Biology*Physics.*

23.0 Bourhis, J., Montay-Gruel, P., Gonçalves Jorge, P., Bailat, C., Petit, B., Ollivier, J., Jeanneret-Sozzi, W., Ozsahin, M., Bochud, F., Moeckli, R., Germond, J. F. and Vozenin, M. C. (2019) 'Clinical translation of FLASH radiotherapy: Why and how?', *Radiother Oncol,* 139, pp. 11-17.

24.0 Bradley, J., Graham, M. V., Winter, K., Purdy, J. A., Komaki, R., Roa, W. H., Ryu, J. K., Bosch, W. and Emami, B. (2005) 'Toxicity and outcome results of RTOG 9311: a phase I-II dose-escalation study using three-dimensional conformal radiotherapy in patients with inoperable non-small-cell lung carcinoma', *International journal of radiation oncology, biology, physics,* 61(2), pp. 318-328.

25.0 Brahmer, J. R., Govindan, R., Anders, R. A., Antonia, S. J., Sagorsky, S., Davies, M. J., Dubinett, S. M., Ferris, A., Gandhi, L., Garon, E. B., Hellmann, M. D., Hirsch, F. R., Malik, S., Neal, J. W., Papadimitrakopoulou, V. A., Rimm, D. L., Schwartz, L. H., Sepesi, B., Yeap, B. Y., Rizvi, N. A. and Herbst, R. S. (2018) 'The Society for Immunotherapy of Cancer consensus statement on immunotherapy for the treatment of non-small cell lung cancer (NSCLC)', *J Immunother Cancer,* 6(1), pp. 75.

26.0 Bral, S., Duchateau, M., Versmessen, H., Engels, B., Tournel, K., Vinh-Hung, V., De Ridder, M., Schallier, D. and Storme, G. (2010) 'Toxicity and outcome results of a class solution with moderately hypofractionated radiotherapy in inoperable Stage III non-small cell lung cancer using helical tomotherapy', *Int J Radiat Oncol Biol Phys,* 77(5), pp. 1352-9.

27.0 Britton, K. R., Starkschall, G., Liu, H., Chang, J. Y., Bilton, S., Ezhil, M., John-Baptiste, S., Kantor, M., Cox, J. D., Komaki, R. and Mohan, R. 2009. Consequences of Anatomic Changes and Respiratory Motion on Radiation Dose Distributions in Conformal Radiotherapy for Locally Advanced Non–Small-Cell Lung Cancer. *International Journal of Radiation Oncology*Biology*Physics.*

28.0 Britton, K. R., Starkschall, G., Tucker, S. L., Pan, T., Nelson, C., Chang, J. Y., Cox, J. D., Mohan, R. and Komaki, R. 2007. Assessment of Gross Tumor Volume Regression and Motion Changes During Radiotherapy for Non–Small-Cell Lung Cancer as Measured by Four-Dimensional Computed Tomography. *International Journal of Radiation Oncology*Biology*Physics.*

29.0 Brower, J. V., Amini, A., Chen, S., Hullett, C. R., Kimple, R. J., Wojcieszynski, A. P., Bassetti, M., Witek, M. E., Yu, M., Harari, P. M. and Baschnagel, A. M. (2016)

'Improved survival with dose-escalated radiotherapy in stage III non-small-cell lung cancer: analysis of the National Cancer Database', *Ann Oncol,* 27(10), pp. 1887-94.

30.0 Cancer Research UK 2016. Lung Cancer Survival Statistics.

31.0 Cancer Research UK (2019) *Lung cancer incidence statistics*. Available at: https://www.cancerresearchuk.org/health-professional/cancer-statistics/statistics-by-cancer-type/lung-cancer/incidence#heading-One.

32.0 Chan, C., Lang, S., Rowbottom, C., Guckenberger, M., Faivre-Finn, C. and Committee, I. A. R. T. (2014) 'Intensity-modulated radiotherapy for lung cancer: current status and future developments', *J Thorac Oncol,* 9(11), pp. 1598-608.

33.0 Chan, M. F., Witztum, A. and Valdes, G. (2020) 'Integration of AI and Machine Learning in Radiotherapy QA', *Frontiers in Artificial Intelligence,* 3(76).

34.0 Chan, O. S., Lee, M. C., Hung, A. W., Chang, A. T., Yeung, R. M. and Lee, A. W. (2011) 'The superiority of hybrid-volumetric arc therapy (VMAT) technique over double arcs VMAT and 3D-conformal technique in the treatment of locally advanced non-small cell lung cancer--a planning study', *Radiother Oncol,* 101(2), pp. 298-302.

35.0 Chang, A. T. Y., Hung, A. W. M., Cheung, F. W. K., Lee, M. C. H., Chan, O. S. H., Philips, H., Cheng, Y. T. and Ng, W. T. (2016) 'Comparison of Planning Quality and Efficiency Between Conventional and Knowledge-based Algorithms in Nasopharyngeal Cancer Patients Using Intensity Modulated Radiation Therapy', *Int J Radiat Oncol Biol Phys,* 95(3), pp. 981-990.

36.0 Chen, C. P., Weinberg, V. K., Jahan, T. M., Jablons, D. M. and Yom, S. S. (2011) 'Implications of delayed initiation of radiotherapy: accelerated repopulation after

induction chemotherapy for stage III non-small cell lung cancer', *J Thorac Oncol,* 6(11), pp. 1857-64.

37.0 Chen, X., Mo, S. and Yi, B. (2022) 'The spatiotemporal dynamics of lung cancer: 30-year trends of epidemiology across 204 countries and territories', *BMC Public Health,* 22(1), pp. 987.

38.0 Chiavassa, S., Bessieres, I., Edouard, M., Mathot, M. and Moignier, A. (2019) 'Complexity metrics for IMRT and VMAT plans: a review of current literature and applications', *Br J Radiol,* 92(1102), pp. 20190270.

39.0 Chin Snyder, K., Kim, J., Reding, A., Fraser, C., Gordon, J., Ajlouni, M., Movsas, B. and Chetty, I. J. (2016) 'Development and evaluation of a clinical model for lung cancer patients using stereotactic body radiotherapy (SBRT) within a knowledge-based algorithm for treatment planning', *J Appl Clin Med Phys,* 17(6), pp. 263-275.

40.0 Cho, B. (2018) 'Intensity-modulated radiation therapy: a review with a physics perspective', *Radiat Oncol J,* 36(1), pp. 1-10.

41.0 Cho, K. H., Ahn, S. J., Pyo, H. R., Kim, K. S., Kim, Y. C., Moon, S. H., Han, J. Y., Kim, H. T., Koom, W. S. and Lee, J. S. (2009) 'A Phase II study of synchronous three-dimensional conformal boost to the gross tumor volume for patients with unresectable Stage III non-small-cell lung cancer: results of Korean Radiation Oncology Group 0301 study', *Int J Radiat Oncol Biol Phys,* 74(5), pp. 1397-404.

42.0 Cox, J. D., Chang, J. Y. and Komaki, R. (2007) *Image-Guided Radiotherapy of Lung Cancer.* CRC Press.

43.0 Crowe, S. B., Kairn, T., Kenny, J., Knight, R. T., Hill, B., Langton, C. M. and Trapp, J. V. (2014) 'Treatment plan complexity metrics for predicting IMRT pre-treatment quality assurance results', *Australas Phys Eng Sci Med,* 37(3), pp. 475-82.

44.0 Cui.W, Yan.H, Fu.G, Dai.J and Li.Y (2015) 'Predicting dosimetric indices in IMRT planning for lung cancer patients', *Biomedical Physics & Engineering Express,* 1(4), pp. 045208.

45.0 Curran, W. J., Jr., Paulus, R., Langer, C. J., Komaki, R., Lee, J. S., Hauser, S., Movsas, B., Wasserman, T., Rosenthal, S. A., Gore, E., Machtay, M., Sause, W. and Cox, J. D. (2011) 'Sequential vs. concurrent chemoradiation for stage III non-small cell lung cancer: randomized phase III trial RTOG 9410', *Journal of the National Cancer Institute,* 103(19), pp. 1452-1460.

46.0 Dan, T. and Williams, N. L. (2017) 'Management of Stage I Lung Cancer with Stereotactic Ablative Radiation Therapy', *Surgical oncology clinics of North America,* 26(3), pp. 393-403.

47.0 Delaney, A. R., Dahele, M., Tol, J. P., Slotman, B. J. and Verbakel, W. F. (2017) 'Knowledge-based planning for stereotactic radiotherapy of peripheral early-stage lung cancer', *Acta Oncologica (Stockholm, Sweden),* 56(3), pp. 490-495.

48.0 Della Gala, G., Dirkx, M. L. P., Hoekstra, N., Fransen, D., Lanconelli, N., van de Pol, M., Heijmen, B. J. M. and Petit, S. F. (2017) 'Fully automated VMAT treatment planning for advanced-stage NSCLC patients', *Strahlentherapie und Onkologie : Organ der Deutschen Rontgengesellschaft ...[et al],* 193(5), pp. 402-409.

49.0 Dieterich, S., Ford, E., Pavord, D. and Zeng, J. (2015) *Practical Radiation Oncology Physics E-Book: A Companion to Gunderson & Tepper's Clinical Radiation Oncology.* Elsevier Health Sciences.

50.0 Diwanji, T. P., Mohindra, P., Vyfhuis, M., Snider, J. W., Kalavagunta, C., Mossahebi, S., Yu, J., Feigenberg, S. and Badiyan, S. N. (2017) 'Advances in radiotherapy techniques and delivery for non-small cell lung cancer: benefits of intensity-modulated radiation therapy, proton therapy, and stereotactic body radiation therapy', *Transl Lung Cancer Res,* 6(2), pp. 131-147.

51.0 Dong, P., Lee, P., Ruan, D., Long, T., Romeijn, E., Low, D. A., Kupelian, P., Abraham, J., Yang, Y. and Sheng, K. (2013) '4π noncoplanar stereotactic body radiation therapy for centrally located or larger lung tumors', *Int J Radiat Oncol Biol Phys,* 86(3), pp. 407-13.

52.0 Doyen, J., Poudenx, M., Gal, J., Otto, J., Guerder, C., Naghavi, A. O., Gérard, A., Leysalle, A., Cohen, C., Padovani, B., Ianessi, A., Schiappa, R., Chamorey, E. and Bondiau, P. Y. (2018) 'Stereotactic ablative radiotherapy after concomitant chemoradiotherapy in non-small cell lung cancer: A TITE-CRM phase 1 trial', *Radiother Oncol,* 127(2), pp. 239-245.

53.0 Dumane, V. A., Kao, J., Green, S., Gupta, V. and Lo, Y. (2010) 'Comparison of Full Arcs, Avoidance Sectors, and Partial Arcs for RapidArc Planning', *International Journal of Radiation Oncology • Biology • Physics,* 78(3), pp. S820-S821.

54.0 Ehrhardt, J. and Lorenz, C. (2013) *4D Modeling and Estimation of Respiratory Motion for Radiation Therapy.* Springer Berlin Heidelberg.

55.0 Emami, B., Lyman, J., Brown, A., Coia, L., Goitein, M., Munzenrider, J. E., Shank, B., Solin, L. J. and Wesson, M. (1991) 'Tolerance of normal tissue to therapeutic irradiation', *Int J Radiat Oncol Biol Phys,* 21(1), pp. 109-22.

56.0 Fleming, C., Cagney, D. N., O'Keeffe, S., Brennan, S. M., Armstrong, J. G. and McClean, B. (2016) 'Normal tissue considerations and dose-volume constraints in the moderately hypofractionated treatment of non-small cell lung cancer', *Radiother Oncol,* 119(3), pp. 423-31.

57.0 Fleming, C., O'Keeffe, S., Dunne, M., Armstrong, J. G., McClean, B. and Vintro, L. L. (2017) 'The potential for increased tumor control probability in non-small cell lung cancer with a hypofractionated integrated boost to the gross tumor volume', *Med Dosim*.

58.0 Fogliata, A., Belosi, F., Clivio, A., Navarria, P., Nicolini, G., Scorsetti, M., Vanetti, E. and Cozzi, L. (2014a) 'On the pre-clinical validation of a commercial model-based optimisation engine: application to volumetric modulated arc therapy for patients with lung or prostate cancer', *Radiotherapy and oncology : journal of the European Society for Therapeutic Radiology and Oncology,* 113(3), pp. 385-391.

59.0 Fogliata, A., Nicolini, G., Bourgier, C., Clivio, A., De Rose, F., Fenoglietto, P., Lobefalo, F., Mancosu, P., Tomatis, S., Vanetti, E., Scorsetti, M. and Cozzi, L. (2015a) 'Performance of a Knowledge-Based Model for Optimization of Volumetric Modulated Arc Therapy Plans for Single and Bilateral Breast Irradiation', *PLoS One,* 10(12), pp. e0145137.

60.0 Fogliata, A., Nicolini, G., Clivio, A., Vanetti, E., Laksar, S., Tozzi, A., Scorsetti, M. and Cozzi, L. (2015b) 'A broad scope knowledge based model for optimization of VMAT

in esophageal cancer: validation and assessment of plan quality among different treatment centers', *Radiation oncology (London, England),* 10, pp. 220-015-0530-5.

61.0 Fogliata, A., Reggiori, G., Stravato, A., Lobefalo, F., Franzese, C., Franceschini, D., Tomatis, S., Mancosu, P., Scorsetti, M. and Cozzi, L. (2017) 'RapidPlan head and neck model: the objectives and possible clinical benefit', *Radiat Oncol,* 12(1), pp. 73.

62.0 Fogliata, A., Wang, P. M., Belosi, F., Clivio, A., Nicolini, G., Vanetti, E. and Cozzi, L. (2014b) 'Assessment of a model based optimization engine for volumetric modulated arc therapy for patients with advanced hepatocellular cancer', *Radiat Oncol,* 9, pp. 236.

63.0 Fowler J K, R. J. G. (1898) *Diseases of the lungs.* London: Longman Greene.

64.0 Fox, J., Ford, E., Redmond, K., Zhou, J., Wong, J. and Song, D. Y. 2009. Quantification of Tumor Volume Changes During Radiotherapy for Non–Small-Cell Lung Cancer. *International Journal of Radiation Oncology*Biology*Physics.*

65.0 Foy, J. J., Marsh, R., Ten Haken, R. K., Younge, K. C., Schipper, M., Sun, Y., Owen, D. and Matuszak, M. M. (2017) 'An analysis of knowledge-based planning for stereotactic body radiation therapy of the spine', *Pract Radiat Oncol,* 7(5), pp. e355-e360.

66.0 Ge, Y. and Wu, Q. J. (2019) 'Knowledge-based planning for intensity-modulated radiation therapy: A review of data-driven approaches', *Med Phys,* 46(6), pp. 2760-2775.

67.0 Gillham, C., Zips, D., Pönisch, F., Evers, C., Enghardt, W., Abolmaali, N., Zöphel, K., Appold, S., Hölscher, T., Steinbach, J., Kotzerke, J., Herrmann, T. and Baumann, M. 2008. Additional PET/CT in week 5–6 of radiotherapy for patients with stage III

non-small cell lung cancer as a means of dose escalation planning? *Radiotherapy and Oncology.*

68.0 Giraud, P., Antoine, M., Larrouy, A., Milleron, B., Callard, P., De Rycke, Y., Carette, M.-F., Rosenwald, J.-C., Cosset, J.-M., Housset, M. and Touboul, E. (2000) 'Evaluation of microscopic tumor extension in non–small-cell lung cancer for three-dimensional conformal radiotherapy planning', *International Journal of Radiation Oncology • Biology • Physics,* 48(4), pp. 1015-1024.

69.0 Guckenberger, M., Richter, A., Wilbert, J., Flentje, M. and Partridge, M. (2011) 'Adaptive radiotherapy for locally advanced non-small-cell lung cancer does not underdose the microscopic disease and has the potential to increase tumor control', *Int J Radiat Oncol Biol Phys,* 81(4), pp. e275-82.

70.0 Gunderson, L. L. and Tepper, J. E. (2015) *Clinical Radiation Oncology E-Book.* Elsevier Health Sciences.

71.0 Higgins, K. A., Pillai, R. N., Chen, Z., Tian, S., Zhang, C., Patel, P., Pakkala, S., Shelton, J., Force, S. D., Fernandez, F. G., Steuer, C. E., Owonikoko, T. K., Ramalingam, S. S., Bradley, J. D. and Curran, W. J. (2017) 'Concomitant Chemotherapy and Radiotherapy with SBRT Boost for Unresectable Stage III Non-Small Cell Lung Cancer: A Phase I Study', *Journal of thoracic oncology : official publication of the International Association for the Study of Lung Cancer,* 12(11), pp. 1687-1695.

72.0 Hoskin, P. (2012) *External Beam Therapy.* OUP Oxford.

73.0 Huang, B. T., Lu, J. Y., Lin, P. X., Chen, J. Z., Kuang, Y. and Chen, C. Z. (2015) 'Comparison of Two RapidArc Delivery Strategies in Stereotactic Body

Radiotherapy of Peripheral Lung Cancer with Flattening Filter Free Beams', *PLoS One,* 10(7), pp. e0127501.

74.0 Hunt, M. A., Jackson, A., Narayana, A. and Lee, N. (2006) 'Geometric factors influencing dosimetric sparing of the parotid glands using IMRT', *International journal of radiation oncology, biology, physics,* 66(1), pp. 296-304.

75.0 Hussein, M., South, C. P., Barry, M. A., Adams, E. J., Jordan, T. J., Stewart, A. J. and Nisbet, A. (2016) 'Clinical validation and benchmarking of knowledge-based IMRT and VMAT treatment planning in pelvic anatomy', *Radiother Oncol,* 120(3), pp. 473-479.

76.0 Indrayani, L., Anam, C., Sutanto, H., Subroto, R. and Dougherty, G. (2022) 'Normal tissue objective (NTO) tool in Eclipse treatment planning system for dose distribution optimization', *Polish Journal of Medical Physics and Engineering,* 28(2), pp. 99-106.

77.0 International Commission on Radiological Units (1993) *ICRU report 50.* (Prescribing, recording, and reporting photon beam therapy vols). International Commission on Radioation Units and Measurements.

78.0 International Commission on Radiological Units (1999) *ICRU report 62.* (Prescribing, recording, and reporting photon beam therapy (supplement to ICRU report 50) vols). International Commission on Radioation Units and Measurements.

79.0 Jabbour, S. K., Kim, S., Haider, S. A., Xu, X., Wu, A., Surakanti, S., Aisner, J., Langenfeld, J., Yue, N. J., Haffty, B. G. and Zou, W. (2015) 'Reduction in Tumor Volume by Cone Beam Computed Tomography Predicts Overall Survival in Non-Small Cell Lung

Cancer Treated With Chemoradiation Therapy', *Int J Radiat Oncol Biol Phys,* 92(3), pp. 627-33.

80.0 Jeremic, B. (2011) *Advances in Radiation Oncology in Lung Cancer.* Springer Berlin Heidelberg.

81.0 Jiang, Z. Q., Yang, K., Komaki, R., Wei, X., Tucker, S. L., Zhuang, Y., Martel, M. K., Vedam, S., Balter, P., Zhu, G., Gomez, D., Lu, C., Mohan, R., Cox, J. D. and Liao, Z. (2012) 'Long-term clinical outcome of intensity-modulated radiotherapy for inoperable non-small cell lung cancer: the MD Anderson experience', *Int J Radiat Oncol Biol Phys,* 83(1), pp. 332-9.

82.0 Juhler-Nottrup, T., Korreman, S. S., Pedersen, A. N., Persson, G. F., Aarup, L. R., Nystrom, H., Olsen, M., Tarnavski, N. and Specht, L. (2008) 'Interfractional changes in tumour volume and position during entire radiotherapy courses for lung cancer with respiratory gating and image guidance', *Acta Oncologica (Stockholm, Sweden),* 47(7), pp. 1406-1413.

83.0 Kanwal, M., Ding, X. J. and Cao, Y. (2017) 'Familial risk for lung cancer', *Oncol Lett,* 13(2), pp. 535-542.

84.0 Kataria, T., Gupta, D., Bisht, S. S., Karthikeyan, N., Goyal, S., Pushpan, L., Abhishek, A., Govardhan, H. B., Kumar, V., Sharma, K., Jain, S., Basu, T. and Srivastava, A. (2014) 'Adaptive radiotherapy in lung cancer: dosimetric benefits and clinical outcome', *The British journal of radiology,* 87(1038), pp. 20130643.

85.0 Kazhdan, M., Simari, P., McNutt, T., Wu, B., Jacques, R., Chuang, M. and Taylor, R. (2009) 'A shape relationship descriptor for radiation therapy planning', *Med Image Comput Comput Assist Interv,* 12(Pt 2), pp. 100-8.

86.0 Kennedy, T. A. C., Corkum, M. T. and Louie, A. V. (2017) 'Stereotactic radiotherapy in oligometastatic cancer', *Chinese clinical oncology,* 6(Suppl 2), pp. S16.

87.0 Kernstine, K. H. and Reckamp, K. L. (2010) *Lung Cancer A multidisciplinary approch to diagnosis and managemet. Clin Chest Med* New York: Demos Medical.

88.0 Khalil, A. A., Hoffmann, L., Moeller, D. S., Farr, K. P. and Knap, M. M. (2015) 'New dose constraint reduces radiation-induced fatal pneumonitis in locally advanced non-small cell lung cancer patients treated with intensity-modulated radiotherapy', *Acta Oncol,* 54(9), pp. 1343-9.

89.0 Khan, F. M. (2012) *The Physics of Radiation Therapy.* 4th edn. Philadelphia, PA 19106, USA: LIPPINCOTT WILLIAMS & WILKIN.

90.0 Kim, J. J. and Tannock, I. F. (2005) 'Repopulation of cancer cells during therapy: an important cause of treatment failure', *Nat Rev Cancer,* 5(7), pp. 516-25.

91.0 Knöös, T., Wieslander, E., Cozzi, L., Brink, C., Fogliata, A., Albers, D., Nyström, H. and Lassen, S. (2006) 'Comparison of dose calculation algorithms for treatment planning in external photon beam therapy for clinical situations', *Phys Med Biol,* 51(22), pp. 5785-807.

92.0 Kong, F. M., Ten Haken, R. K., Schipper, M. J., Sullivan, M. A., Chen, M., Lopez, C., Kalemkerian, G. P. and Hayman, J. A. (2005) 'High-dose radiation improved local tumor control and overall survival in patients with inoperable/unresectable non-

small-cell lung cancer: long-term results of a radiation dose escalation study', *International journal of radiation oncology, biology, physics,* 63(2), pp. 324-333.

93.0 Kwint, M., Conijn, S., Schaake, E., Knegjens, J., Rossi, M., Remeijer, P., Sonke, J. J. and Belderbos, J. (2014) 'Intra thoracic anatomical changes in lung cancer patients during the course of radiotherapy', *Radiotherapy and oncology : journal of the European Society for Therapeutic Radiology and Oncology,* 113(3), pp. 392-397.

94.0 Langendijk, J. A., Doornaert, P., Verdonck-de Leeuw, I. M., Leemans, C. R., Aaronson, N. K. and Slotman, B. J. (2008) 'Impact of late treatment-related toxicity on quality of life among patients with head and neck cancer treated with radiotherapy', *J Clin Oncol,* 26(22), pp. 3770-6.

95.0 Leary, A. (2012) *Lung Cancer A Multidiscoplinary Approach.* Oxford: Wiley-Blackwell.

96.0 Lee, C. B., Stinchcombe, T. E., Rosenman, J. G. and Socinski, M. A. 2006. Therapeutic Advances in Local-Regional Therapy for Stage III Non-Small-Cell Lung Cancer: Evolving Role of Dose-Escalated Conformal (3-Dimensional) Radiation Therapy. *Clinical Lung Cancer.*

97.0 Levitt, S. H., Brady, L. W., Heilmann, H. P., Purdy, J. A., Perez, C. A., Molls, M., Vijayakumar, S. and Nieder, C. (2008) *Technical Basis of Radiation Therapy: Practical Clinical Applications.* Springer Berlin Heidelberg.

98.0 Li, X. A. (2011) *Adaptive radiation therapy. Imaging in medical diagnosis and therapy* Boca Raton, Fla.: CRC Press.

99.0 Li, Y., Wang, J., Tan, L., Hui, B., Ma, X., Yan, Y., Xue, C., Shi, X., Drokow, E. K. and Ren, J. (2018) 'Dosimetric comparison between IMRT and VMAT in irradiation for peripheral and central lung cancer', *Oncol Lett,* 15(3), pp. 3735-3745.

100.0 Maciejewski, B. and Majewski, S. (1991) 'Dose fractionation and tumour repopulation in radiotherapy for bladder cancer', *Radiother Oncol,* 21(3), pp. 163-70.

101.0 Maconachie, R., Mercer, T., Navani, N., McVeigh, G. and Committee, G. (2019) 'Lung cancer: diagnosis and management: summary of updated NICE guidance', *BMJ,* 364, pp. l1049.

102.0 Mao, B., Verma, V., Zheng, D., Zhu, X., Bennion, N. R., Bhirud, A. R., Poole, M. A. and Zhen, W. (2017) 'Target migration from re-inflation of adjacent atelectasis during lung stereotactic body radiotherapy', *World journal of clinical oncology,* 8(3), pp. 300-304.

103.0 Marcu, L., Bezak, E. and Allen, B. (2012) *Biomedical Physics in Radiotherapy for Cancer.* CSIRO Publishing.

104.0 Marks, L. B., Bentzen, S. M., Deasy, J. O., Kong, F. M., Bradley, J. D., Vogelius, I. S., El Naqa, I., Hubbs, J. L., Lebesque, J. V., Timmerman, R. D., Martel, M. K. and Jackson, A. (2010a) 'Radiation dose-volume effects in the lung', *Int J Radiat Oncol Biol Phys,* 76(3 Suppl), pp. S70-6.

105.0 Marks, L. B., Lawrence, M. V., Hubbs, J. L., Das, S. K., Zhang, J., Wong, T. Z., Jaszczak, R. J. and Zhou, S. (2009) 'The Impact of “Low-dose Lung Bath” on the Sensitivity of

the Lung to Radiation: Are There Neighborhood Effects in the Lung?', *International Journal of Radiation Oncology • Biology • Physics,* 75(3), pp. S46.

106.0 Marks, L. B., Yorke, E. D., Jackson, A., Ten Haken, R. K., Constine, L. S., Eisbruch, A., Bentzen, S. M., Nam, J. and Deasy, J. O. (2010b) 'Use of normal tissue complication probability models in the clinic', *Int J Radiat Oncol Biol Phys,* 76(3 Suppl), pp. S10-9.

107.0 Massion P P, S. L. V. P. W. (2016) 'Biology of Lung Cancer', *Textbook of Respiratory Medicine*. Philadelphia: Elsevier, pp. 912.

108.0 Mayles, P., Nahum, A. and Rosenwald, J. C. (2007) *Handbook of Radiotherapy Physics: Theory and Practice.* New York London: Taylor and Francis.

109.0 Mayo, C. S., Urie, M. M., Fitzgerald, T. J., Ding, L., Lo, Y. C. and Bogdanov, M. (2008) 'Hybrid IMRT for treatment of cancers of the lung and esophagus', *Int J Radiat Oncol Biol Phys,* 71(5), pp. 1408-18.

110.0 Meyer, P., Noblet, V., Mazzara, C. and Lallement, A. (2018) 'Survey on deep learning for radiotherapy', *Computers in Biology and Medicine,* 98, pp. 126-146.

111.0 Miften, M., Olch, A., Mihailidis, D., Moran, J., Pawlicki, T., Molineu, A., Li, H., Wijesooriya, K., Shi, J., Xia, P., Papanikolaou, N. and Low, D. A. (2018) 'Tolerance limits and methodologies for IMRT measurement-based verification QA: Recommendations of AAPM Task Group No. 218', *Med Phys,* 45(4), pp. e53-e83.

112.0 Moller, D. S., Holt, M. I., Alber, M., Tvilum, M., Khalil, A. A., Knap, M. M. and Hoffmann, L. (2016) 'Adaptive radiotherapy for advanced lung cancer ensures target coverage and decreases lung dose', *Radiotherapy and oncology : journal of the European Society for Therapeutic Radiology and Oncology,* 121(1), pp. 32-38.

113.0 Moore, K. L., Schmidt, R., Moiseenko, V., Olsen, L. A., Tan, J., Xiao, Y., Galvin, J., Pugh, S., Seider, M. J., Dicker, A. P., Bosch, W., Michalski, J. and Mutic, S. (2015) 'Quantifying Unnecessary Normal Tissue Complication Risks due to Suboptimal Planning: A Secondary Study of RTOG 0126', *Int J Radiat Oncol Biol Phys,* 92(2), pp. 228-35.

114.0 Moya-Horno, I., Viteri, S., Karachaliou, N. and Rosell, R. (2018) 'Combination of immunotherapy with targeted therapies in advanced non-small cell lung cancer (NSCLC)', *Therapeutic Advances in Medical Oncology,* 10, pp. 1758834017745012.

115.0 Nahum, A., Uzan, J., Jain, P., Malik, Z., Fenwick, J. and Baker, C. (2011) 'SU-E-T-657: Quantitative Tumour Control Predictions for the Radiotherapy of Non-Small-Cell Lung Tumours', *Medical Physics,* 38(6Part21), pp. 3641-3641.

116.0 Nakamura, K., Kodaira, T., Shikama, N., Kagami, Y., Ishikura, S., Shibata, T. and Hiraoka, M. (2008) 'Accelerated fractionation versus conventional fractionation radiation therapy for glottic cancer of T1-2N0M0 Phase III study: Japan Clinical Oncology Group study (JCOG 0701)', *Jpn J Clin Oncol,* 38(5), pp. 387-9.

117.0 National Cancer Institute (2009) 'Common Terminology Criteria for Adverse Events v4.0'.

118.0 National Cancer Registration & Analysis Service and Cancer Research UK (2017) 'Chemotherapy, Radiotherapy and Tumour Resections in England: 2013-2014'. Available at: https://www.cancerresearchuk.org/health-professional/cancer-statistics/statistics-by-cancer-type/lung-cancer/diagnosis-and-treatment#heading-Two (Accessed 19/02/2021).

119.0 Neal, A. J. and Hoskin, P. J. (2012) *Clinical Oncology basic principles and practice.* London: Taylor & Francis Group.

120.0 Nelms, B. E., Robinson, G., Markham, J., Velasco, K., Boyd, S., Narayan, S., Wheeler, J. and Sobczak, M. L. (2012) 'Variation in external beam treatment plan quality: An inter-institutional study of planners and planning systems', *Practical radiation oncology,* 2(4), pp. 296-305.

121.0 Newhauser, W. (2009) 'ICRUPrescribing, Recording and Reporting Photon Beam Therapy. International Commissions on Radiation Units and Measurements (Supplement to ICRU Report 50): Bethesda, MD, USA. Report 62', *Radiation Protection Dosimetry - RADIAT PROT DOSIM,* 133, pp. 60-62.

122.0 Nielsen, T. B., Hansen, O., Schytte, T. and Brink, C. (2014) 'Inhomogeneous dose escalation increases expected local control for NSCLC patients with lymph node involvement without increased mean lung dose', *Acta Oncologica (Stockholm, Sweden),* 53(1), pp. 119-125.

123.0 Nuraini, R. and Widita, R. (2019) 'Tumor Control Probability (TCP) and Normal Tissue Complication Probability (NTCP) with Consideration of Cell Biological Effect', *Journal of Physics: Conference Series,* 1245(1), pp. 012092.

124.0 Nwankwo, O., Mekdash, H., Sihono, D. S., Wenz, F. and Glatting, G. (2015) 'Knowledge-based radiation therapy (KBRT) treatment planning versus planning by experts: validation of a KBRT algorithm for prostate cancer treatment planning', *Radiation oncology (London, England),* 10, pp. 111-015-0416-6.

125.0 Nyman, J., Hallqvist, A., Lund, J., Brustugun, O. T., Bergman, B., Bergström, P., Friesland, S., Lewensohn, R., Holmberg, E. and Lax, I. (2016) 'SPACE - A randomized study of SBRT vs conventional fractionated radiotherapy in medically inoperable stage I NSCLC', *Radiother Oncol,* 121(1), pp. 1-8.

126.0 Oh, D., Ahn, Y. C., Park, H. C., Lim, D. H. and Han, Y. (2009) 'Prediction of radiation pneumonitis following high-dose thoracic radiation therapy by 3 Gy/fraction for non-small cell lung cancer: analysis of clinical and dosimetric factors', *Jpn J Clin Oncol,* 39(3), pp. 151-7.

127.0 Oliver, M., Gagne, I., Popescu, C., Ansbacher, W. and Beckham, W. A. (2009) 'Analysis of RapidArc optimization strategies using objective function values and dose-volume histograms', *J Appl Clin Med Phys,* 11(1), pp. 3114.

128.0 Olofsson, N. (2012) 'Evaluation of IMRT beam complexity metrics to be used in the IMRT QA process', pp. 30, *https://www.radfys.gu.se/digitalAssets/1360/1360092_niklas-olofsson-rapport.pdf*, Available at: University of Gothenburg.

129.0 Ozyigit, G., Selek, U. and Topkan, E. (2016) *Principles and practice of radiotherapy techniques in thoracic malignancies.* Springer International Publishing.

130.0 Paz-Ares, L., Spira, A., Raben, D., Planchard, D., Cho, B. C., Özgüroğlu, M., Daniel, D., Villegas, A., Vicente, D., Hui, R., Murakami, S., Spigel, D., Senan, S., Langer, C. J., Perez, B. A., Boothman, A. M., Broadhurst, H., Wadsworth, C., Dennis, P. A., Antonia, S. J. and Faivre-Finn, C. (2020) 'Outcomes with durvalumab by tumour PD-L1 expression in unresectable, stage III non-small-cell lung cancer in the PACIFIC trial', *Ann Oncol*.

131.0 Petereit, D. G., Sarkaria, J. N., Chappell, R., Fowler, J. F., Hartmann, T. J., Kinsella, T. J., Stitt, J. A., Thomadsen, B. R. and Buchler, D. A. (1995) 'The adverse effect of treatment prolongation in cervical carcinoma', *Int J Radiat Oncol Biol Phys,* 32(5), pp. 1301-7.

132.0 Powis, R., Bird, A., Brennan, M., Hinks, S., Newman, H., Reed, K., Sage, J. and Webster, G. (2017) 'Clinical implementation of a knowledge based planning tool for prostate VMAT', *Radiation oncology (London, England),* 12(1), pp. 81-017-0814-z.

133.0 'Preface', (2017) *Journal of the International Commission on Radiation Units and Measurements,* 14(2), pp. 1-1.

134.0 Pugachev, A. and Xing, L. (2002) 'Incorporating prior knowledge into beam orientation optimization in IMRT', *International journal of radiation oncology, biology, physics,* 54(5), pp. 1565-1574.

135.0 Pursley, J., Damato, A. L., Czerminska, M. A., Margalit, D. N., Sher, D. J. and Tishler, R. B. (2017) 'A comparative study of standard intensity-modulated radiotherapy and RapidArc planning techniques for ipsilateral and bilateral head and neck irradiation', *Medical Dosimetry,* 42(1), pp. 31-36.

136.0 Pöttgen, C., Eberhardt, W., Stamatis, G. and Stuschke, M. (2017) 'Definitive radiochemotherapy versus surgery within multimodality treatment in stage III non-small cell lung cancer (NSCLC) - a cumulative meta-analysis of the randomized evidence', *Oncotarget,* 8(25), pp. 41670-41678.

137.0 Quan, E. M., Chang, J. Y., Liao, Z., Xia, T., Yuan, Z., Liu, H., Li, X., Wages, C. A., Mohan, R. and Zhang, X. (2012) 'Automated volumetric modulated Arc therapy treatment

planning for stage III lung cancer: how does it compare with intensity-modulated radio therapy?', *Int J Radiat Oncol Biol Phys,* 84(1), pp. e69-76.

138.0 Ramella, S., Fiore, M., Silipigni, S., Zappa, M. C., Jaus, M., Alberti, A. M., Matteucci, P., Molfese, E., Cornacchione, P., Greco, C., Trodella, L., Ippolito, E. and D'Angelillo, R. M. 2017. Local Control and Toxicity of Adaptive Radiotherapy Using Weekly CT Imaging: Results from the LARTIA Trial in Stage III NSCLC. *Journal of Thoracic Oncology.*

139.0 Ramroth, J., Cutter, D. J., Darby, S. C., Higgins, G. S., McGale, P., Partridge, M. and Taylor, C. W. (2016) 'Dose and Fractionation in Radiation Therapy of Curative Intent for Non-Small Cell Lung Cancer: Meta-Analysis of Randomized Trials', *International journal of radiation oncology, biology, physics,* 96(4), pp. 736-747.

140.0 Rana, S. (2013) 'Intensity modulated radiation therapy versus volumetric intensity modulated arc therapy', *J Med Radiat Sci,* 60(3), pp. 81-3.

141.0 Rana, S. B. and Cheng, C. (2013) 'Investigating VMAT planning technique to reduce rectal and bladder dose in prostate cancer treatment plans', *Clinical Cancer Investigation Journal,* 2(3), pp. 212-217.

142.0 Rancati, T., Ceresoli, G. L., Gagliardi, G., Schipani, S. and Cattaneo, G. M. (2003) 'Factors predicting radiation pneumonitis in lung cancer patients: a retrospective study', *Radiother Oncol,* 67(3), pp. 275-83.

143.0 Reinard, J. C. (2006) *Communication Research Statistics.* SAGE Publications.

144.0 Ren, C., Ji, T., Liu, T., Dang, J. and Li, G. (2018) 'The risk and predictors for severe radiation pneumonitis in lung cancer patients treated with thoracic reirradiation', *Radiat Oncol,* 13(1), pp. 69.

145.0 Rengan, R., Rosenzweig, K. E., Venkatraman, E., Koutcher, L. A., Fox, J. L., Nayak, R., Amols, H., Yorke, E., Jackson, A., Ling, C. C. and Leibel, S. A. 2004. Improved local control with higher doses of radiation in large-volume stage III non–small-cell lung cancer. *International Journal of Radiation Oncology*Biology*Physics.*

146.0 Rosca, F., Kirk, M., Soto, D., Sall, W. and McIntyre, J. (2012) 'Reducing the low-dose lung radiation for central lung tumors by restricting the IMRT beams and arc arrangement', *Med Dosim,* 37(3), pp. 280-6.

147.0 Rosenzweig, K. E., Fox, J. L., Yorke, E., Amols, H., Jackson, A., Rusch, V., Kris, M. G., Ling, C. C. and Leibel, S. A. (2005) 'Results of a phase I dose-escalation study using three-dimensional conformal radiotherapy in the treatment of inoperable nonsmall cell lung carcinoma', *Cancer,* 103(10), pp. 2118-27.

148.0 Schreibmann, E. and Fox, T. (2014) 'Prior-knowledge treatment planning for volumetric arc therapy using feature-based database mining', *Journal of applied clinical medical physics,* 15(2), pp. 4596.

149.0 Schulze, R., Heil, U., Gross, D., Bruellmann, D. D., Dranischnikow, E., Schwanecke, U. and Schoemer, E. (2011) 'Artefacts in CBCT: a review', *Dentomaxillofac Radiol,* 40(5), pp. 265-73.

150.0 Shah, J. L. and Loo, B. W., Jr. (2017) 'Stereotactic Ablative Radiotherapy for Early-Stage Lung Cancer', *Seminars in radiation oncology,* 27(3), pp. 218-228.

151.0 Sher, T., Dy, G. K. and Adjei, A. A. (2008) 'Small cell lung cancer', *Mayo Clin Proc,* 83(3), pp. 355-67.

152.0 Sibolt, P., Ottosson, W., Sjostrom, D., Larsen, C. and Behrens, C. F. (2015) 'Adaptation requirements due to anatomical changes in free-breathing and deep-inspiration breath-hold for standard and dose-escalated radiotherapy of lung cancer patients', *Acta Oncologica (Stockholm, Sweden),* 54(9), pp. 1453-1460.

153.0 Spoelstra, F. O., Pantarotto, J. R., van Sornsen de Koste, J. R., Slotman, B. J. and Senan, S. (2009) 'Role of adaptive radiotherapy during concomitant chemoradiotherapy for lung cancer: analysis of data from a prospective clinical trial', *International journal of radiation oncology, biology, physics,* 75(4), pp. 1092-1097.

154.0 Steel, G. G. (2002) *Basic Clinical Radiobiology, 3Ed.* Taylor & Francis.

155.0 Sun, B., Brooks, E. D., Komaki, R. U., Liao, Z., Jeter, M. D., McAleer, M. F., Allen, P. K., Balter, P. A., Welsh, J. D., O'Reilly, M. S., Gomez, D., Hahn, S. M., Roth, J. A., Mehran, R. J., Heymach, J. V. and Chang, J. Y. (2017) '7-year follow-up after stereotactic ablative radiotherapy for patients with stage I non-small cell lung cancer: Results of a phase 2 clinical trial', *Cancer,* 123(16), pp. 3031-3039.

156.0 Symonds, P. R., Deehan, C., Meredith, C. and Mills, J. A. (2012) *Walter and Miller's Textbook of Radiotherapy E-book.* Elsevier Health Sciences.

157.0 Tambe, N. S., Pires, I. M., Moore, C., Cawthorne, C. and Beavis, A. W. (2020) 'Validation of in-house knowledge-based planning model for advance-stage lung

cancer patients treated using VMAT radiotherapy', *Br J Radiol,* 93(1106), pp. 20190535.

158.0 Tekatli, H., van 't Hof, S., Nossent, E. J., Dahele, M., Verbakel, W. F. A. R., Slotman, B. J. and Senan, S. (2017) 'Use of Stereotactic Ablative Radiotherapy (SABR) in Non-Small Cell Lung Cancer Measuring More Than 5 cm', *Journal of thoracic oncology : official publication of the International Association for the Study of Lung Cancer,* 12(6), pp. 974-982.

159.0 Tennyson, N., Weiss, E., Sleeman, W., Rosu, M., Jan, N. and Hugo, G. D. 2017. Effect of variations in atelectasis on tumor displacement during radiation therapy for locally advanced lung cancer. *Advances in Radiation Oncology.*

160.0 Teoh, M., Clark, C. H., Wood, K., Whitaker, S. and Nisbet, A. (2011) 'Volumetric modulated arc therapy: a review of current literature and clinical use in practice', *Br J Radiol,* 84(1007), pp. 967-96.

161.0 Tepper, J. E. (2020) *Gunderson & Tepper's Clinical Radiation Oncology, E-Book.* Elsevier Health Sciences.

162.0 The Royal College of Radiologists (2008) *On Target: Ensuring Geometric Accuracy In Radiotherapy*. Available at: http://www.rcr.ac.uk/publications.aspx?PageID=149&PublicationID=292.

163.0 The Royal College of Radiologists (2022) *Radiotherapy target volume definition and peer review*. Available at: https://www.rcr.ac.uk/system/files/publication/field_publication_files/radiotherapy-peer-review-2022.pdf.

164.0 Tol, J. P., Dahele, M., Peltola, J., Nord, J., Slotman, B. J. and Verbakel, W. F. (2015a) 'Automatic interactive optimization for volumetric modulated arc therapy planning', *Radiat Oncol,* 10, pp. 75.

165.0 Tol, J. P., Delaney, A. R., Dahele, M., Slotman, B. J. and Verbakel, W. F. (2015b) 'Evaluation of a knowledge-based planning solution for head and neck cancer', *International journal of radiation oncology, biology, physics,* 91(3), pp. 612-620.

166.0 Tran, A., Zhang, J., Woods, K., Yu, V., Nguyen, D., Gustafson, G., Rosen, L. and Sheng, K. (2017) 'Treatment planning comparison of IMPT, VMAT and 4π radiotherapy for prostate cases', *Radiat Oncol,* 12(1), pp. 10.

167.0 Tseng, H.-H., Luo, Y., Ten Haken, R. K. and El Naqa, I. (2018) 'The Role of Machine Learning in Knowledge-Based Response-Adapted Radiotherapy', *Frontiers in Oncology,* 8(266).

168.0 UK SABR Consortium (2016) *Stereotactic Ablative Body Radiation Therapy (SABR): A Resource*, UK: The Faculty of Clinical Oncology of The Royal College of Radiologists.

169.0 UK SABR Consortium (2019) *Stereotactic Ablative Body Radiation Therapy (SABR): A Resource*, UK: The Faculty of Clinical Oncology of The Royal College of Radiologists.

170.0 Uzan, J. and Nahum, A. E. (2012) 'Radiobiologically guided optimisation of the prescription dose and fractionation scheme in radiotherapy using BioSuite', *Br J Radiol,* 85(1017), pp. 1279-86.

171.0 van Zwienen, M., van Beek, S., Belderbos, J., van Kranen, S., Rasch, C., van Herk, M. and Sonke, J. 2008. Anatomical Changes during Radiotherapy of Lung Cancer Patients. *International Journal of Radiation Oncology*Biology*Physics.*

172.0 Vozenin, M. C., Bourhis, J. and Durante, M. (2022) 'Towards clinical translation of FLASH radiotherapy', *Nat Rev Clin Oncol*.

173.0 Wall, P. D. H., Carver, R. L. and Fontenot, J. D. (2018) 'An improved distance-to-dose correlation for predicting bladder and rectum dose-volumes in knowledge-based VMAT planning for prostate cancer', *Phys Med Biol,* 63(1), pp. 015035.

174.0 Wang, H., Xue, J., Chen, T., Qu, T., Barbee, D., Tam, M. and Hu, K. (2020a) 'Adaptive radiotherapy based on statistical process control for oropharyngeal cancer', *J Appl Clin Med Phys,* 21(9), pp. 171-177.

175.0 Wang, J., Hu, W., Yang, Z., Chen, X., Wu, Z., Yu, X., Guo, X., Lu, S., Li, K. and Yu, G. (2017) 'Is it possible for knowledge-based planning to improve intensity modulated radiation therapy plan quality for planners with different planning experiences in left-sided breast cancer patients?', *Radiation oncology (London, England),* 12(1), pp. 85-017-0822-z.

176.0 Wang, S., Liao, Z., Wei, X., Liu, H. H., Tucker, S. L., Hu, C. S., Mohan, R., Cox, J. D. and Komaki, R. (2006) 'Analysis of clinical and dosimetric factors associated with treatment-related pneumonitis (TRP) in patients with non-small-cell lung cancer (NSCLC) treated with concurrent chemotherapy and three-dimensional conformal radiotherapy (3D-CRT)', *Int J Radiat Oncol Biol Phys,* 66(5), pp. 1399-407.

177.0 Wang, X., Palaskas, N. L., Yusuf, S. W., Abe, J. I., Lopez-Mattei, J., Banchs, J., Gladish, G. W., Lee, P., Liao, Z., Deswal, A. and Lin, S. H. (2020b) 'Incidence and Onset of Severe Cardiac Events After Radiotherapy for Esophageal Cancer', *J Thorac Oncol,* 15(10), pp. 1682-1690.

178.0 Webb, S. (2003) 'Use of a quantitative index of beam modulation to characterize dose conformality: illustration by a comparison of full beamlet IMRT, few-segment IMRT (fsIMRT) and conformal unmodulated radiotherapy', *Phys Med Biol,* 48(14), pp. 2051-62.

179.0 Webb, S. (2015) *Intensity-Modulated Radiation Therapy.* CRC Press.

180.0 Whitson, G. L. (1972) *Concepts in radiation cell biology, edited by Gary L. Whitson. Cell biology: a series of monographs* New York,: Academic Press.

181.0 Wijsman, R., Dankers, F., Troost, E. G. C., Hoffmann, A. L., van der Heijden, E. H. F. M., de Geus-Oei, L. F. and Bussink, J. (2017) 'Comparison of toxicity and outcome in advanced stage non-small cell lung cancer patients treated with intensity-modulated (chemo-)radiotherapy using IMRT or VMAT', *Radiother Oncol,* 122(2), pp. 295-299.

182.0 Winchester, D. J., Winchester, D. P., Hudis, C. A. and Norton, L. (2006) *Breast Cancer.* B.C. Decker.

183.0 Withers, H. R., Peters, L. J., Taylor, J. M., Owen, J. B., Morrison, W. H., Schultheiss, T. E., Keane, T., O'Sullivan, B., van Dyk, J. and Gupta, N. (1995) 'Local control of carcinoma of the tonsil by radiation therapy: an analysis of patterns of fractionation in nine institutions', *Int J Radiat Oncol Biol Phys,* 33(3), pp. 549-62.

184.0 Withers, H. R., Taylor, J. M. and Maciejewski, B. (1988) 'The hazard of accelerated tumor clonogen repopulation during radiotherapy', *Acta Oncol,* 27(2), pp. 131-46.

185.0 Wolthaus, J. W., Sonke, J. J., van Herk, M., Belderbos, J. S., Rossi, M. M., Lebesque, J. V. and Damen, E. M. (2008) 'Comparison of different strategies to use four-dimensional computed tomography in treatment planning for lung cancer patients', *Int J Radiat Oncol Biol Phys,* 70(4), pp. 1229-38.

186.0 Wu, B., Pang, D., Simari, P., Taylor, R., Sanguineti, G. and McNutt, T. (2013) 'Using overlap volume histogram and IMRT plan data to guide and automate VMAT planning: a head-and-neck case study', *Med Phys,* 40(2), pp. 021714.

187.0 Wu, B., Ricchetti, F., Sanguineti, G., Kazhdan, M., Simari, P., Chuang, M., Taylor, R., Jacques, R. and McNutt, T. (2009) 'Patient geometry-driven information retrieval for IMRT treatment plan quality control', *Medical physics,* 36(12), pp. 5497-5505.

188.0 Xia, P., Godley, A., Shah, C., Gregory M. M. Videtic, M. D. C. M. F. and Suh, J. (2018) *Strategies for Radiation Therapy Treatment Planning.* Springer Publishing Company.

189.0 Yan, D., Vicini, F., Wong, J. and Martinez, A. (1997) 'Adaptive radiation therapy', *Physics in Medicine and Biology,* 42(1), pp. 123-132.

190.0 Yin, L., Wu, H., Gong, J., Geng, J. H., Jiang, F., Shi, A. H., Yu, R., Li, Y. H., Han, S. K., Xu, B. and Zhu, G. Y. (2012) 'Volumetric-modulated arc therapy vs. c-IMRT in esophageal cancer: a treatment planning comparison', *World J Gastroenterol,* 18(37), pp. 5266-75.

191.0 Yom, S. S. (2015) 'Accelerated repopulation as a cause of radiation treatment failure in non-small cell lung cancer: review of current data and future clinical strategies', *Semin Radiat Oncol,* 25(2), pp. 93-9.

192.0 Yom, S. S., Liao, Z., Liu, H. H., Tucker, S. L., Hu, C. S., Wei, X., Wang, X., Wang, S., Mohan, R., Cox, J. D. and Komaki, R. (2007) 'Initial evaluation of treatment-related pneumonitis in advanced-stage non-small-cell lung cancer patients treated with concurrent chemotherapy and intensity-modulated radiotherapy', *Int J Radiat Oncol Biol Phys,* 68(1), pp. 94-102.

193.0 Yoneda, K., Kuwata, T., Kanayama, M., Mori, M., Kawanami, T., Yatera, K., Ohguri, T., Hisaoka, M., Nakayama, T. and Tanaka, F. (2019) 'Alteration in tumoural PD-L1 expression and stromal CD8-positive tumour-infiltrating lymphocytes after concurrent chemo-radiotherapy for non-small cell lung cancer', *Br J Cancer,* 121(6), pp. 490-496.

194.0 Younge, K. C., Roberts, D., Janes, L. A., Anderson, C., Moran, J. M. and Matuszak, M. M. (2016) 'Predicting deliverability of volumetric-modulated arc therapy (VMAT) plans using aperture complexity analysis', *J Appl Clin Med Phys,* 17(4), pp. 124-131.

195.0 Yu, X. J., Dai, W. R. and Xu, Y. (2017) 'Survival Outcome after Stereotactic Body Radiation Therapy and Surgery for Early Stage Non-Small Cell Lung Cancer: A Meta-Analysis', *Journal of investigative surgery : the official journal of the Academy of Surgical Research*, pp. 1-8.

196.0 Yuan, L., Ge, Y., Lee, W. R., Yin, F. F., Kirkpatrick, J. P. and Wu, Q. J. (2012) 'Quantitative analysis of the factors which affect the interpatient organ-at-risk dose sparing variation in IMRT plans', *Medical physics,* 39(11), pp. 6868-6878.

197.0 Zappa, C. and Mousa, S. A. (2016) 'Non-small cell lung cancer: current treatment and future advances', *Transl Lung Cancer Res,* 5(3), pp. 288-300.

198.0 Zawadzka, A., Nesteruk, M., Brzozowska, B. and Kukolowicz, P. F. (2017) 'Method of predicting the mean lung dose based on a patients anatomy and dose-volume histograms', *Medical dosimetry : official journal of the American Association of Medical Dosimetrists,* 42(1), pp. 57-62.

199.0 Zehentmayr, F., Grambozov, B., Kaiser, J., Fastner, G. and Sedlmayer, F. (2020) 'Radiation dose escalation with modified fractionation schedules for locally advanced NSCLC: A systematic review', *Thorac Cancer,* 11(6), pp. 1375-1385.

200.0 Zhang, X., Li, X., Quan, E. M., Pan, X. and Li, Y. (2011a) 'A methodology for automatic intensity-modulated radiation treatment planning for lung cancer', *Phys Med Biol,* 56(13), pp. 3873-93.

201.0 Zhang, X., Li, X., Quan, E. M., Pan, X. and Li, Y. (2011b) 'A methodology for automatic intensity-modulated radiation treatment planning for lung cancer', *Physics in Medicine and Biology,* 56(13), pp. 3873-3893.

202.0 Zhen, H., Nelms, B. E. and Tome, W. A. (2011) 'Moving from gamma passing rates to patient DVH-based QA metrics in pretreatment dose QA', *Med Phys,* 38(10), pp. 5477-89.

203.0 Zhu, X., Ge, Y., Li, T., Thongphiew, D., Yin, F. F. and Wu, Q. J. (2011) 'A planning quality evaluation tool for prostate adaptive IMRT based on machine learning', *Medical physics,* 38(2), pp. 719-726.

204.0 Zhuang, H., Yuan, Z., Chang, J. Y., Wang, J., Pang, Q., Zhao, L. and Wang, P. (2014) 'Radiation pneumonitis in patients with non--small-cell lung cancer treated with erlotinib concurrent with thoracic radiotherapy', *J Thorac Oncol,* 9(6), pp. 882-5.